

COLD EXPANSION EFFECTS ON CRACKED FASTENER HOLES
UNDER CONSTANT AMPLITUDE AND SPECTRUM LOADING
IN THE 2024-T351 ALUMINUM ALLOY

by

Jacob John Warner

A thesis submitted to the faculty of
The University of Utah
in partial fulfillment of the requirements for the degree of

Master of Science

Department of Mechanical Engineering

The University of Utah

May 2012

Report Documentation Page

*Form Approved
OMB No. 0704-0188*

Public reporting burden for the collection of information is estimated to average 1 hour per response, including the time for reviewing instructions, searching existing data sources, gathering and maintaining the data needed, and completing and reviewing the collection of information. Send comments regarding this burden estimate or any other aspect of this collection of information, including suggestions for reducing this burden, to Washington Headquarters Services, Directorate for Information Operations and Reports, 1215 Jefferson Davis Highway, Suite 1204, Arlington VA 22202-4302. Respondents should be aware that notwithstanding any other provision of law, no person shall be subject to a penalty for failing to comply with a collection of information if it does not display a currently valid OMB control number.

1. REPORT DATE 03 JUL 2012	2. REPORT TYPE N/A	3. DATES COVERED -	
4. TITLE AND SUBTITLE Cold Expansion Effects on Cracked Fastener Holes Under Constant Amplitude and Spectrum Loading in the 2024-T351		5a. CONTRACT NUMBER	
		5b. GRANT NUMBER	
		5c. PROGRAM ELEMENT NUMBER	
6. AUTHOR(S) Jacob John Warner		5d. PROJECT NUMBER	
		5e. TASK NUMBER	
		5f. WORK UNIT NUMBER	
7. PERFORMING ORGANIZATION NAME(S) AND ADDRESS(ES) Department of Mechanical Engineering The University of Utah AND A-10 Systems Program Office (SPO) at Hill AFB, Utah		8. PERFORMING ORGANIZATION REPORT NUMBER	
		10. SPONSOR/MONITOR'S ACRONYM(S)	
9. SPONSORING/MONITORING AGENCY NAME(S) AND ADDRESS(ES)		11. SPONSOR/MONITOR'S REPORT NUMBER(S)	
		12. DISTRIBUTION/AVAILABILITY STATEMENT Approved for public release, distribution unlimited	
13. SUPPLEMENTARY NOTES The original document contains color images.			
14. ABSTRACT			
15. SUBJECT TERMS			
16. SECURITY CLASSIFICATION OF:			17. LIMITATION OF ABSTRACT
a. REPORT unclassified	b. ABSTRACT unclassified	c. THIS PAGE unclassified	UU
			18. NUMBER OF PAGES 194
			19a. NAME OF RESPONSIBLE PERSON

Copyright © Jacob John Warner 2012

All Rights Reserved

ABSTRACT

Current United States Air Force maintenance techniques require that any discontinuity (crack, pit, gouge, or other defect) detected in a hole be removed by oversizing the hole or replacing the part. What if cold expansion could be proved to extend the life of a cracked component well beyond the time to the next required inspection? This research investigates the effects of cold expansion on cracked holes.

This research compares the fatigue lives of clean (no detected discontinuities) cold-expanded holes with the fatigue lives of holes cold-expanded after a 0.050 inch fatigue crack had nucleated. The experiments conducted herein investigate various stress levels under constant amplitude and spectrum loading conditions. The percent cold expansion is calculated for each specimen, and the amount of crack growth from cold expansion was measured.

Finally, this work compares the tested fatigue lives with analytical predictions using Lextech Inc. AFGROW software utilizing an assumed 0.005 inch initial crack size to account for the benefit of cold expansion, consistent with most industrial aerospace damage tolerance analysis.

I would like to dedicate this work to my wonderful
wife Sarah, and to our daughter-to-be.

TABLE OF CONTENTS

ABSTRACT.....	iv
LIST OF TABLES.....	viii
ACKNOWLEDGEMENTS.....	x
1. INTRODUCTION	1
1.1. History of Fatigue Damage in Fastener Holes	1
1.2. History of Fatigue Designs.....	2
1.3. Current DTA Inspections	5
1.4. Fatigue Improvement Methods	6
1.5. Role of Cold Expansion in Maintenance and Life Extension Programs.....	8
1.6. Scope of Project	13
1.7. Goals of Project.....	15
2. TESTING SETUP AND PROCEDURES.....	20
2.1. Equipment Used.....	20
2.2. Test Specimens.....	25
2.3. Specimen Preparation.....	28
2.4. Test Procedure.....	28
2.5. Test Matrix	33
3. DATA COLLECTION AND ANALYSIS.....	49
3.1. Measurement Procedure.....	49
3.2. Time to Failure.....	51
3.3. Crack Growth Rate.....	52

3.4.	AFGROW Simulations	53
4.	RESULTS	70
4.1.	Constant Amplitude Loading	71
4.2.	Spectrum Loading	72
5.	DISCUSSION.....	92
5.1.	Cold-Expanded Holes and Precracked Cold-Expanded Holes	92
5.2.	Benefit of Cold Expansion on Precracked Holes	92
5.3.	AFGROW Predictions.....	95
5.4.	Error in Spectrum Loading.....	98
6.	SUMMARY	106
6.1.	Conclusions	106
6.2.	Recommendations	107
6.3.	Further Research Possibilities	108
APPENDICES		
A.	MATERIAL CERTIFICATION SHEET	110
B.	FATIGUE CRACK GROWTH TEST DATA SHEETS	112
C.	SPECIMEN CRACK GROWTH CURVES	153
D.	AFGROW PREDICTIONS	172
E.	FRACTOGRAPHIC IMAGES	177
F.	da/dN VS. ΔK DATA.....	182
G.	DAMAGE TOLERANCE ANALYSIS GROUND RULES FOR A-10A RECONFIGURED POST DESERT STORM SPECTRUM.....	184
	REFERENCES	191

LIST OF TABLES

<u>Table</u>	<u>Page</u>
1. Final Test Matrix	19
2. Original Test Matrix	48
3. Tested and Predicted Fatigue Lives for ASTM E 647 Standard Tests	66
4. AFGROW Baseline Aspect Ratio Analysis Results for Lookup File B	66
5. AFGROW SOLR Analysis Results.....	67
6. Average AFGROW SOLR Results with Interpolated Values.....	67
7. Test Data Summary	77
8. Weibull β Parameter	78
9. Constant Amplitude Test and Prediction Averages	80
10. Spectrum Test and Prediction Averages	82
11. Test and Prediction Results for 25.00 ksi Spectrum	82
12. Test and Prediction Results for 33.00 ksi Spectrum	84
13. Test and Prediction Results for NCX 43.25 ksi Spectrum	87
14. Crack Extension from Cold Expansion and Percent Cold Expansion.....	102
15. AFGROW Prediction Average Percent Disagreement for Precracked Cold-Expanded Tests.....	103
16. Ratios of Tested Life to AFGROW Predicted Life for Precracked Cold-Expanded Tests.....	104
17. Spectrum Stress Distributions	104

18. Maximum and Average Error Calculated from FRAG Log Files 105

19. Spectrum Loading Validation Tests 105

ACKNOWLEDGEMENTS

I would like to thank all those who have assisted me in completing this work. I am very grateful to all of the teachers and mentors I have had along the way. I am especially grateful toward the A-10 Aircraft Structural Integrity Program group, for their knowledge and wisdom. I am especially grateful to Paul Clark and Mark Thomsen for their previous expertise and wisdom of fatigue testing and machinery, as well as their knowledge of fracture mechanics and their willingness to teach and mentor me. I am very grateful toward Robert Pilarczyk and Scott Carlson for their previous fatigue work and the background and insight they provided.

I am very grateful to Dallen Andrew, a fellow student and friend who has helped me along every step of the way, especially for his patience and assistance at operating StressCheck and AFGROW programs. I am also very grateful to him and his family for his staying late in the lab so I could finish long experiments.

I am grateful to all of my professors at the University of Utah, especially Dr. David Hoepfner who is serving as the chair on my committee. Thanks to him for his knowledge, wisdom, and background in fatigue and fracture mechanics.

I am grateful to FTI Inc. and Kaiser Aluminum for their permission in the use of their copyrighted figures. I am grateful for the SMART scholarship program that has funded me through this program.

I would like to thank all of the lab employees that trained me on the equipment there and for permitting me to use the equipment. Namely, I am grateful to Dr. Hansen, George Lamar, Jeff Wandrey, and Eric Billings for permitting me to use the lab, and to Bryce Jolley, Cody Hone, and others who trained and assisted me on use of the lab equipment.

Finally, I would like to thank my family. I am so grateful to my wonderful wife Sarah for her love, patience, and support. I am very appreciative of the sacrifices she has made, and the incredible confidence, support, and love she demonstrates. I am grateful to parents and siblings as well for their examples and encouragement, and to the Lord for blessing me with this wonderful opportunity.

1. INTRODUCTION

1.1. History of Fatigue Damage in Fastener Holes

Fatigue damage has been the cause of catastrophic failures since before the Wright brothers first achieved flight in 1903. The first known fatigue tests were published in 1837 by Wilhelm Albert who was researching the life of conveyor belt chains used in mining. Numerous catastrophic fatigue failures occurred in the 1800's, including the Versailles train axle fatigue failure in 1842 which killed 60 people.¹ These failures motivated fatigue research that has led to the current knowledge of today.

Catastrophic fatigue failures continue to occur today in a number of different industries. A recent example is the Southwest Airlines flight 812 on April 1, 2011 which caused depressurization of the fuselage.² The focus of this document will be on the fatigue of fasteners holes in United States Air Force (USAF) A-10 aircraft.

To begin discussing metal fatigue, there must first be a common understanding of fatigue. The ASTM E1823 standard definition of fatigue.³

*The process of progressive localized permanent structural change occurring in a material subjected to conditions that produce fluctuating stresses and strains at some point or points and that may culminate in cracks or complete fracture after a sufficient number of fluctuations.*³

One critical point to be understood from this definition is that fatigue is a process. Some amount of damage is accumulated each time the component is used, and that damage may or may not be detectable before it is large enough to cause catastrophic

failure of the component. This time dependent nature of fatigue is one reason that fatigue must be accounted for from the initial stages of design.

1.2. History of Fatigue Designs

1.2.1. Safe Life Design

The United States Air Force (USAF) has primarily used two design paradigms for fatigue thus far. These paradigms are the Safe Life, and the Damage Tolerance fatigue designs. The American Society for Metals (ASM) Handbook 11 on Failure Analysis and Prevention describes safe life fatigue design: “The safe-life approach attempts to maintain safety by designing structural components to have a fatigue life longer than their expected use or by replacing them long before they suffer failure.”⁴ One of the first documented safe life fatigue designs was recommended for train axles by August Wohler in 1860.¹

There are a number of inherent problems with the safe life design. One is the possible early termination of components that are still functional and have some unknown/undetermined remaining life. Likewise, there is also possible catastrophic failure before the component has reached the assumed safe life. The possible early failure is a result of the safe life paradigm methodology. Generally the safe life of a component is determined from fatigue tests of carefully manufactured parts. The actual components used in service, however, may have any number of scratches or discontinuities from manufacturing, assembling, and processing that may nucleate cracks earlier than the tested components.

1.2.2. Damage Tolerance Design

Damage tolerance design incorporates key components of analysis, inspection, and design to provide a more accurate design approach than the safe life design. The damage tolerance design paradigm makes extensive use of fracture mechanics to determine the residual strength of a component for some crack shape and size. Damage tolerance also makes use of modern technology to perform a Nondestructive Inspection (NDI) to assess the amount of damage incurred on a component. Damage tolerance analysis incorporates fracture mechanics, NDI results, loading data, and crack growth rate data to predict the remaining life of a component given the defect size found by NDI. Each component to the damage tolerance design paradigm will be explained in more detail.

1.2.2.1. Fracture Mechanics History

In 1920 Alan Arnold Griffith published a paper entitled *Phenomena of Rupture and Flow in Solids* which was the result of his research on rupture strength of glass tubes and spheres. Griffith derived what is known as the Griffith Criterion, which is a relationship of the fracture stress and the surface energy.⁵ Irwin, Orowan, and Williams contributed to modifications of the Griffith criterion which replaced the surface energy with the material plane strain fracture toughness and a geometric correction factor. This relationship is commonly used in modern fracture mechanics and is given in Equation 1.⁶

$$K_{Ic} = \beta\sigma\sqrt{\pi a} \quad (1)$$

Where K_{IC} is the plane strain fracture toughness, β is the geometric correction factor, σ is the applied stress, and a is the crack length. This relationship is used to determine the stress and crack length that will cause fracture of a component.

1.2.2.2. Nondestructive Inspection

Modern technology has created a number of devices to detect crack, or crack-like discontinuities, in components without damaging the components. This process is known as NDI. There are a number of different types of NDI, to name a few: dye penetrate, magnetic particle, and eddy current. Each method has advantages, disadvantages, and limitations. The NDI method most commonly used for fastener holes in aircraft is the eddy current inspection because of its repeatability, capability to inspect multiple layers, and its small detectable flaw size. (Limits of detectable flaw size will be discussed later in the text. Also, “flaw” is taken to mean defect, discontinuity, crack, pit, etc.)

1.2.2.3. Damage Tolerance Analysis

The ASM handbook 19 on fatigue and fracture describes Damage Tolerance Analysis (DTA). “The objective of damage tolerance evaluation is to provide a crack growth and residual strength analysis, based on the expected use of the aircraft, so that an inspection program can be developed to maintain safety during service.”⁷ Damage tolerance design assumes each critical component to have some initial crack or crack-like discontinuity. It then applies fracture mechanics theory and uses test data to predict the fatigue life that will nucleate and propagate that discontinuity to the critical crack size. That life is then divided by some factor to define a time for inspection of the component.

After the component has reached the time specified for inspection, an NDI is conducted to assess the structural integrity of the component. The damage assessed from the inspection, if any, is removed or repaired, if possible, and the remaining component life is recalculated. The process is then repeated until the component is retired, unrepairable, or fails. A flowchart of the damage tolerance design process is shown in Fig. 1. The USAF Military Standard (MIL STD) 1530C describes the damage tolerance of a material, “Damage tolerance is the attribute of a structure that permits it to retain its required residual strength for a period of unrepaired usage after the structure has sustained specific levels of fatigue, corrosion, accidental, and/or discrete source damage.”⁸

1.3. Current DTA Inspections

The current maintenance practice within the USAF for fastener holes is to inspect the hole for defects with a specified NDI technique. A bolt hole eddy current probe is commonly used for this inspection. The bolt hole eddy current inspection returns an “indication” of a crack in a fastener hole. In some cases the “indication” detected may not be crack-like and could be an inclusion, void, or other material discontinuity that may or may not form a crack. Standard procedure requires any hole with a crack “indication” to be oversized until NDI no longer detects a discontinuity. This can lead to a fastener hole being unnecessarily oversized any number of times to remove a “phantom crack.” Unnecessarily oversizing a fastener hole weakens the structure by removing material. This can increase stresses in surrounding structure, often causes issues with short edge margins, and requires costly maintenance during which the structure can be further

damaged. All of these diminish the availability of the aircraft, thus weakening support to the war fighter.

1.4. Fatigue Improvement Methods

Some fatigue improvement methods create a residual compressive stress in the fatigue critical location of the component to reduce the mean stress in that area. Two common fatigue improvement methods used in the aerospace industry are cold expansion and shot peening. Shot peening blasts a surface with a laser or beads made of glass, ceramic, or some metal to create a residual compressive stress on the blasted surface. As it is difficult to blast the inside of a fastener hole with particles, shot peening is generally not used on fastener holes.

1.4.1. Cold Expansion

The cold expansion method expands the fastener hole diameter to create a residual stress field around the hole as shown in Fig. 2.⁹ This is done by forcing a tapered mandrel with a lubricated split sleeve through the fastener hole as shown in Fig. 3.⁹ A side effect is the split sleeve leaves a small indent, as shown in Fig. 4, and therefore should be aligned in the load direction of the component so it is 90 degrees from the most likely location for a crack to nucleate.

Cold expansion is easily applied to a number of components because it only requires access to one side of the hole. Care must be taken, however, to track the entrance and exit side of the mandrel as the residual stress field is not uniform through the thickness, and induces “P shape” crack fronts as shown in Fig. 5.

Another benefit to cold expansion is that it can be performed on nearly every hole independent of size, and a hole can be cold-expanded any number of times. Some research shows double cold expanding a hole, or cold expanding a hole twice consecutively, can provide a further fatigue benefit compared to cold expanding only once.¹⁰

The cold expansion process was invented by Boeing in 1965. Boeing then licensed the technology to some small businesses. One such business was then called International Wire and Metal Forming Incorporated, and is now known as Fatigue Technology Incorporated (FTI). FTI developed and patented a disposable lubricated split sleeve along with a number of other parts for cold expansion.¹¹

1.4.2. Interference Fit Fasteners

Interference fit fasteners refers to a fastener which has a larger diameter than the hole for the fastener, thus creating an interference fit of the fastener and the component. Interference fit fasteners can also increase the fatigue life of a component, as they maintain the shape of the hole, impeding deformation and strain from loading. The work of Y. C. Lam at Monash University indicated that interference fit fasteners could increase the fatigue life by a factor of 10.¹² It has also been shown that a combination of cold expansion and interference fit fasteners can provide a greater benefit than either cold expansion or interference fasteners acting independently.^{13,14}

1.5. Role of Cold Expansion in Maintenance and Life Extension Programs

As industry continues to push aircraft to fly longer, life extension programs become more and more common. Life extension programs are aimed to evaluate the incurred damage from usage up to the design life and then determine what maintenance and refurbishment is necessary for safe operation through some extended life.

1.5.1. The Role of Cold Expansion in Life Extension Programs

As cold expansion can improve the fatigue life of a fastener hole by large factors (up to 100 or more), is a relatively inexpensive procedure, and only requires access to one side of the component, it is widely utilized by life extension programs to improve fatigue life. As life extension programs are constantly dealing with cracked, or potentially cracked, fastener holes it becomes necessary to understand the effects of fatigue improvement techniques on cracked fastener holes. More specifically, it becomes necessary to understand the effects of cold expanding a cracked fastener hole. Some effects that require understanding are:

- How much, if any, crack extension will occur upon cold expansion?
- What benefit, if any, will there be for cold expanding a crack fastener hole?
- What modifications, if any, need to be made to analysis methods to accurately model the crack growth rate of a cracked, cold-expanded fastener hole?

Perhaps the most critical crack size at which these effects need to be understood is the assumed maximum crack size that is missed by NDI methods, in this case that would be 0.050 inches. MIL STD 1530C specifies that the minimum detectable crack size be the size for which there is a 90 percent probability of detection with 95 percent confidence (90/95).⁸ The minimum detectable crack size, then, for a bolt hole eddy

current inspection is specified in the Air Force Structures Bulletin (EN-SB-09-012 rev A) and is 0.050 inches.¹⁵ As the minimum detectable crack size is a critical value to damage tolerance analysis this research has been based around a 0.050 inch initial crack size (IFS).

1.5.2. Previous Research

The work of Ball and Lowry investigated cold expansion effects on precracked fastener holes with through thickness and part through thickness (corner) cracks under constant amplitude and spectrum loading for 2124-T851 aluminum plate. They found that for constant amplitude loading the fatigue life improved by a factor of 10 to 15 with cold expansion, and that under spectrum loading the fatigue life benefit was two to four. The spectrum loading was based on a wing root bending moment for fighter aircraft with all compressive loads removed.¹⁶

Research performed at the Aeronautical Research Laboratory in Australia demonstrated that for 0.59 inch (15 mm) thick sections the 2214-T651 aluminum alloy, cold expansion benefited the fatigue life by a factor of seven irrespective of if a crack was present before cold expansion or not. They also found that the crack growth rate of non-cold-expanded specimens increased almost linearly with crack length, while for cold-expanded specimens the crack growth rate decreased to a constant value until dramatically increasing before failure. Finally, they made some conclusions about the unique “P shape” crack front of cold-expanded specimens.¹⁷

The development of the characteristic “bulbous nose” crack front at cold-expanded holes in thick sections is not the result of earlier crack initiation near the mandrel entry face; rather it is a consequence (during the latter portion of the fatigue crack life) of an increase of the crack propagation rate adjacent to the

mandrel entry face compared with that at the exit face. This faster growth may be a result of the crack near the entry face passing into the decreasing compressive hoop stress field sooner than that near the exit face.¹⁷

Research performed by Zhang and Wang also indicated that:

In all cases cracks grew faster on the mandrel entry face than on the mandrel exit face. This can be explained by the fact that the mandrel exit face has higher compressive residual stress levels compared to the mandrel entry face. The difference in the residual tangential stress at the entry and exit faces has been attributed to the level of retained expansion and to the material volume carried by the mandrel movement.¹⁸

Phillips thoroughly investigated sleeve cold expansion and identified optimum cold expansion methods for aluminum, titanium, and steel alloys.¹⁹ Fatigue Technology Inc. investigated the effects of Split Sleeve Cold Expansion™ on test specimens that were precycled for 60% to 80% of a baseline fatigue life. The tests found that cold expansion of these specimens demonstrated an increase in fatigue life by a factor of two.¹⁰ The work of Pir M. Toor showed that tensile overloads during testing of cold-expanded holes further increased the fatigue life, while compressive overloads reduced the life.¹⁴

A number of documents have shown that cold expansion does not affect crack nucleation, only crack propagation after growing approximately 0.039 inches.^{17,20} Cold expansion in 2024-T351 aluminum was shown by the University of Bristol to significantly reduce the crack growth rate for cracks about 0.078 inches in length and larger, but that cold expansion had only a small influence on cracks shorter than 0.039 inches.²¹

A study done by the Department of Aeronautical Engineering at the Israel Institute of Technology observed that the life improvement for a cold-expanded hole without a crack was double the life of a non-cold-expanded hole, while the life

improvement for a cold-expanded hole with a prior 0.039 inch crack was four times that of a non-cold-expanded hole in the 7075-T7351 aluminum alloy.²² Buch and Berkovits also demonstrated that the fatigue life of a hole that was cracked before cold expansion is greater than the fatigue life of a hole that was not cracked before cold expansion.²² Similarly, the work of Zhang and Wang indicated that cold expansion of the 2024-T351 aluminum alloy was optimal after 25% of the baseline fatigue life. Zhang and Wang also observed that holes with cracks greater than the radius of the hole do not demonstrate any benefit from cold expansion.¹⁸ Buxbaum and Huth also showed that holes with cracks greater than the radius of the hole should not be cold-expanded.²³ Petrak and Stewart demonstrated that for 7075-T6 aluminum cracks up to 0.1 inches long can successfully be retarded with cold expansion and interference fit fasteners.²⁴

Buxbaum and Huth showed that using life improvement factors for cold-expanded specimens under constant amplitude loading will yield nonconservative predictions of cold-expanded specimens under spectrum loading for the 2024-T3 aluminum alloy.²³ Andrew also demonstrated that the life improvement factor from cold expansion for spectrum loaded tests was less than that of constant amplitude tests.²⁵

Carlson investigated the benefit of cold expansion on the 2024-T351 aluminum alloy under constant amplitude loading.²⁶ Pilarczyk performed similar research on the 7075-T651 aluminum alloy.²⁷ Andrew investigated the effects of cold expansion under spectrum loading for holes with short edge margins in the 2024-T351 aluminum alloy.²⁵

Some authors applied fracture mechanics principles incorporating residual stresses to accurately estimate fatigue life of cracks emanating from cold-expanded

fastener holes.^{20,28} Some authors estimated fatigue life of cracks in cold-expanded fastener holes with good agreement utilizing Lextech Inc. AFGROW software.^{18,29}

1.5.3. Current Research

Inspection methods for identifying cracks or crack-like flaws in fastener holes are only reliable down to some determined length known as the detectable flaw size. As a result, damage tolerance techniques must assume that a crack the length of the minimum detectable flaw size exists even after being inspected. This research is focused on the effects of cold expansion and wing spectrum on the fatigue of holes with approximately 0.050 inch cracks at various stress levels.

Similar research has been done on different materials and/or with different spectrum files. This work differs from previous work because it is focused on the fatigue life benefit of cold-expanded holes with preexisting cracks the length of the minimum detectable flaw size for USAF hole inspection. These differences are important because they represent a common maintenance situation for USAF aircraft. The current research also explores the effects of an A-10 wing spectrum on the fatigue life of precracked cold-expanded components, which has not been explored in any other research found by the author.

Another significant difference that makes this research unique is that it compares the predicted life using AFGROW and an assumed 0.005 inch IFS to account for the crack growth retardation effects of cold expansion with the tested fatigue life. The 0.005 inch IFS was used because it is the maximum benefit that can be assumed under current

USAF guidelines for cold expansion.¹⁵ This prediction was done for both spectrum and constant amplitude loading scenarios at various stress levels.

1.6. Scope of Project

A brief summary of the conditions tested are displayed in Table 1. The test matrix will be discussed in further detail later on, but is provided here for assistance in understanding the test plan.

1.6.1. Establish and Validate Baseline for Specimen

Size/Loading Conditions

The first phase of this project was to validate the manufacturing and testing procedures, and create a baseline condition for comparison purposes. The American Society for Testing and Materials (ASTM) is an organization that creates standards for material testing procedures and criteria. In 1990 ASTM released the Standard Test Method for Plane-Strain Fracture Toughness of Metallic Materials, or ASTM E 399.³⁰ In 2008 ASTM adopted the Standard Test Method for Measurement of Fatigue Crack Growth Rates, ASTM E 647.³¹ The ASTM E 647 standard depicts geometry and crack growth requirements for a fatigue test. The test specimen geometry used for this research was patterned after the requirements of a middle tension specimen for the ASTM E 647 test standard.

Two test specimens were dedicated to validating the testing procedure to be followed for the remainder of the tests. These two tests were also used as a baseline to validate crack growth prediction models, and to validate comparison with similar testing performed previously by Scott Carlson. Scott Carlson performed testing in 2007 through

2008 analyzing the fatigue effects of cold expansion on fastener holes in the 2024-T351 aluminum alloy.²⁶

1.6.2. Quantify Effects of Precracking on Cold-Expanded Holes

Carlson performed non-cold-expanded and cold-expanded experiments under constant amplitude loading for the 2024-T351 aluminum alloy. Carlson's work can be used to quantify a fatigue improvement for cold expansion of an uncracked fastener hole. A main goal of this research, however, is to quantify the effects of cold expansion on a hole with a preexisting corner fatigue crack of 0.050 inches. The results from the experiments conducted herein will be compared with the results from Carlson to quantify a reduction in fatigue benefit due to the existence of a fatigue crack prior to cold expansion. The equipment used for this research was the same equipment used by Carlson in his research, thus minimizing equipment induced variables.

1.6.3. Quantify A-10 Spectrum Effects on Fatigue Crack Growth Rates

The simplest and most common form of fatigue testing is constant amplitude testing, wherein the same maximum and minimum loads are applied to the test specimen each cycle. A far more useful fatigue experiment incorporates the approximate loading that the component observes during operation, which is known as a load spectrum. This research performed experiments using an A-10 wing spectrum to simulate flight loads on the test specimen to quantify fatigue effects of the A-10 WING spectrum. The results were then used as a baseline condition for fatigue life under spectrum loading conditions.

1.6.4. Quantify Cold Expansion Benefit on Precracked

Holes with Spectrum Loading

For a life extension program perhaps one of the most useful pieces of information would be to know the fatigue life of a cold-expanded hole with a prior crack the length of the minimum detectable flaw size. This presents a worst case scenario to baseline fatigue analyses and predictions. This research makes an attempt to quantify the fatigue benefit of cold expansion for a precracked hole under spectrum loading.

1.6.5. Perform AFGROW Prediction Models to Compare with Test Data

The test data obtained from this research will be compared against fatigue prediction models using LexTech Inc. AFGROW software. AFGROW is the standard fatigue prediction tool used by the A-10 Aircraft Structural Integrity Program (ASIP), and the predictions obtained from AFGROW will be compared against the test data obtained for comparison and validation purposes.

1.7. Goals of Project

The goals of this research project are:

1. Quantify the fatigue benefit of precracked cold-expanded holes under constant amplitude loading.
2. Quantify the fatigue life of non-cold-expanded holes under A-10 wing spectrum loading.
3. Quantify the fatigue benefit of precracked cold-expanded holes under A-10 WING spectrum loading.
4. Validate AFGROW fatigue life prediction models.

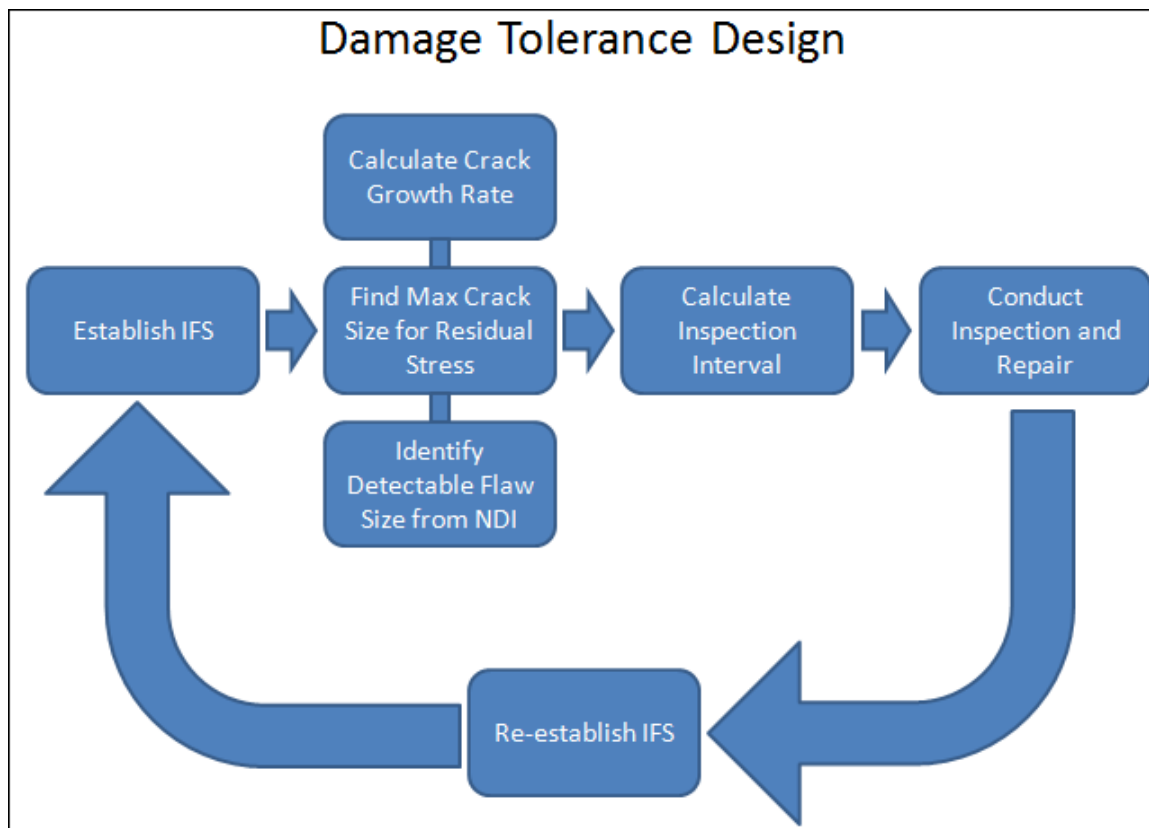


Fig. 1 Basic Damage Tolerance Design Flow Chart

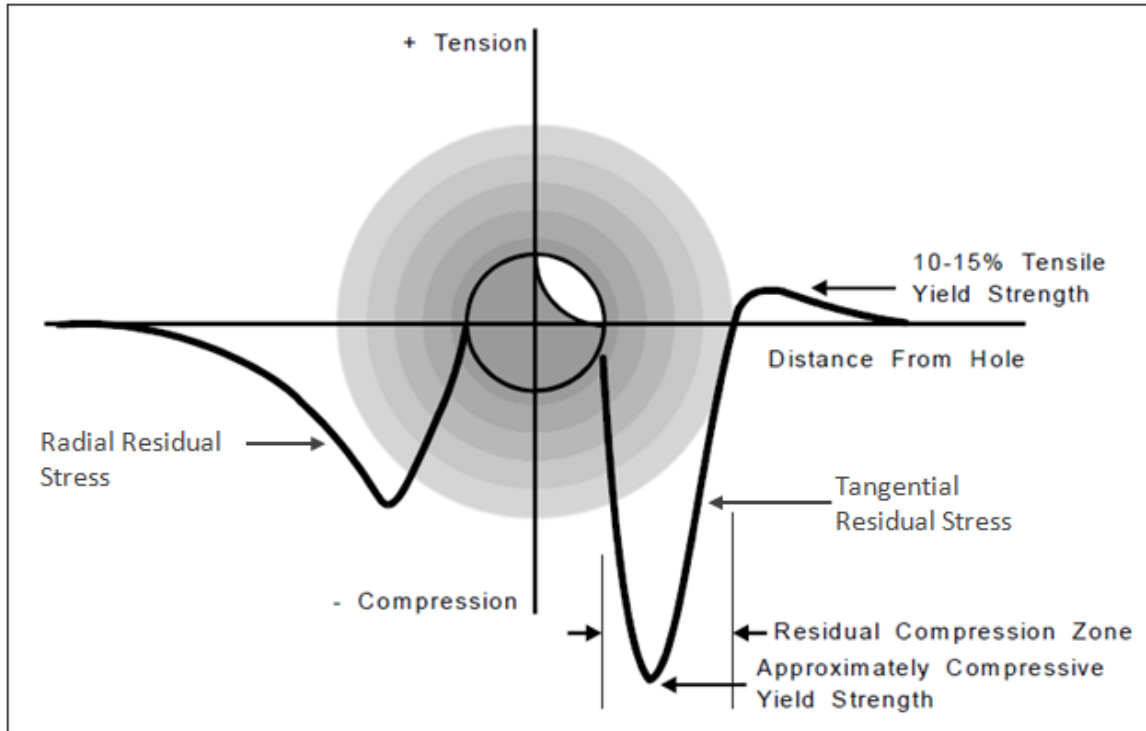


Fig. 2 Residual Stress Field from Split Sleeve Cold Expansion™⁹

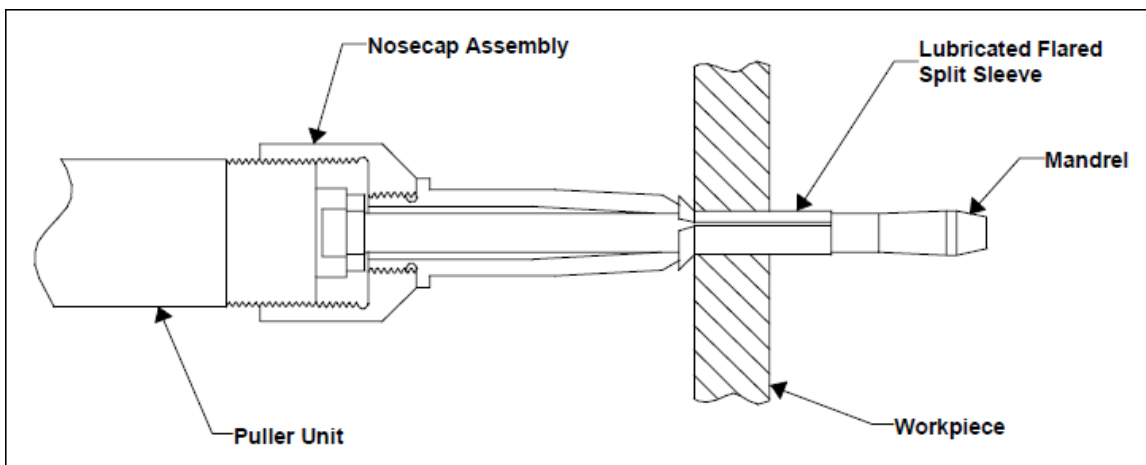


Fig. 3 Split Sleeve Cold Expansion™ Assembly⁹

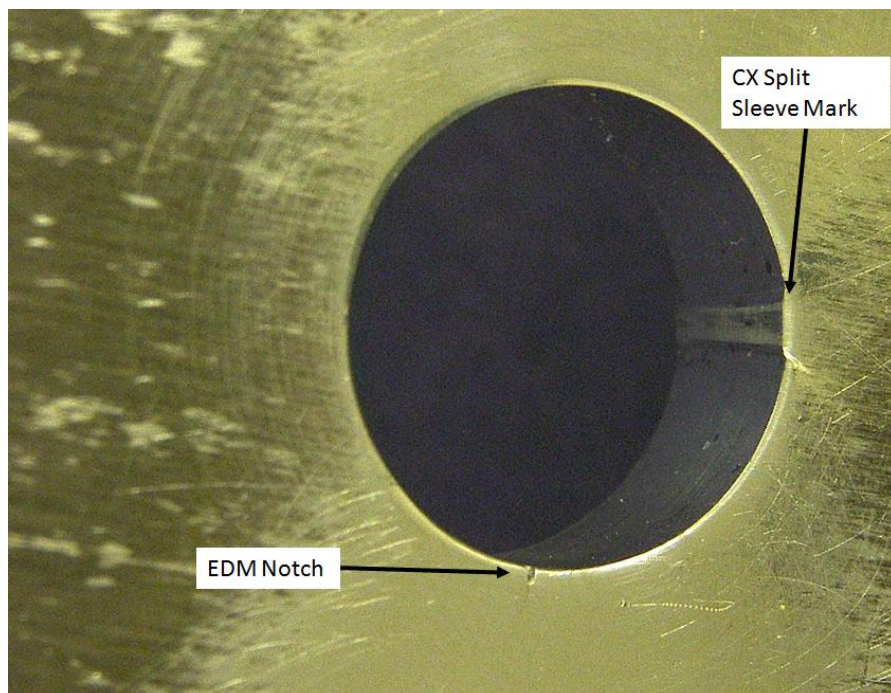


Fig. 4 Split Sleeve Ridge in Cold-Expanded Hole

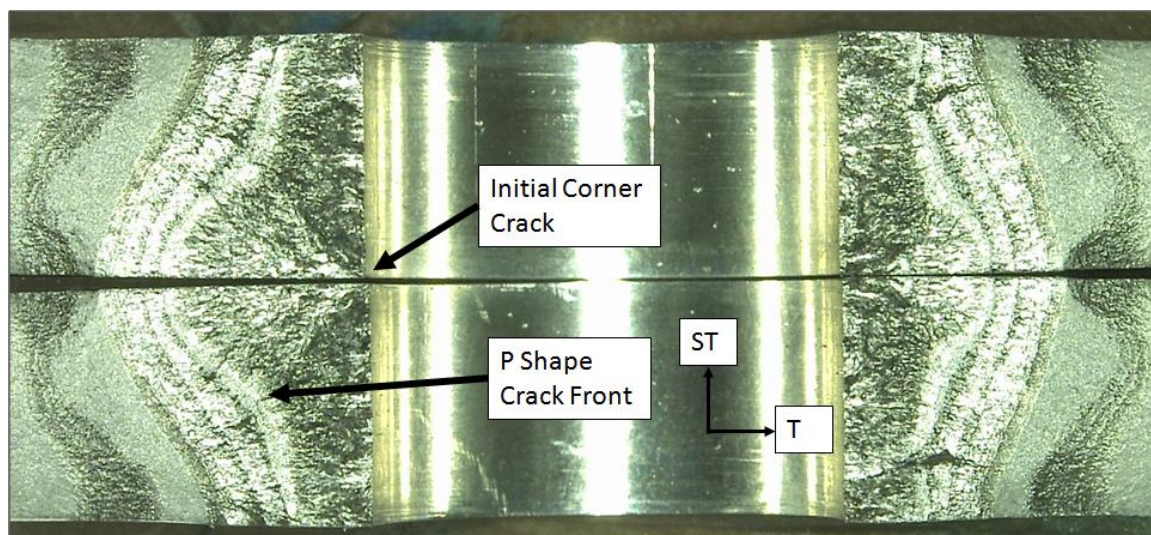


Fig. 5 Characteristic P shape Crack Front from Cold Expansion

Table 1 Final Test Matrix

CX/NON-CX	CA or Spectrum	Peak Stress (ksi)	Specimens Tested	Specimen ID's
NON-CX	CA (ASTM E647)	11.25	2	2024-1;-2
NON-CX	Spectrum	25.00	3	NCX 2024-1 thru -3
		33.00	3	NCX 2024-4 thru -6
		43.25	1	NCX 2024-7
CX	CA	20.00	4	PC-CX 2024-9;-10;-11
		25.00	3	PC-CX 2024-15;-16;-17
	Spectrum	25.00	1	PC-CX 2024-5
		30.00	3	PC-CX 2024-4;-12;-13
		33.00	3	PC-CX 2024-1 thru -3
		43.25	3	PC-CX 2024-6 thru -8

2. TESTING SETUP AND PROCEDURES

2.1. Equipment Used

2.1.1. Servo-Hydraulic Fatigue Equipment

The fatigue equipment used is owned and maintained by the USAF Hill Air Force Base (HAFB) Science and Engineering Laboratory. Use of the lab equipment for these experiments was made possible by an agreement with the lab supervisor and director. A labeled image of the general fatigue equipment used is shown in Fig. 6, and a more specific image of the load frame and gripping fixtures is shown in Fig. 7.

2.1.1.1. Interlaken Technology Corporation Load Frame

The fatigue testing was carried out on an Interlaken Technology Corporation Series 3300 Test Frame. The maximum capacity for this load frame is 55,000 lbf (55 kip).

2.1.1.2. MTS Systems Corporation Grips

While there were hydraulic wedge grips manufactured by Interlaken Technology Corporation for use with this load frame, they were not large enough to satisfactorily grip the test specimens used in these experiments and therefore were not used. A set of MTS Systems Corporation hydraulic wedge grips, model 647.25A-01, was selected instead as they can grip specimens four inches wide and over on quarter inch thick. MTS 398378-

01 wedges were used with the hydraulic grips. A threaded step stud was used to mount the MTS grips to the Interlaken load frame as the diameter of the mount on the grip differed from the mount on the load frame.

In addition to the MTS grips used, an MTS 685.60 Hydraulic Grip Supply intensifier was used to increase the grip pressure, therefore preventing slip of the test specimen during loading. The intensifier is capable of ramping the hydraulic pressure up to 10,000 psi. The grip pressure used in this research was 5,000 psi. This pressure was selected because it was the grip pressure used when the load cell was calibrated and loaded up to 50 kip. As no slipping was observed during this loading, and the loading conducted in this research only reached 43.3 kip it was assumed that the 5,000 psi grip pressure was adequate. Furthermore, increasing the grip pressure may have increased the probability of a premature failure due to cracks nucleating at the grips, so a higher grip pressure would not have been desirable.

A magnetic base stand assembly was mounted to the top grip and connected to a dial indicator, which was used to measure the concentricity of the top grip and the lower grip by spinning the actuator and observing the deflection of the dial indicator. The grips were found to be concentric within 0.015 inches, which was found to be satisfactory as the error of mounting each specimen in the grips is estimated to be greater than 0.015 inches. Furthermore, the ASTM E 647 standard does not require any maximum deflection of concentricity, rather it states the following.

It is important that attention be given to achieving good alignment in the force train through careful machining of all gripping fixtures. Misalignment can cause non-symmetric cracking, ... If non-symmetric cracking occurs, the use of a strain-gaged specimen to identify and minimize misalignment might prove useful.³¹

As there was not any nonsymmetric cracking observed during any testing, and all of the measurements for the ASTM E 647 specimens were within the limits of the standard it was assumed that any concentricity issues in the load train were not significant.

2.1.1.3. Instron Servo-Hydraulic Controller and Software

The fatigue actuator was controlled by an Instron Fast Track 8800 controller. The controller has an independent control panel for basic operation, but the interface primarily used with the controller was a standard personal computer running on the Windows 7 operating system. Using this interface, tensile and compressive load and position limits were set to prevent overloading the specimen and for safety concerns.

The software program used for constant amplitude loading was Instron DADN version 8.4.12 software package. This software was selected for the constant amplitude loading because it has the capability of pausing the test and holding the mean load for visual measurement purposes. It also has active auto tuning processes built into it, ensuring precise and accurate loading.

The software used for variable amplitude loading was Instron Random version 8.0.1 software. This program was selected because it allows for a user created spectrum text file to be uploaded to define load patterns. It also provides an instantaneous command and feedback plot allowing the user to monitor the test performance and accuracy. Another beneficial feature of this software is that it records a detailed log file including all loading points where the command and feedback differed by a percentage defined by the user. For the testing carried out herein that percentage was set to 2.0%.

The controller used feedback from an Interface 50 kip load cell, model 1032AF-50K-B, to measure the load applied to the specimen. The load cell was installed and calibrated by Instron on May 20, 2011 using the ASTM E4 standard procedure.

2.1.2. Measurement Equipment

The width and thickness of each specimen was measured using Max-Cal digital calipers manufactured by Fowler and NSK with an accuracy of ± 0.0005 inches. The calipers were calibrated on March 30, 2011.

The hole diameters were measured using a Fowler Bowers Hologic. The Hologic is a bore gauge measurement tool accurate to ± 0.00005 inches.

To track the length of a fatigue crack during testing, two Gaertner Scientific traveling microscopes with 32x magnification were used.³² These microscopes were mounted to the load frame using custom fixtures so as to not affect specimen loading, and to remain in the same location for consistency purposes. Two eyepieces were used with the microscopes, one for a focal length of 60 millimeters, and one for a focal length of 80 millimeters. The microscopes use a Fagor Automation digital readout to measure distances and displays values to ± 0.00002 inches. While the digital readout displays values to ± 0.00002 inches, the accuracy of the scopes as listed by Gaertner Scientific is only ± 0.00005 inches.³³ The accuracy required in the ASTM E 647 standard is only ± 0.004 inches.³¹ A picture of the traveling microscopes and the digital readouts are shown in Fig. 8.

Two Bausch and Lomb Fiber-Lite® lamps were used with snake light and magnifier attachments to aid in viewing the crack. These were selected because the

snake light allowed the angle of the light to be changed easily to best view the crack. The ASTM E 647 standard states that the crack tip is more easily viewed under indirect lighting, and the indirect light was facilitated as the crack grew using these lights.³¹ An image of one of the lights is shown in Fig. 7.

2.1.3.Reaming and Polishing Equipment

The holes were reamed using a standard 12 flute, ½ inch reamer. The specimens were reamed on a standard Bridgeport mill. Each specimen was individually centered on the mill to within 0.001 inches using a dial indicator that mounts to the mill spindle and touches the bore of the hole. An image of the mill is shown in Fig. 9.

Each specimen was polished after the final ream using one micron diamond paste. The diamond paste was placed onto the surface and then a Dremel hand tool was used with a cloth polishing attachment to refine the surface to a mirror finish.

2.1.4.Cold Expansion Equipment

The test specimens were cold-expanded using the FTI Split Sleeve Cold Expansion™ method with an FTI 16-0-N cold expansion tooling kit. An FD 200 Power Pack pump, shown in Fig. 10, was used with a 100 psi compressed air line to power the puller as shown in Fig. 11. An FTI small diameter, 30 pound puller was used with an FTI 33-I-02 nose cap and an FTI 16-O-N cold expansion kit to cold-expand each specimen. The nose cap and mandrel setup are shown in Fig. 12. New FTI split sleeves, shown in Fig. 13, were used on each specimen for cold expansion, and the FTI Go-No-Go gauge was used on the mandrel, as well as the hole before and after cold expansion for each specimen. An image of the cold expansion setup used shown in Fig. 14.

To ensure the cold expansion process was performed properly, FTI employee Greg Kimoto instructed the author on the proper FTI cold expansion method. He assisted in the cold expansion of the first two batches of specimens as well.

2.1.5. Imaging and Fractography Equipment

After each specimen failed the fracture surface was cut out of the specimen using a Struers Exotom 150 wet saw. The fracture surfaces were cut out of the specimen such that they could fit easily under a microscope for fractography purposes. An image of the wet saw is shown in Fig. 15.

A Keyence VHX 600 digital microscope was used to take images of the fracture surfaces up to 50X. The Keyence microscope was also used to record a short video of a fatigue crack growing from a hole out to failure of the component. A picture of the Keyence microscope is shown in Fig. 16.

For identifying fatigue nucleation points, viewing striations, and detailed crack front images a JEOL JSM-6490LV Scanning Electron Microscope (SEM) was used. This tool was extremely useful for identifying various characteristics on the fracture surface as it is capable of magnification up to 300,000X. A picture of the SEM is shown in Fig. 17.

2.2. Test Specimens

Three different test specimen configurations were used in the experiments conducted. Two specimens were designed and tested to follow the ASTM E 647 standard, and 24 others were made to model common aircraft geometry. Seven of these 24 were not cold-expanded after precracking to create a baseline condition. The

remaining 17 were cold-expanded after being precracked. A picture of one of the specimens is shown in Fig. 18.

2.2.1. ASTM E 647 Standard Specimens

The test specimen geometry was patterned after the middle tension specimen geometry specifications outlined in Annex 2 of the ASTM E 647 standard.³¹ Two test specimens were designed to expressly follow the specifications of the ASTM E 647 standard to demonstrate accuracy in the manufacturing and testing procedures being used. These specimens were four inches wide, 16 inches long, and one quarter inch thick. These specimens also had a 0.100 inch hole drilled in the center of the specimen with through thickness Electronic Discharge Machining (EDM) notches on both sides of the hole from which cracks were to nucleate. A drawing of these specimens is shown in Fig. 19.

2.2.2. Non-Cold-Expanded Specimens

In addition to the two E 647 specimens, 24 other specimens were made with similar geometry. These 24 specimens were designed to follow the guidelines of the ASTM E 647 standard while incorporating some similitude to aircraft components. Seven of the 24 were not cold-expanded in order to create a baseline condition for comparison with the cold-expanded tests. The primary differences from the non-cold-expanded specimens and the E 647 specimens are a 0.474-0.477 inch initial hole size and an EDM notch on only one corner of the hole. A drawing of the initial geometry for these specimens is shown in Fig. 20.

2.2.3. Cold-Expanded Specimens

The remaining 17 specimens were cold-expanded after being precracked to investigate the effects of cold expansion on a precracked hole. The only geometric difference from the cold-expanded specimens and the non-cold-expanded specimens is that the cold-expanded specimens had 0.63 inch thick aluminum tabs bonded to the specimen ends where the specimens were gripped in the fatigue machine. The purpose of these tabs was simply to protect the test specimen from possible crack nucleations due to the hydraulic grips. A drawing for the initial geometry of the 17 cold-expanded specimens is shown in Fig. 21.

2.2.4. Specimen Identification and Test Matrix

In order to keep track of each specimen throughout the machining, testing, analysis, and fractography processes each specimen was given an identification code. These codes abbreviate non-cold-expanded with NCX, and precracked cold-expanded with PC-CX. The identification code for each specimen was stamped on the both ends of the specimen. Table 2 shows the test matrix for these experiments and the specimen identification for each test that was conducted.

For simplicity and consistency in identifying the orientation of each test specimen during testing and analysis, the primary sides and faces of each specimen were named. The four inch wide face of a specimen was referred to as the “EDM” face if it was the face of the specimen where the notch was located. The face was referred to as “NEDM” if it was opposite face. The side of the specimen, or the half of the specimen, on which side the hole had the EDM notch was referred to as side “A”. Similarly, the side of the

specimen that did not have the EDM notch was referred to as side “B”. A picture of a specimen with the sides and faces labeled are shown in Fig. 22.

2.3. Specimen Preparation

The test specimens were prepared by the Southwest Research Institute (SwRI) in San Antonio, Texas with 0.25 inch 2024-T351 aluminum plate purchased from Kaiser Aluminum. SwRI was responsible for:

1. Cutting and milling specimen dimensions from the plate material
2. Stamping specimen identification on both ends of each specimen
3. Drilling and reaming the initial hole
4. Using EDM to cut a notch in the corner of the hole approximately 0.020x0.020 inches
5. Bonding tabs to the specimens (only applicable to specimens that were cold-expanded.)

The test specimens were then shipped to HAFB in Clearfield, Utah where the author carried out the following procedures:

1. Measured hole diameter, width, and thickness
2. Precracked to 0.050 inch surface crack
3. Performed cold expansion where applicable
4. Performed final hole reaming to 0.5 inch diameter
5. Polished the new hole surface
6. Fatigue cycled to failure

2.4. Test Procedure

2.4.1. Specimen Handling Process

Upon receiving the test specimens from SwRI, the following procedure was carried out for the ASTM E 647 standard specimens:

1. Specimen thickness, width, and hole diameter were measured

2. Specimen was precracked to 0.050 inches at a max load of 11.4 kip and a stress ratio of 0.1
3. Specimen was fatigue tested to failure being paused regularly for visual measurements
4. Fracture surface was cut out from specimen
5. Fracture surface was analyzed under microscope

The following procedure was followed for all of the non-cold-expanded specimens after receiving them from SwRI:

1. Specimen thickness, width, and hole diameter were measured
2. Specimen was precracked to 0.050 inches at a max stress of 20.00 ksi and a stress ratio of 0.1
3. Specimen hole diameter was measured
4. Specimen hole was reamed to 0.50 inches
5. Specimen hole diameter was measured
6. Specimen was fatigue tested to failure being paused regularly for visual measurements
7. Fracture surface was cut out from specimen
8. Fracture surface was analyzed under microscope

Finally, the procedure that was followed for the cold-expanded specimens after receiving them from SwRI:

1. Specimen thickness, width, and hole diameter were measured
2. Specimen was precracked to 0.050 inches at a max stress of 20.00 ksi and a stress ratio of 0.1
3. Specimen hole diameter was measured
4. Specimen was cold-expanded following the FTI Split Sleeve Cold Expansion™ Method
5. Specimen hole diameter was measured
6. Specimen hole was reamed to 0.50 inches
7. Specimen hole diameter was measured
8. Specimen was fatigue tested to failure being paused regularly for visual measurements
9. Fracture surface was cut out from specimen
10. Fracture surface was analyzed under microscope

Each of the above test configuration procedures is summarized in Fig. 23 and Fig. 24.

2.4.2. Fatigue Testing Process

The Instron console for the controller has a feature called Specimen Protect. When this feature is enabled the controller keeps the actuator active and constantly adjusts the actuator to maintain the load on the specimen below some specified value (100 lbs for this research). The Specimen Protect feature was used whenever a specimen was inserted or removed from the load frame to prevent extraneous/unknown loads on the specimen.

To install a specimen in the load frame the frame crosshead was locked, and the actuator was moved to an approximate height for gripping the specimen. Specimen Protect was turned on, and both grips were opened. The specimen was then slid in between the grip wedges such that the EDM face of the specimen was facing the operator and the side A was on the operator's right hand side. The top of the specimen was then aligned with the top of the grip wedge, and the sides of the specimen were also lined up with the sides of the grip wedges (the grip wedges were four inches wide). While the specimen was held in this position the top grip was closed. A picture of a specimen properly aligned in the wedges is shown in Fig. 25. After the top grip was closed the operator verified that the specimen was straight by verifying that the sides of the specimen were lined up with the sides of the bottom wedge grips as well as the sides of the top wedge grips. The actuator was adjusted so the bottom of the specimen lined up with the bottom of the lower grip wedge, and the bottom grip was then closed.

Once the specimen was properly inserted into the load frame the Specimen Protect feature was turned off, and the controller was transferred to load control. The tuning parameters were checked and adjusted if necessary. Some tests were cycled

briefly to identify proper tuning parameters. The specimen was then loaded to the mean load, and baseline measurements were taken for the EDM size, and crack size (if precracked). The load was then returned to zero pounds, and all necessary testing parameters were put into the software. The test was then started and ran continuously until failure, except when paused by the operator for visual measurements.

All constant amplitude tests were run at a stress ratio of 0.1 and a constant frequency of 20 Hz. All specimens were also precracked under constant amplitude loading at a stress ratio of 0.1 and a frequency of 20 Hz. The stresses at which specimens were precracked varied based on the max stress of the final testing for that specimen, but most were precracked at a max stress of 20.00 ksi.

All spectrum loading tests were done at a constant load rate of 500,000 lbs per second. In other words, the frequency varied throughout the test for spectrum loading because high loads would take longer to reach than low loads. Although the constant load rate would indicate a triangular wave form, the Instron Random Loading software automatically smoothed the waveform to be more sinusoidal. An image of the command and feedback from one of the tests is shown in Fig. 26.

2.4.3. Reaming Process

After precracking was completed each specimen was reamed. Cold-expanded specimens were cold-expanded first and then reamed. The same eight flute reamer was used to ream each specimen. To set up the reaming, a specimen was first mounted securely to the mill with the EDM face up. In other words, the reamer entered the specimen from the EDM face. This was done so that the chatter from the reamer entering

the hole would occur on the EDM side, where a crack already existed. It was assumed that since a crack was already present on the EDM face, any chatter induced by the reaming process would not nucleate and grow another crack.

The drive shaft of the mill was then centered over the existing hole to within 0.005 inches. The table was then locked into place, and the mill was turned on. The reamer was gently lowered through the hole, and once the reamer had penetrated the entire thickness of the specimen the mill was shut off and the reamer was raised only after the spindle had come to a complete stop. This was done to prevent pulling any cut material back through the hole and gouging the bore of the hole. This method does, however, sometimes cause lines from the reamer flutes to be inscribed on the bore as shown in Fig. 27. These lines were generally removed during polishing.

2.4.4. Cold Expansion Process

For cold expansion an FTI FD 200 PowerPak hydraulic pump was hooked up to a 100 psi compressed air line for power. The pump was then connected to an FTI small diameter 30 lb. puller with a nose cap adapter (part 33-I-02) for the 16-O-N mandrel. For consistency the puller was mounted in a vice, and a new FTI 16-O-N split sleeve was slid onto the mandrel. The test specimen was then slid onto the mandrel, over the split sleeve, with EDM face of the specimen facing out, or toward the cold expansion entrance side, and with the split sleeve 90 degrees to the left of the EDM notch. The trigger on the puller was then pulled and held down until the mandrel had retracted completely through the material.

2.5. Test Matrix

The original test matrix outlined for this research is shown in Table 2. This matrix was selected to investigate the effects of cold expansion on a cracked fastener hole under spectrum loading at maximum stresses of 25.00 and 33.00 ksi, and the effects of cold expansion of a cracked fastener hole under constant amplitude loading at maximum stresses of 20.00 and 25.00 ksi. The spectrum stress levels were selected from the maximum and minimum stress levels observed at a critical point on the A-10 aircraft.³⁴ The constant amplitude stress levels were selected so that the results of this research could be compared with the results from Carlson's work to quantify the benefit of a clean, or uncracked, cold-expanded hole compared to a 0.050 inch precracked cold-expanded hole.²⁶

As testing continued it was observed that the 25.00 ksi maximum stress level for cold-expanded specimens under spectrum loading was sufficiently low that those tests would either need to be truncated or eliminated to complete testing in a timely manner. Furthermore, it became of interest to investigate the 43.25ksi maximum stress level, as that is the maximum stress observed in A-10 wing panels.³⁴ (The actual max stress measured in the wing was 43.252 ksi. However, the load cell used is only accurate to ± 20 lbf. Therefore 43.25 ksi was used in this report.) It also came of interest to investigate the 30.00 ksi stress level for cold-expanded, spectrum loaded specimens as that is the maximum stress observed at a half inch diameter hole under A-10 wing spectrum loading.³⁴ As a result, many of the specimens originally intended to be spares and 25.00 ksi cold-expanded spectrum tests were tested at the 30.00 ksi and 43.25 ksi maximum stresses. The revised test matrix is shown in Table 1.

As the original test plan did not include the 30.00 or 43.25 ksi stress levels, and by the time it was decided to investigate these stress levels all of the non-cold-expanded specimens had been tested. It was decided to take one specimen which was intended to be cold-expanded, but had not yet been cold-expanded, and use it as a non-cold-expanded baseline test for the 43.25 ksi stress level. A baseline for the 30.00 ksi stress level was interpolated from the 25.00 ksi and 33.00 ksi stress levels.



Fig. 6 Fatigue Machine Equipment

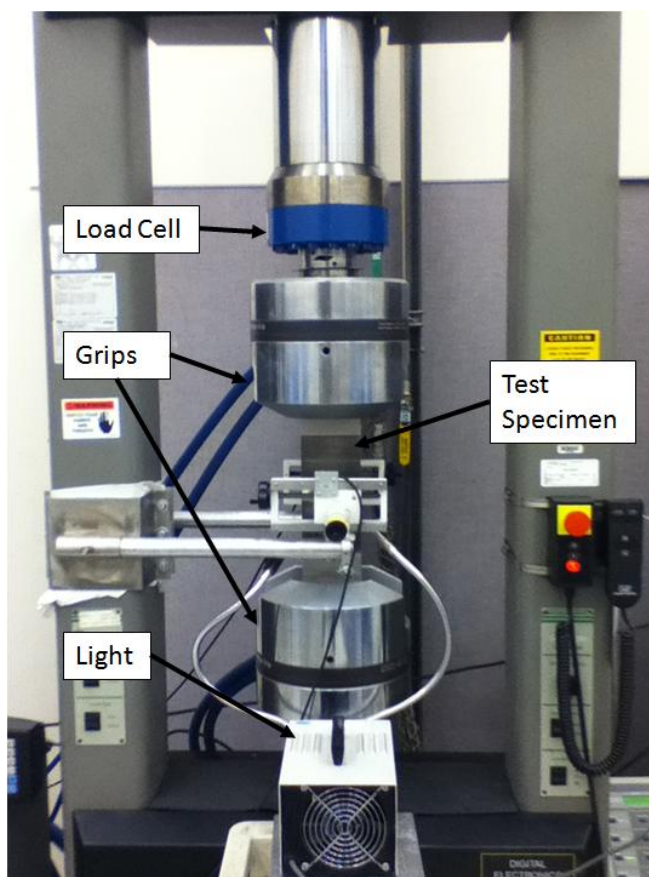


Fig. 7 Load Frame Equipment

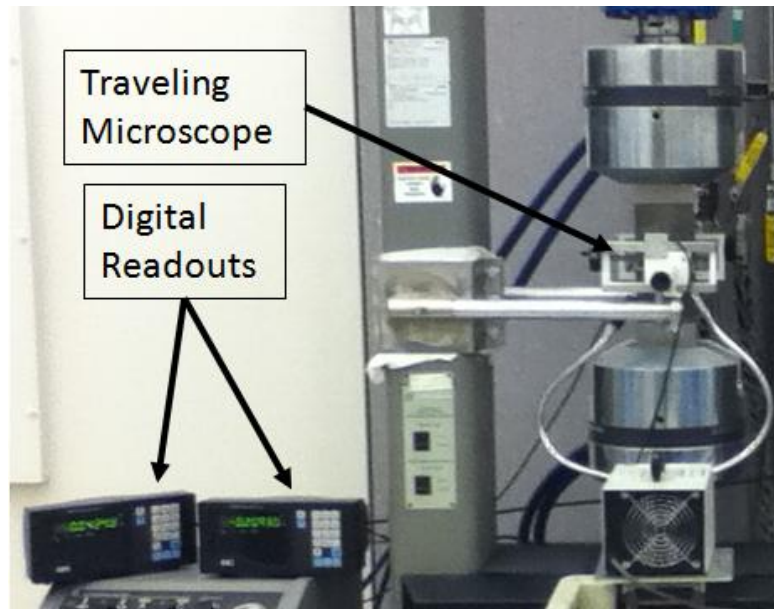


Fig. 8 Crack Measurement Equipment

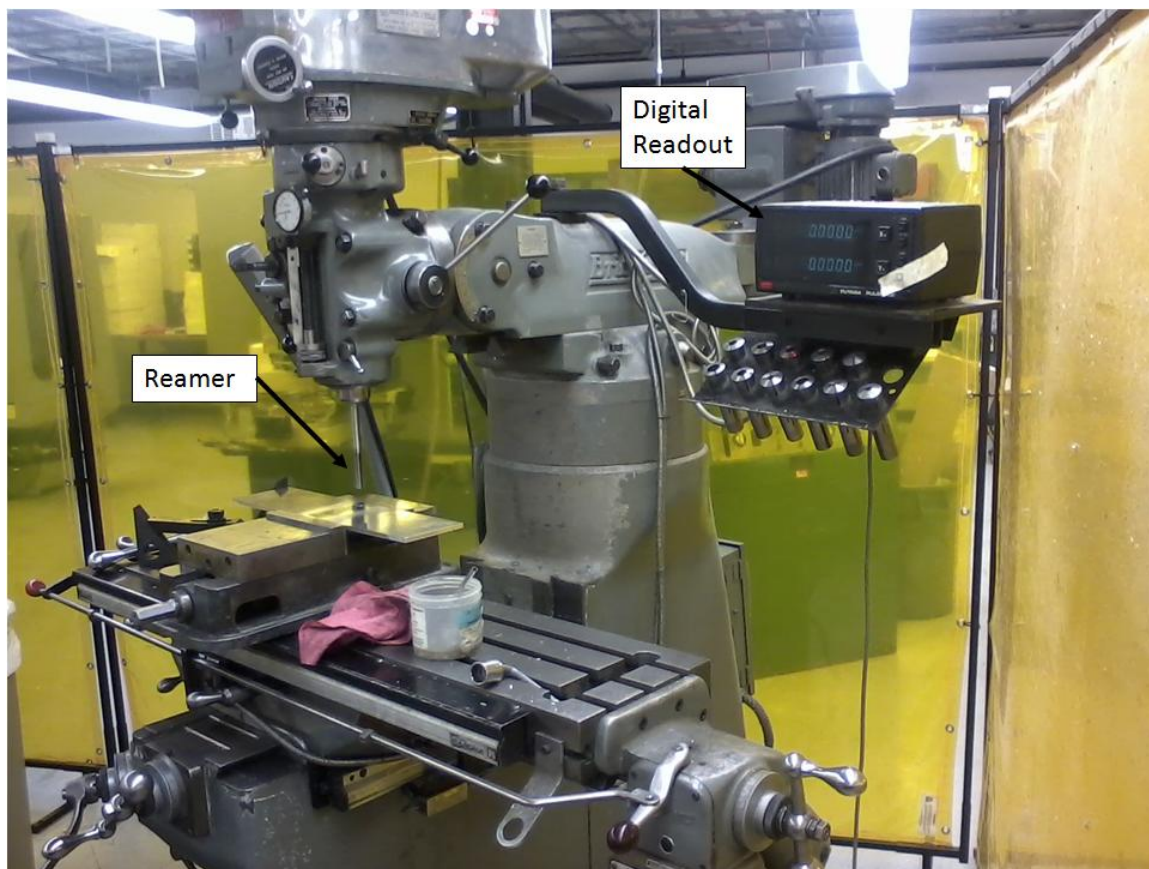


Fig. 9 Milling Machine for Reaming Final Diameters



Fig. 10 FTI Hydraulic PowerPak for Cold Expansion



Fig. 11 Cold Expansion Gun Mounted in Vice

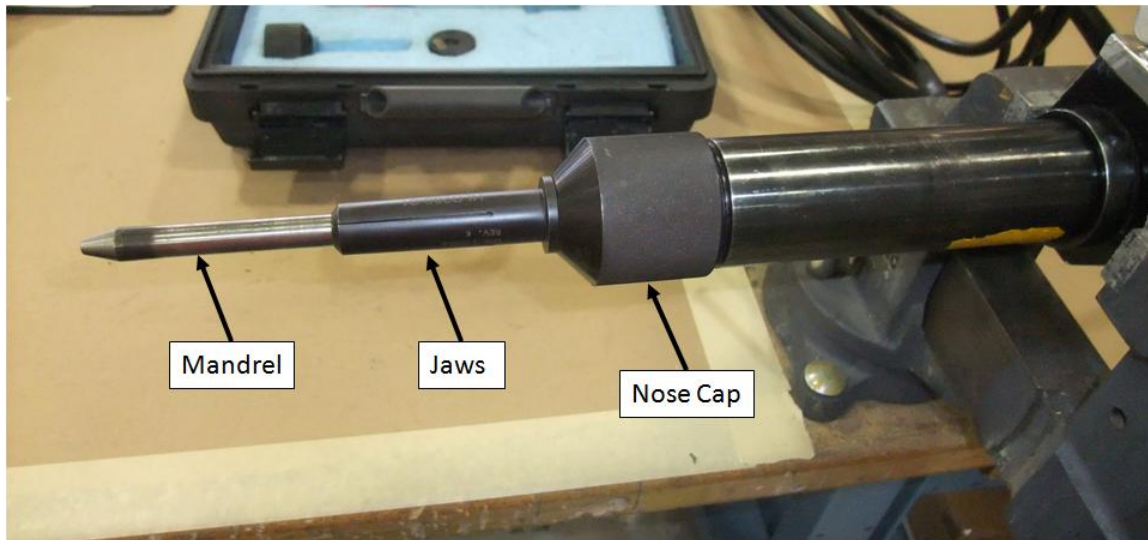


Fig. 12 Cold Expansion Mandrel Assembly



Fig. 13 Cold Expansion Split Sleeves



Fig. 14 Cold Expansion Setup and Process



Fig. 15 Exotom 150 Wet Saw



Fig. 16 Keyence Digital Microscope



Fig. 17 Scanning Electron Microscope

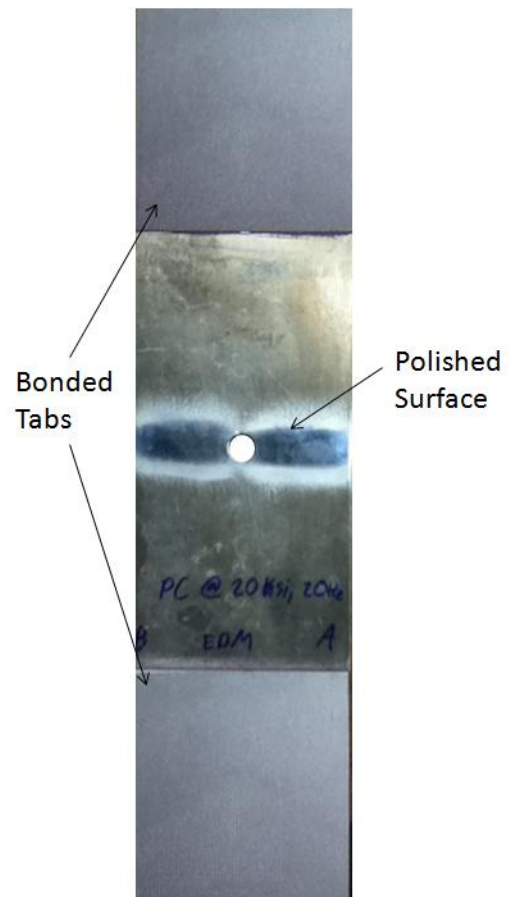


Fig. 18 Test Specimen with Bonded Tabs

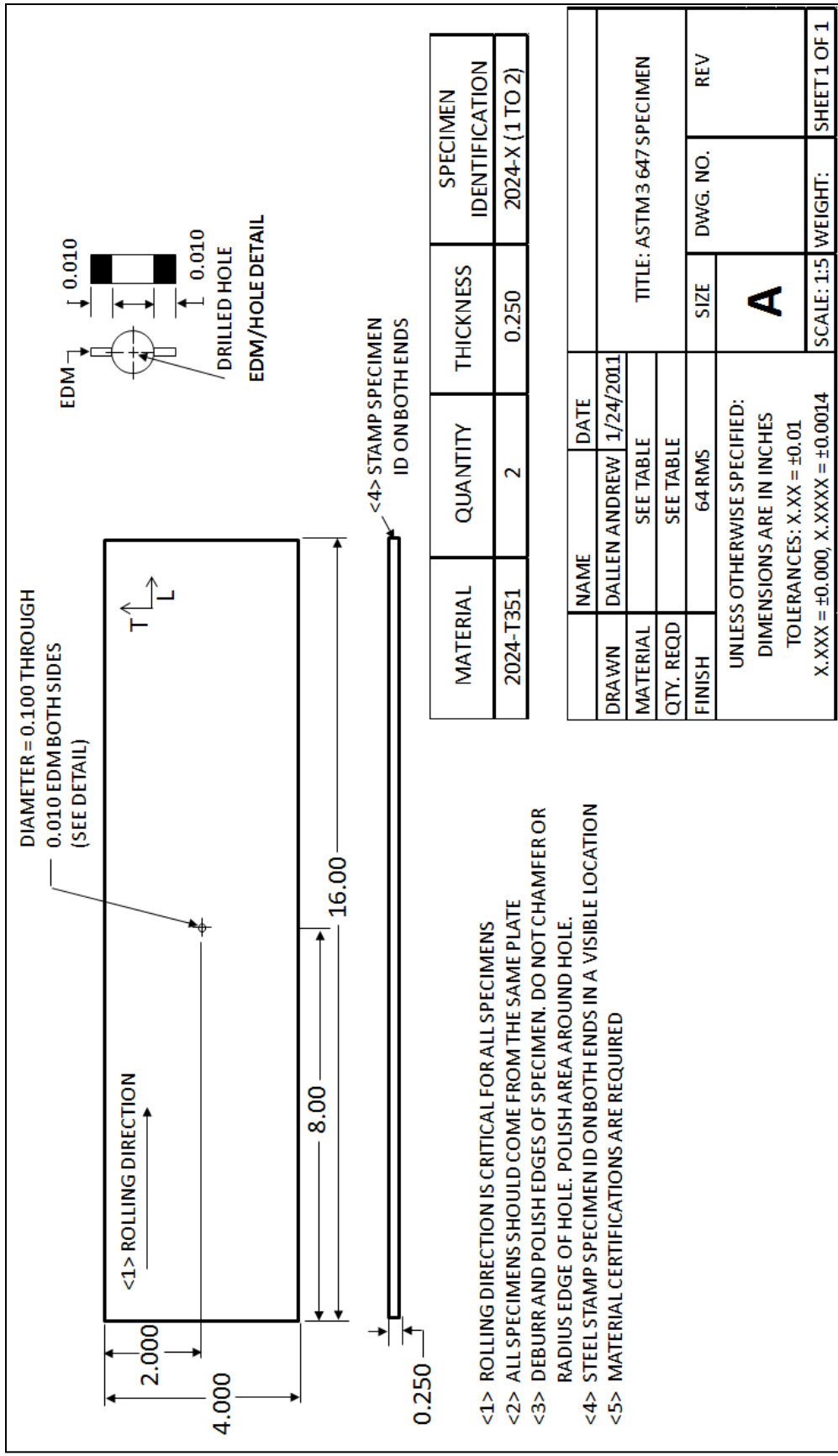


Fig. 19 ASTM E 647 Standard Specimen Drawing

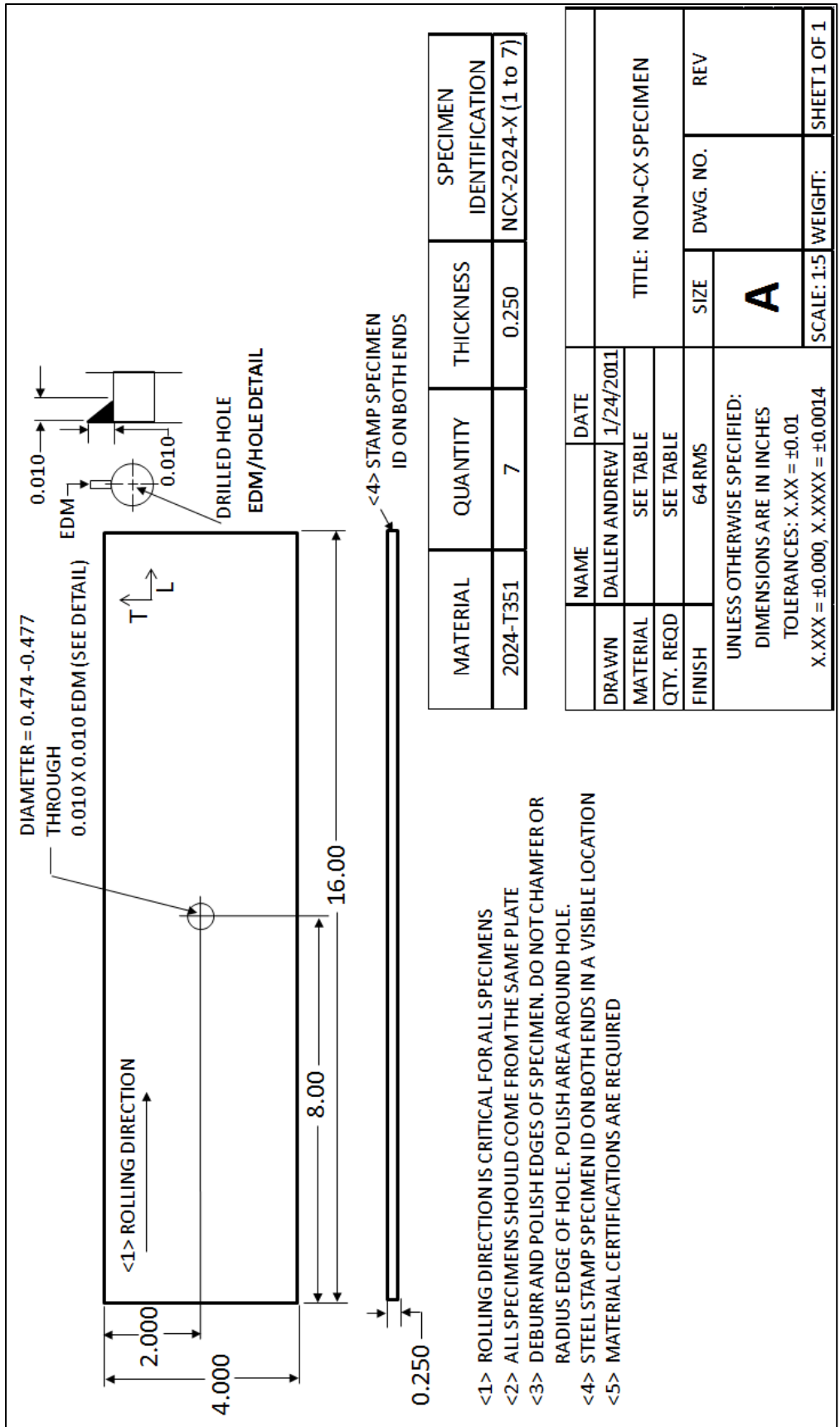


Fig. 20 Non Cold Expanded Specimen Drawing

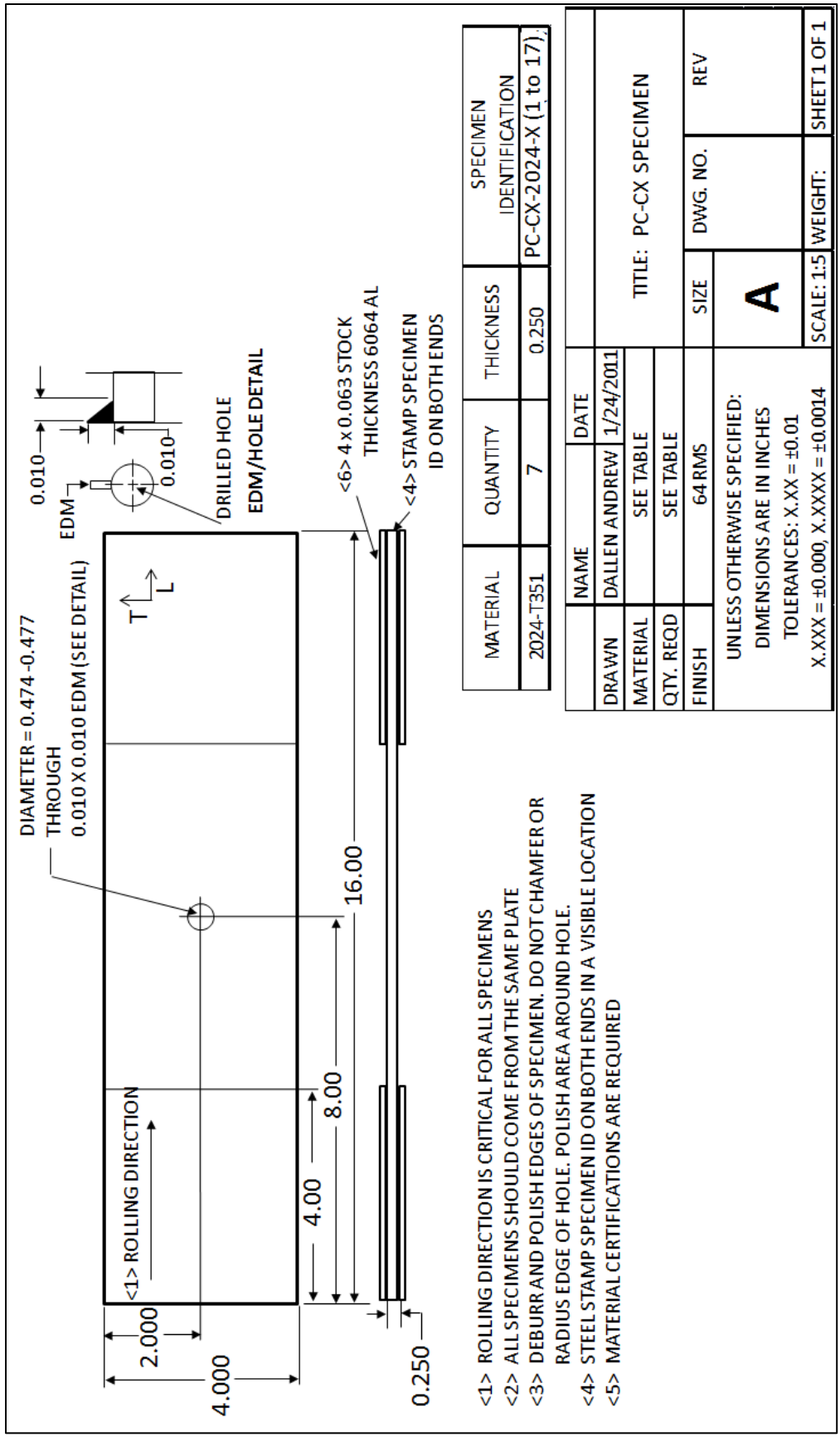


Fig. 21 Cold Expanded Specimen Drawing

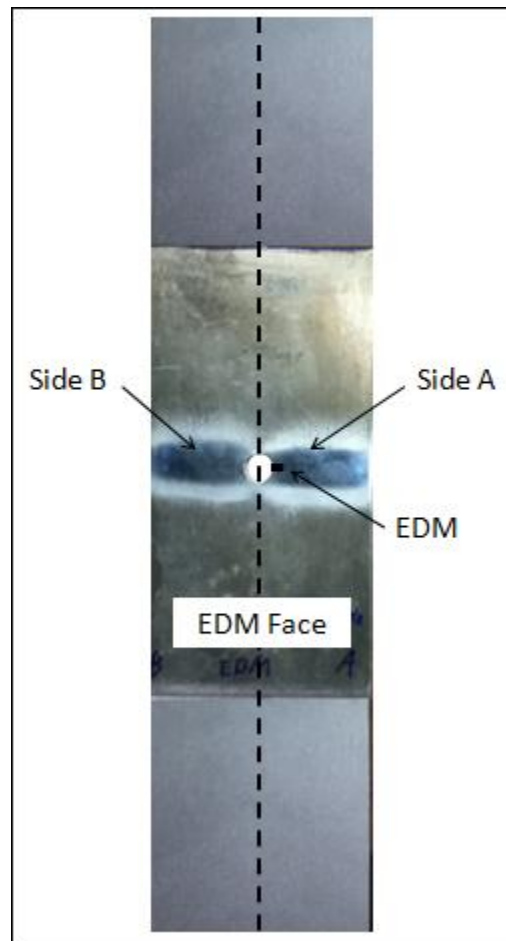


Fig. 22 Specimen Orientation Pattern

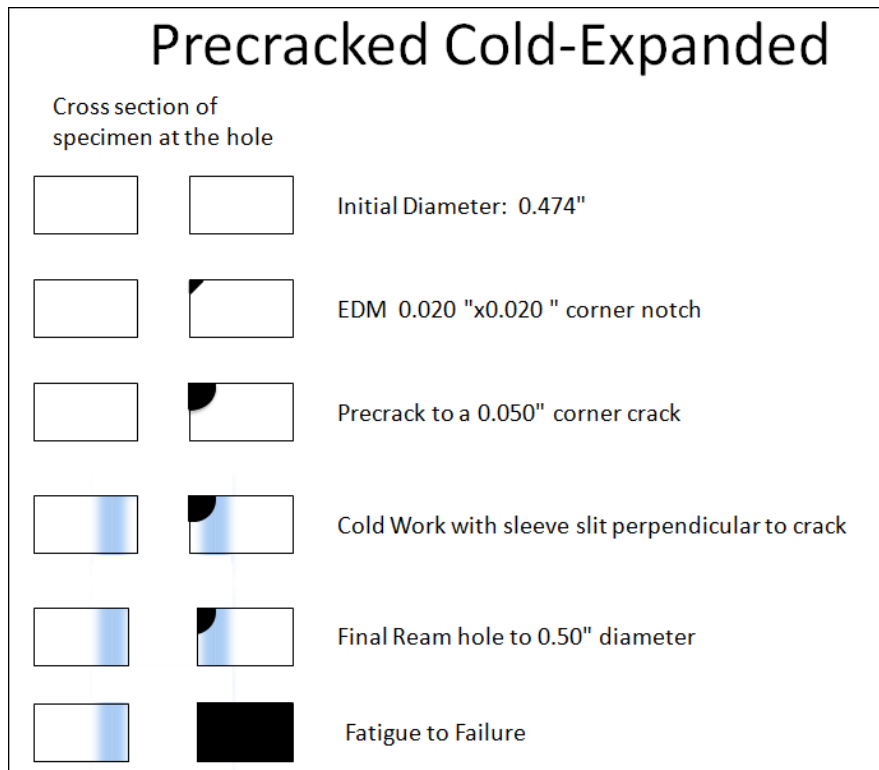


Fig. 23 Precracked Cold-Expanded Specimens

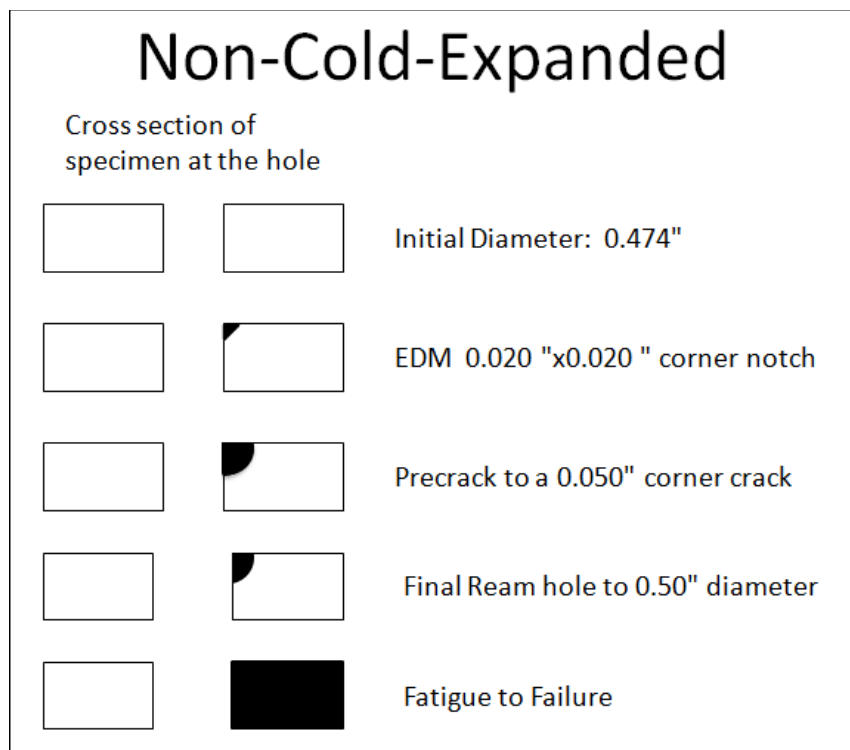


Fig. 24 Non-Cold-Expanded Specimens

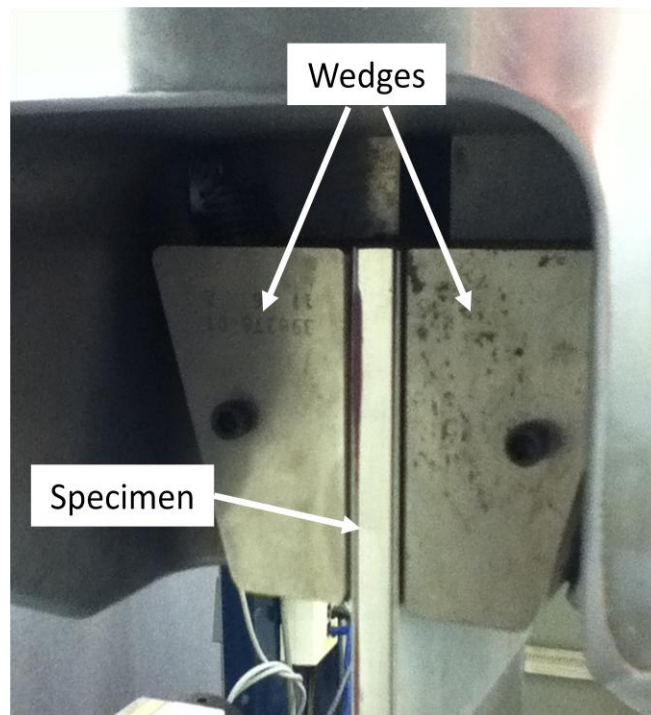


Fig. 25 Specimen Alignment in Wedges

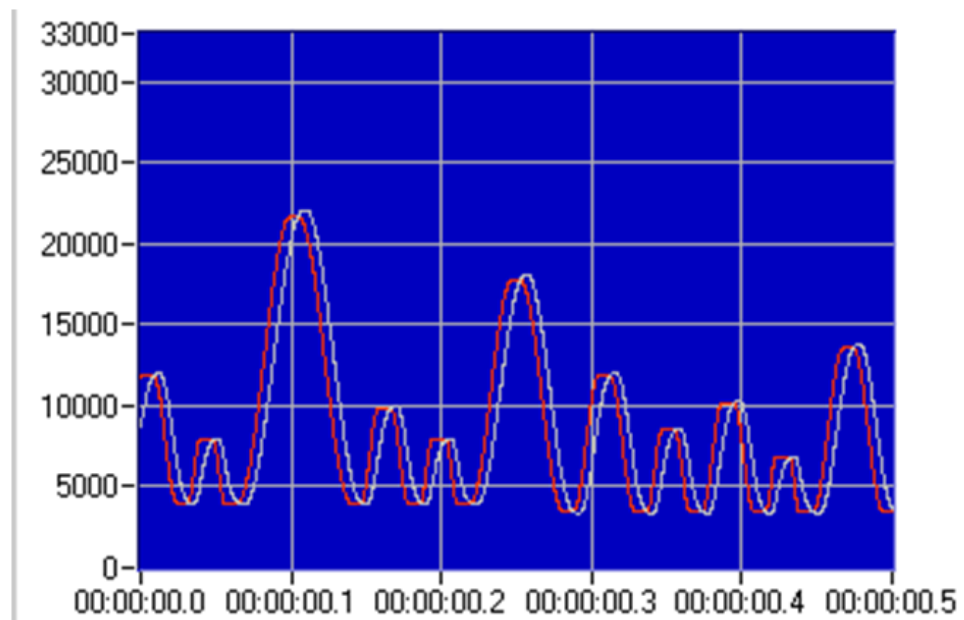
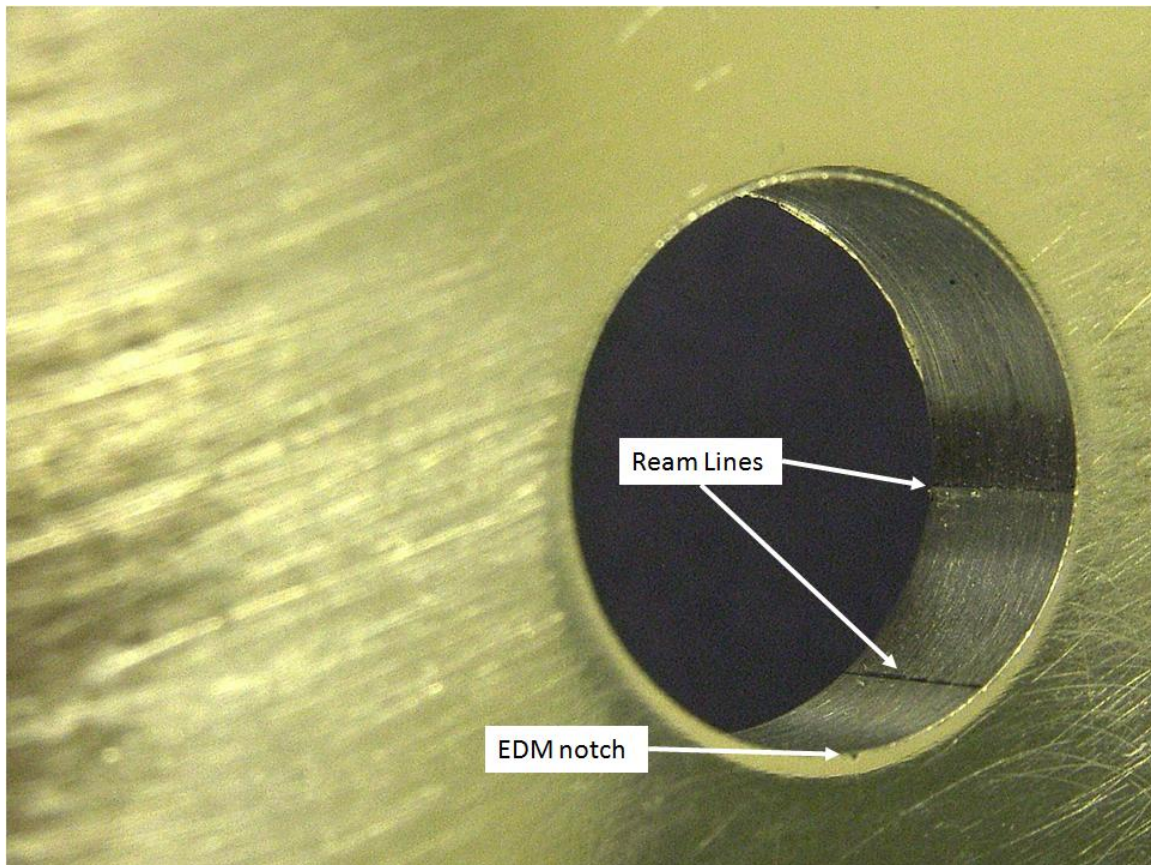


Fig. 26 Command (red) and Feedback (white) of Waveform for Spectrum Loading

Table 2 Original Test Matrix

CX/NON-CX	CA or Spectrum	Peak Stress (ksi)	Specimens		Specimen ID's
			Tested	Spares	
NON-CX	CA (ASTM E647)	11.25	2	0	2024-1;-2
NON-CX	Spectrum	25.00	2	1	NCX 2024-1;-6
		33.00	2	1	
CX	CA	20.00	4	1	PC-CX 2024-9;-18
		25.00	4	1	
	Spectrum	25.00	3	1	PC-CX 2024-1;-8
		33.00	3	1	

**Fig. 27 Ream Lines**

3. DATA COLLECTION AND ANALYSIS

3.1. Measurement Procedure

The two traveling microscopes were used to measure the cracks on five surfaces. One microscope was mounted in front of the EDM face of the specimen to track the cracks on both sides of the EDM face. The second microscope was cocked at angle at the beginning of a test and during precracking to measure the crack in the bore of the specimen on side A. Once the crack had grown through the bore to the NEDM face, that microscope was readjusted to track cracks growing on both sides of the NEDM face.

3.1.1. Measurement Recording

To measure the cracks the test was paused, and the load was held at the mean load (or for spectrum at the current load when the test was stopped). The number of cycles or segments was recorded, and then the operator scrolled the microscope to the edge of the hole, zeroed the digital readout, and scrolled carefully to the crack tip. The value reported on the digital readout was recorded, and the operator performed the same procedure for each tracked surface of the specimen. An important thing to note is that the digital readout was zeroed for each measurement, thus eliminating any induced error by the microscope being moved.

After the measurements were recorded the microscope on the EDM face was scrolled 0.020 inches ahead of the crack tip on side A to provide an approximation of the next point at which the test would be paused to measure the crack lengths. The test was then resumed.

3.1.2. Bore Measurement Calculations

To track crack lengths down the bore of the hole on side A the microscope facing the NEDM face was adjusted to be pointing down the bore of the hole at some angle. This allowed the operator to see and measure values that represented the crack length in the bore of the hole.

To convert the measured values to actual surface distances in the bore of the hole the following trigonometric conversion was done. The angle of the microscope to the bore surface was derived by measuring the apparent thickness of the bore as seen through the microscope, this value is represented in Fig. 28 as “D”. Since the actual thickness (B) was previously known, the angle θ can then be found easily using the relationship:

$$\sin(\theta) = \frac{D}{B} \quad (2)$$

Once the angle has been calculated a similar procedure can be used to find the actual crack length. A crack in the bore will appear in the scope as the distance “a” shown in Fig. 29. Since the angle θ was previously determined, the only unknown quantity in the triangle shown in Fig. 29 is the actual bore crack length “c”. This quantity can be found by using the relationship in Eq. 4.

$$c = \frac{a}{\sin(\theta)} \quad (3)$$

The procedure described above was used to calculate each crack length measured in the bore for every specimen tested.

3.2. Time to Failure

The recorded measurements were plotted along with the number of cycles or segments to generate crack length vs. time curves (a vs. N curves) for each specimen tested. These plots are commonly used and are very useful for identifying how crack length and time affected the crack growth rate of the test specimen at each stress level. Combine plots of a vs. N curves for non-cold-expanded and cold-expanded specimens were also generated to demonstrate the effects and benefits of cold expansion. Examples of these plots for constant amplitude loading as well as spectrum loading for non-cold-expanded and precracked cold-expanded tests are shown in Fig. 30, Fig. 31, and Fig. 32 respectively.

For constant amplitude tests the time to failure was reported in cycles, as recorded by the cycle counter on the Instron software system used. For spectrum loading tests the software provided a count of the number of segments run in the test. A segment is a single point load, a peak or a valley. The spectrum file used for testing contains 14736 segments, and is equivalent to 240 flight hours.³⁴ Thus, the time to failure for all spectrum loading tests were converted from segments into flight hours using the formula below.

$$\# \textit{Flight Hours} = (\# \textit{of Segments}) * \frac{240 \textit{ flight hours}}{14736 \textit{ Segments}} \quad (4)$$

3.3. Crack Growth Rate

The test data obtained from constant amplitude tests were also used to generate crack growth rate data. The ASTM E 647 standard recommends one of two methods for calculating the crack growth rate from the measured data. The two methods recommended in the standard are the secant method and the incremental polynomial method. The secant method was used for this research. The secant method, “simply involves calculating the slope of the straight line connecting two adjacent data points on the a versus N curve.”³¹ The mathematical relationship for calculating the crack growth rate using the secant method is:³¹

$$\left(\frac{da}{dN} \right)_a = \frac{a_{i+1} - a_i}{N_{i+1} - N_i} \quad (5)$$

The stress intensity factor range, ΔK , was calculated for the average crack size at each point as well. Values for β at each crack length were obtained using AFGROW software. The stress intensity factor range for the average crack size was then calculated using the relationship:

$$\Delta K = \Delta \sigma * \beta \sqrt{\pi a} \quad (6)$$

The crack growth rate was plotted against the calculated value of the stress intensity factor range, ΔK , for the average crack size, as the crack growth rate calculation

under the secant method is also an average crack growth rate. A crack growth rate vs. stress intensity factor range (da/dN vs. ΔK) plot was then created as shown in Fig. 33.

3.4. AFGROW Simulations

AFGROW is a very powerful crack prediction software tool that allows the user to predict crack growth for a wide variety of geometry and loading situations. The guidelines followed for conducting the AFGROW analyses in this research are the same guidelines used by the A-10 USAF ASIP group for damage tolerance analysis.^{35,36}

3.4.1. ASTM E 647 Baseline

The most simple fatigue crack growth prediction model is a through crack in a wide plate as the only correction factor is a finite width correction. The ASTM E 647 standard geometry somewhat patterns this geometry by creating a small hole in a plate with notches on both sides of the hole. Therefore, the E 647 standard test specimens were used as a baseline for the AFGROW Internal Through Crack prediction model as no cold expansion, spectrum, or geometry effects were incorporated into the prediction model.

3.4.1.1. Tabular Lookup File

AFGROW allows for a number of simulation models to predict crack growth. The prediction method used for this research uses a tabular lookup file to determine the crack growth for the given stress state. This lookup file contains the crack growth rate data for two stress ratios and then AFGROW interpolates or extrapolates that data for all

other stress states. For this research the tabular lookup file for crack growth rate data at a stress ratio of 0.1 was obtained from the E 647 test specimen data. The data for the second stress ratio was obtained from a standard lookup file used by the A-10 USAF ASIP group at a stress ratio of 0.8.

In creating the tabular lookup data for the stress ratio of 0.1 a lookup file was created that produced conservative predictions for all but one of the E 647 tests performed. This lookup file is the lookup file that was used by Andrew in his work on short edge margin holes.²⁵ The author created another lookup file that yielded predictions with a smaller percent of disagreement from the test data, however, half of the predictions were not conservative. A plot of the test data and the AFGROW predictions using the two lookup files are shown in Fig. 34 and Fig. 35. It was decided beneficial to run prediction models with both lookup files for comparison of scatter effects and variation in prediction results from different lookup files. For simplicity in referencing these two lookup files the lookup file used in the work by Andrew will be referred to as “lookup file A”, and the lookup file created by the author will be referred to as “lookup file B” for the remainder of this paper.

3.4.1.2. Standard E 647 Baseline Prediction Model

To validate the tabular lookup files generated from crack growth rate data, AFGROW models were created with the measured geometry values for each specimen. A prediction was then run for each specimen using the tabular lookup files, and the predictions were compared to the tested life of the specimen to quantify the agreement between prediction and test. The average percent agreement between prediction and test

using the lookup file A was 11.88%, and the averaged percent agreement using lookup file B was -1.03%, with a negative percentage indicating an unconservative prediction. The tested life and the predicted life for all E 647 tests are reported in Table 3.

AFGROW predictions were also obtained for prediction techniques other than the tabular lookup file, including the Forman and NASGRO equations. However, the tabular lookup file predictions had a far greater percent agreement with test data than the other prediction techniques. As a result only the tabular lookup file predictions are analyzed in this research.

3.4.2. Geometry Baseline

With the material tabular lookup file established the next step was to create a baseline for the test geometry. The test geometry of all other specimens in this research incorporated a 0.50 inch diameter hole in the center of the specimen with a corner crack. A baseline was needed to compare the agreement of prediction for this geometry with test. Two tests from Scott Carlson's research were selected for this baseline as they were tested under constant amplitude loading and were not cold-expanded.²⁶ The tests from Scott Carlson's research also had the same geometry as the tests performed in this research.

A key parameter for any corner crack is the aspect ratio. The aspect ratio is the ratio of the crack length down the bore to the crack length along the surface of the specimen, as depicted in Fig. 36. For corner crack predictions, AFGROW allows the user to maintain the aspect ratio constant for the prediction, or to allow AFGROW to vary the

aspect ratio as the crack grows. The user can average the crack lengths before entering them into AFGROW to create an aspect ratio equal to one.

In order to assess whether the aspect ratio should be held constant or not, and whether or not the crack lengths should be averaged, predictions were run for each scenario. It was found that the greatest agreement between prediction and test was obtained when the crack lengths were averaged and the aspect ratio was held constant. This same conclusion was found by Dallen Andrew in his research.²⁵ As a result this method was used for all predictions in this research. The average percent disagreement between prediction and test for this method using lookup file B was 6.58%. The predictions for each variation of the aspect ratio and crack length using lookup file B is shown in Table 4.

3.4.3. Spectrum Baseline

The final baseline for AFGROW predictions was the spectrum retardation effects. AFGROW offers a number of retardation models. The retardation model most commonly used by A-10 ASIP is the Generalized Willenborg model. The AFGROW help file describes the approach.³⁷

The Willenborg model uses an ‘effective’ stress intensity factor based on the size of the yield zone in front of the crack tip to account for the effect of load sequence on crack growth rate. ... The Generalized Willenborg retardation model is one of the most commonly used retardation models in crack-growth life prediction programs. The model is based on early fracture mechanics work at Wright-Patterson AFB, OH and was named after a student who worked on the model. The model uses an ‘effective’ stress intensity factor based on the size of the yield zone in front of the crack tip.³⁷

The Generalized Willenborg model uses an input parameter called the Shutoff Overload Ratio (SOLR). The SOLR parameter controls the retardation effects on the prediction. A smaller SOLR causes greater growth retardation, and therefore a greater predicted life.

In order to identify the proper SOLRs for the tests conducted in this research, AFGROW predictions were run for each test (that was spectrum loaded and not cold-expanded) at varying SOLR values until the optimum SOLR for each stress level was identified. This was done using both lookup files A and B, as well as the standard A-10 lookup file to verify the trend in SOLRs between stress levels. The optimum SOLR values found for each specimen are shown in Table 5, and the average SOLR values for each stress level are shown in Table 6. It should be noted that as there were not any non-cold-expanded specimens tested at the 30.00 ksi maximum stress level, the SOLR was interpolated from the 25.00 ksi and 33.00 ksi average SOLR values.

To further analyze which lookup file and SOLR was in most agreement with the test data, plots were created of the test data and AFGROW crack growth prediction data to compare curve fits. It was observed that lookup file A always had the greatest agreement of curve shape with the test data as seen in Fig. 37.

The trend for SOLR values typically used by the A-10 ASIP group decrease with increasing stress. This means that greater retardation is included into models with higher stress levels. This same trend, however, was not observed in the SOLR values derived for this research, as the SOLR for the 43.25 ksi test prediction was the greatest for any given lookup file used. This change in the trend of SOLR values was attributed to the conservative nature of the standard A-10 lookup file. The baseline E 647 tests performed

for this research demonstrated a slight “knee” in the upper region of the da/dN vs. ΔK chart as shown in Fig. 38. Lookup file A and lookup file B were modified to capture this feature of the da/dN vs. ΔK relationship, while the standard A-10 lookup file simply maintains a nearly constant slope through that region. It was, therefore, concluded, that the standard A-10 lookup file needed greater retardation effects at higher stresses to compensate for the conservative crack growth rate at such stress levels.

3.4.4. Cold-Expanded Predictions

The current USAF approach to account for the retardation effects of corner cracks in fastener holes due to cold expansion is to change the assumed initial flaw size (IFS) to 0.005 inches.³⁸ As a result, all predictions for cold-expanded specimens in this research used the IFS of 0.005 inches independent of the actual initial flaw size.

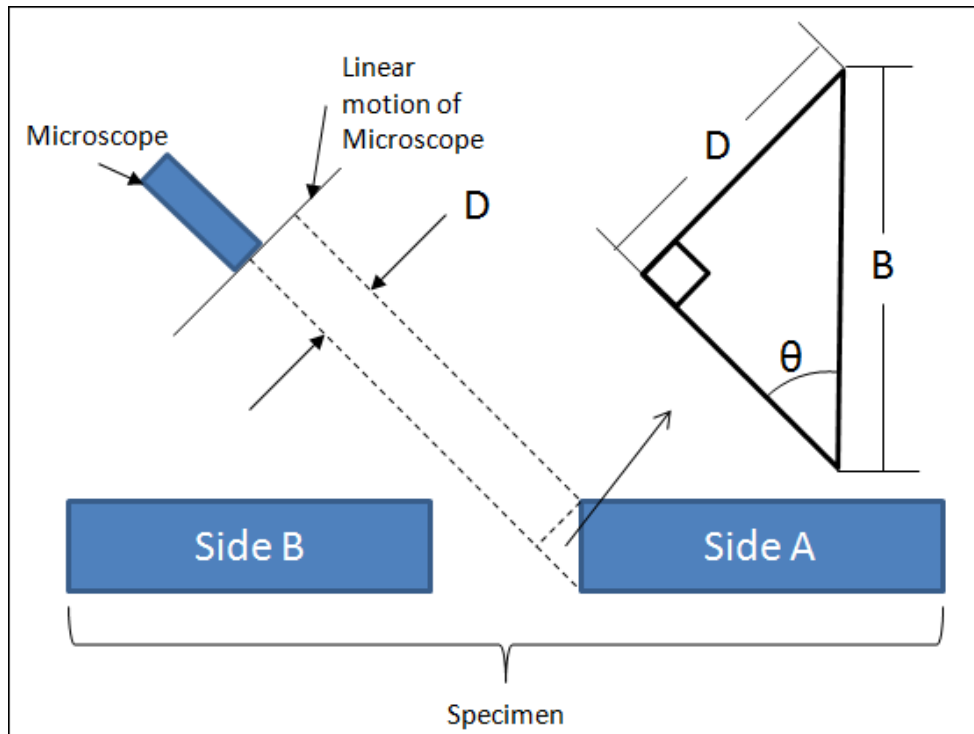


Fig. 28 Bore Measurement Setup, How to Find Angle θ

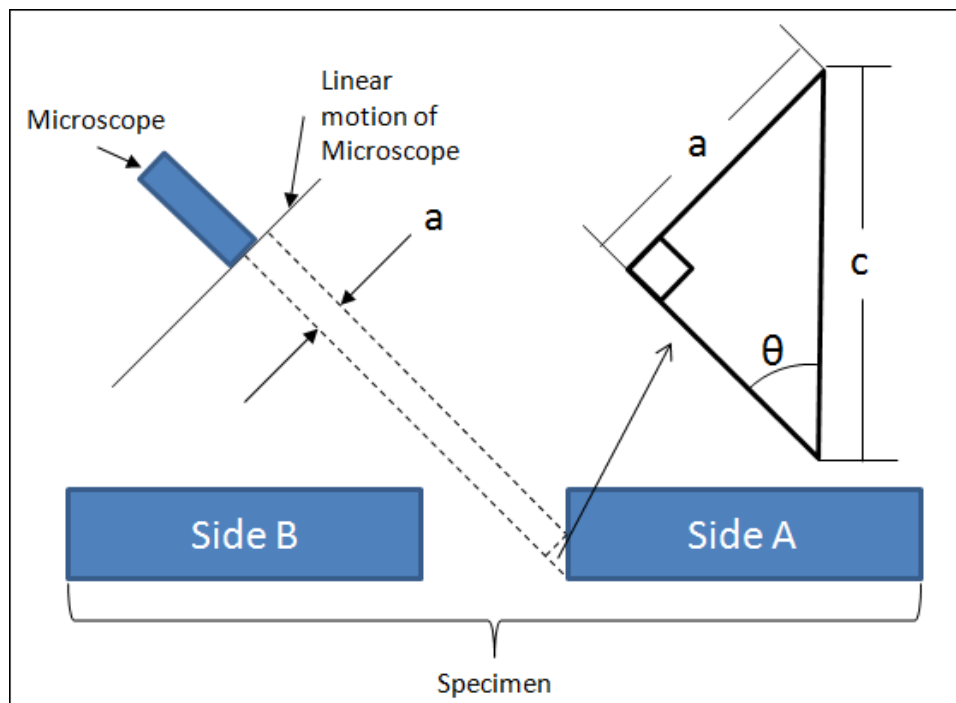


Fig. 29 Bore Measurement Setup, How to Find Crack Length "a"

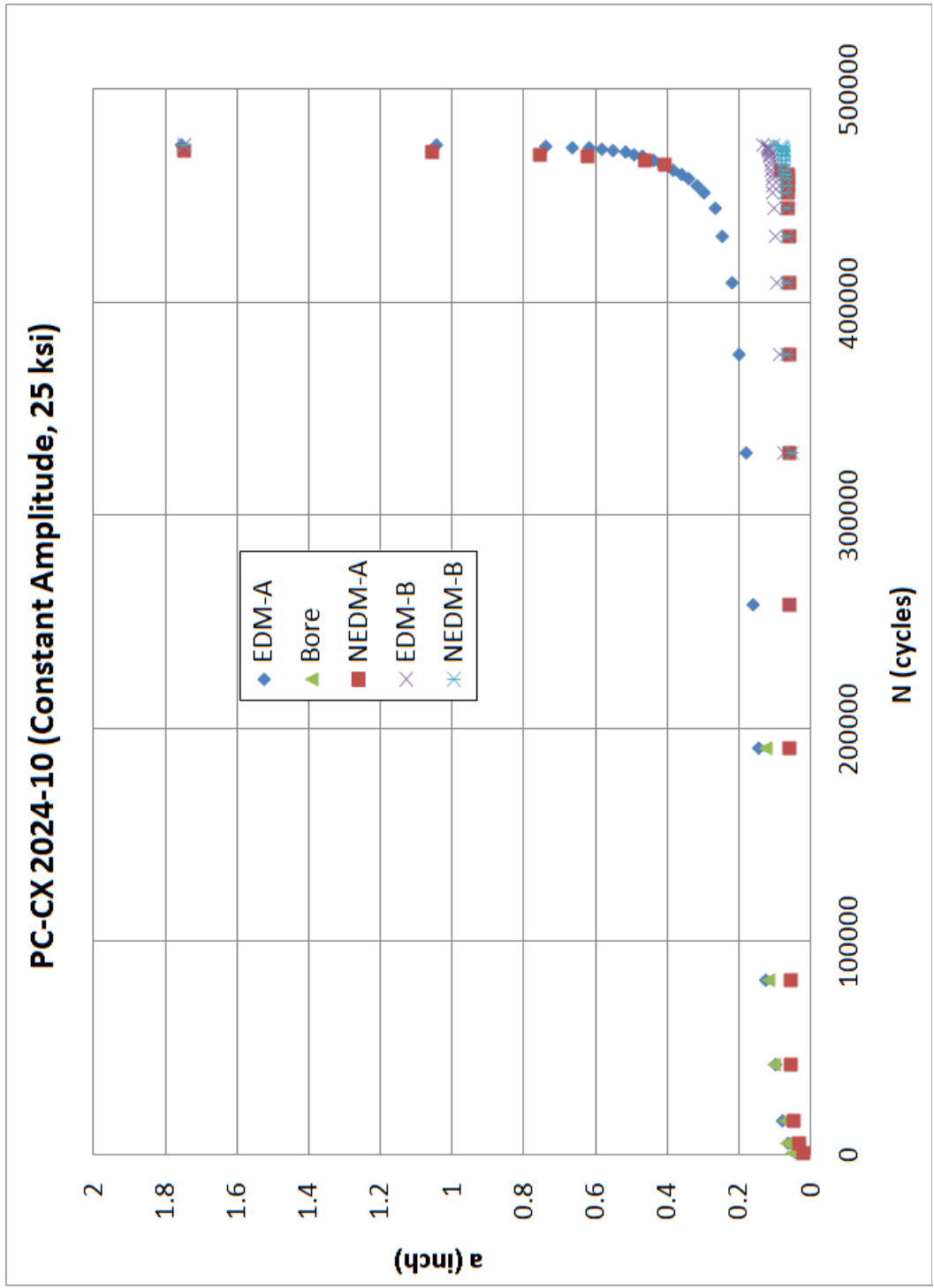


Fig. 30 a vs. N plot for a Precracked Cold-Expanded Test under Constant Amplitude Loading

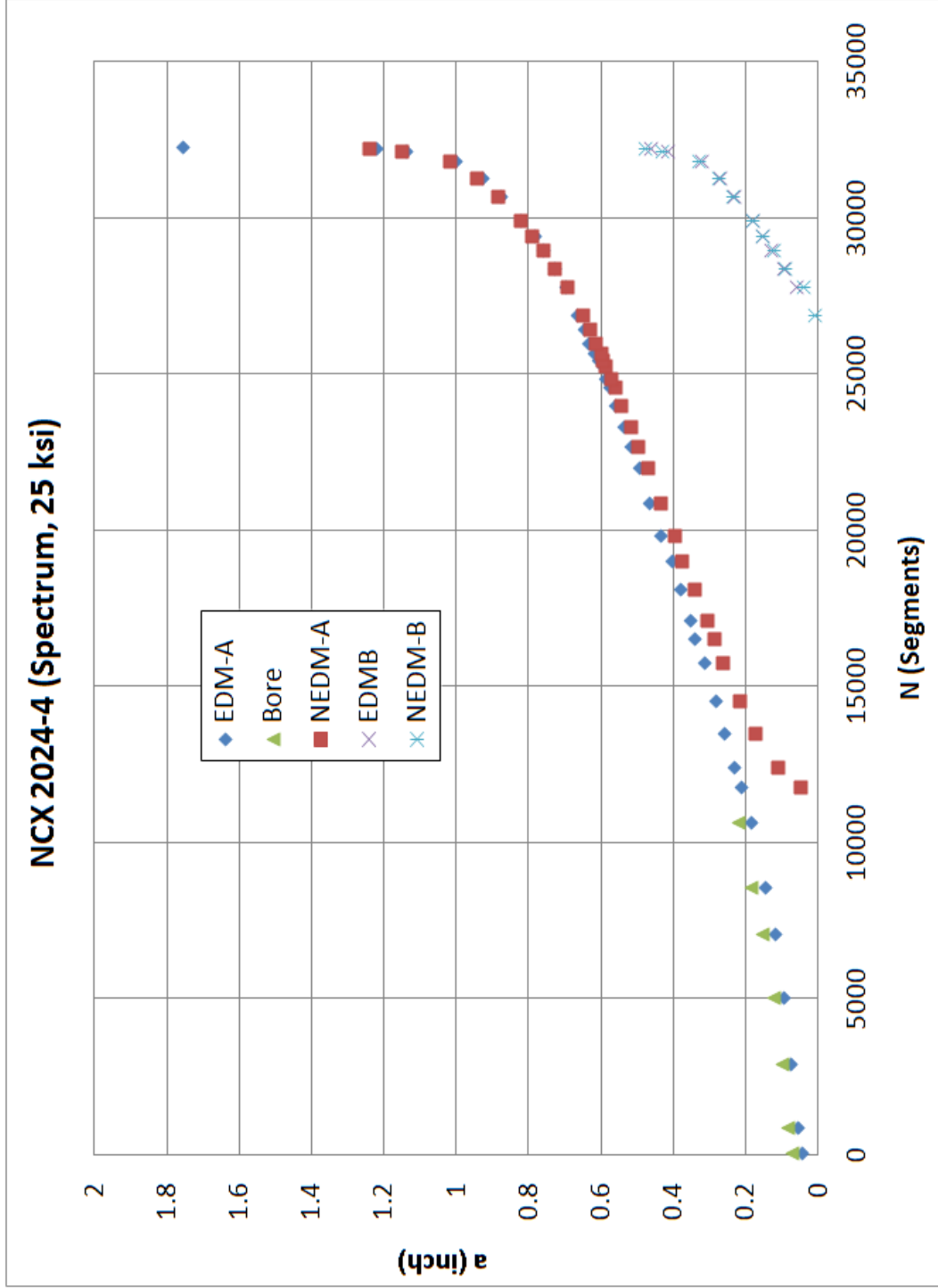


Fig. 31 a vs. N Plot for a Non-Cold-Expanded Test under Spectrum Loading

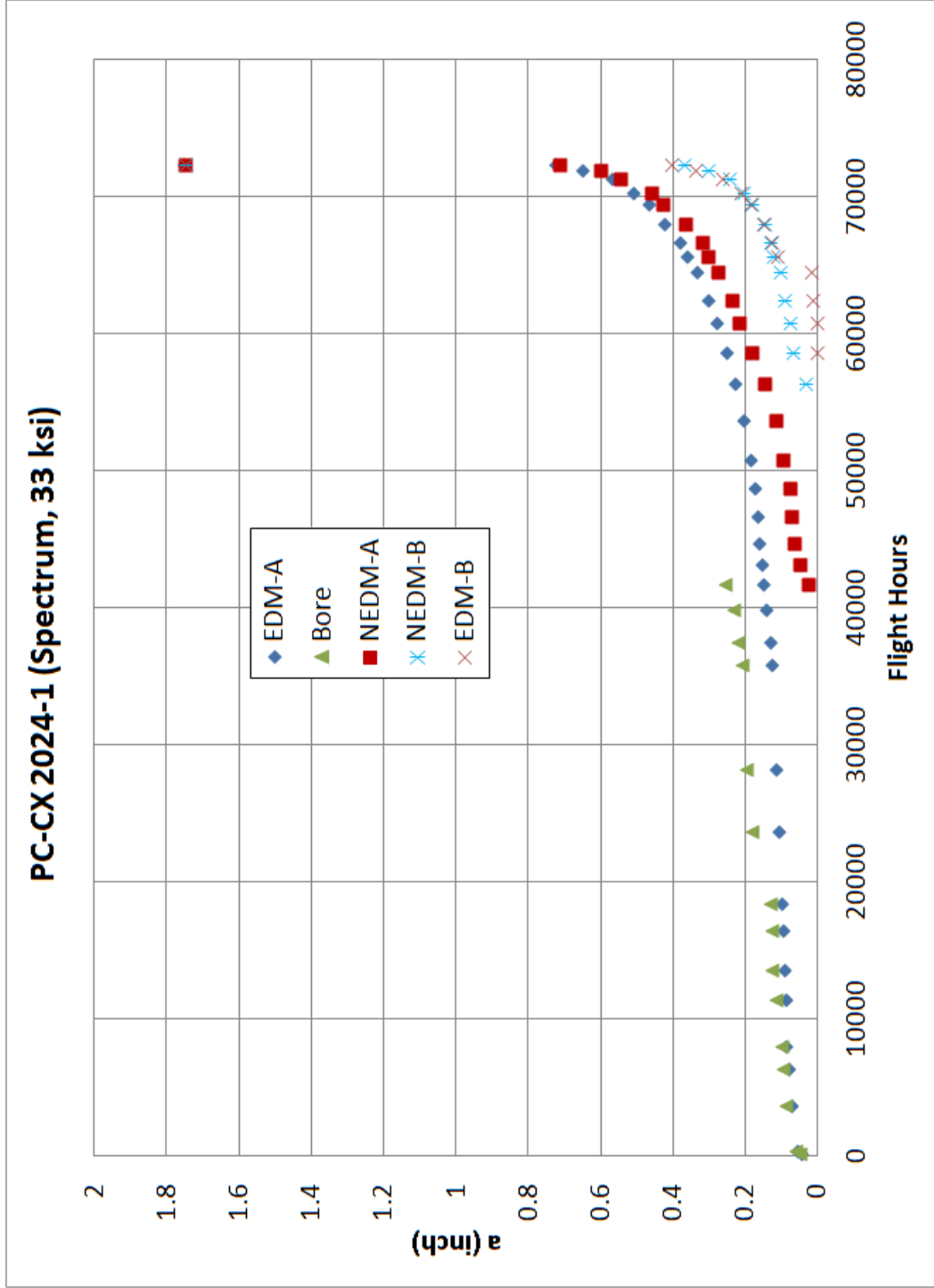


Fig. 32 a vs. N Plot for Pre-cracked Cold-Expanded Test under Spectrum Loading

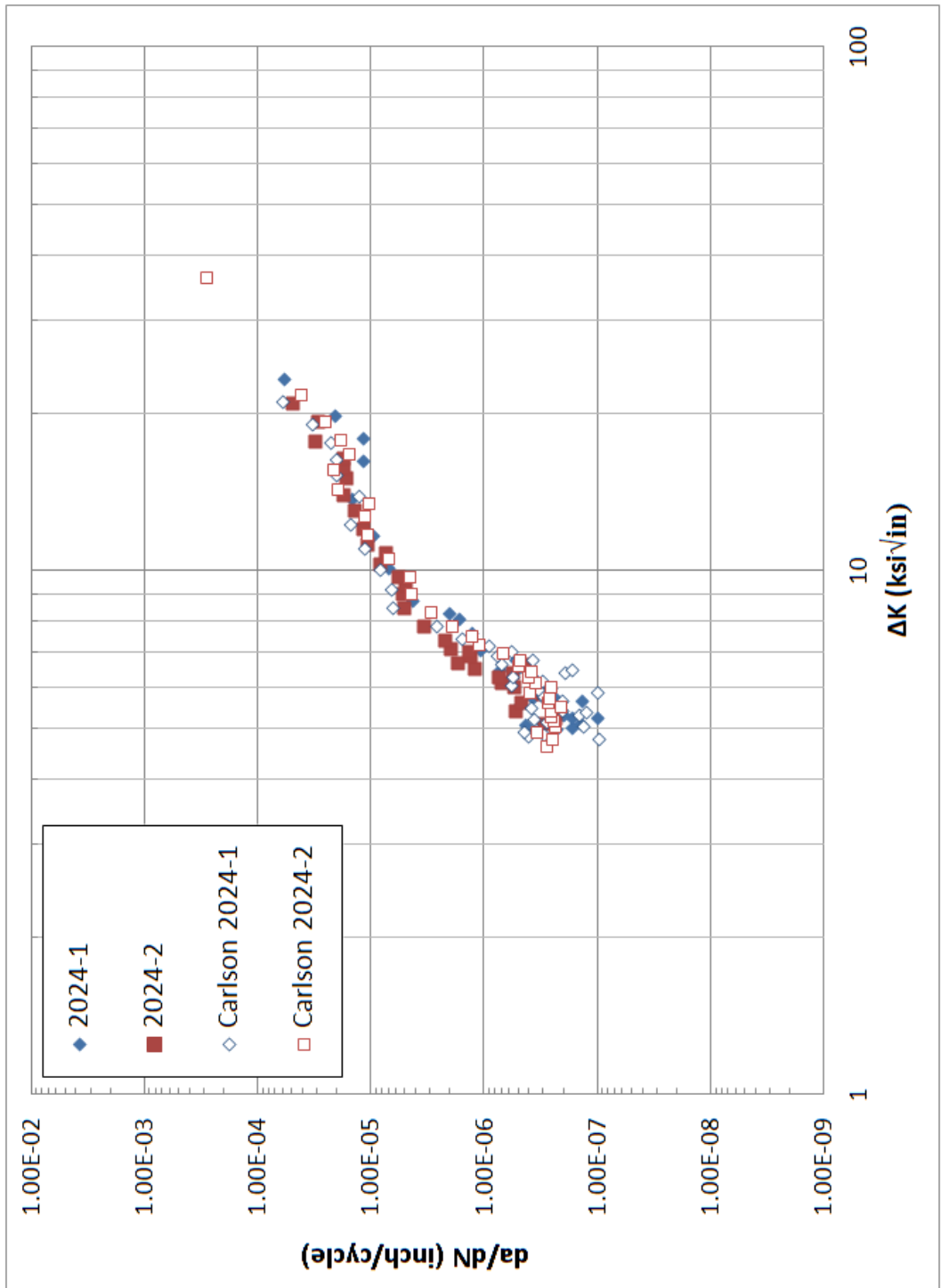


Fig. 33 da/dN vs. Delta K Data from ASTM E 647 Standard Tests

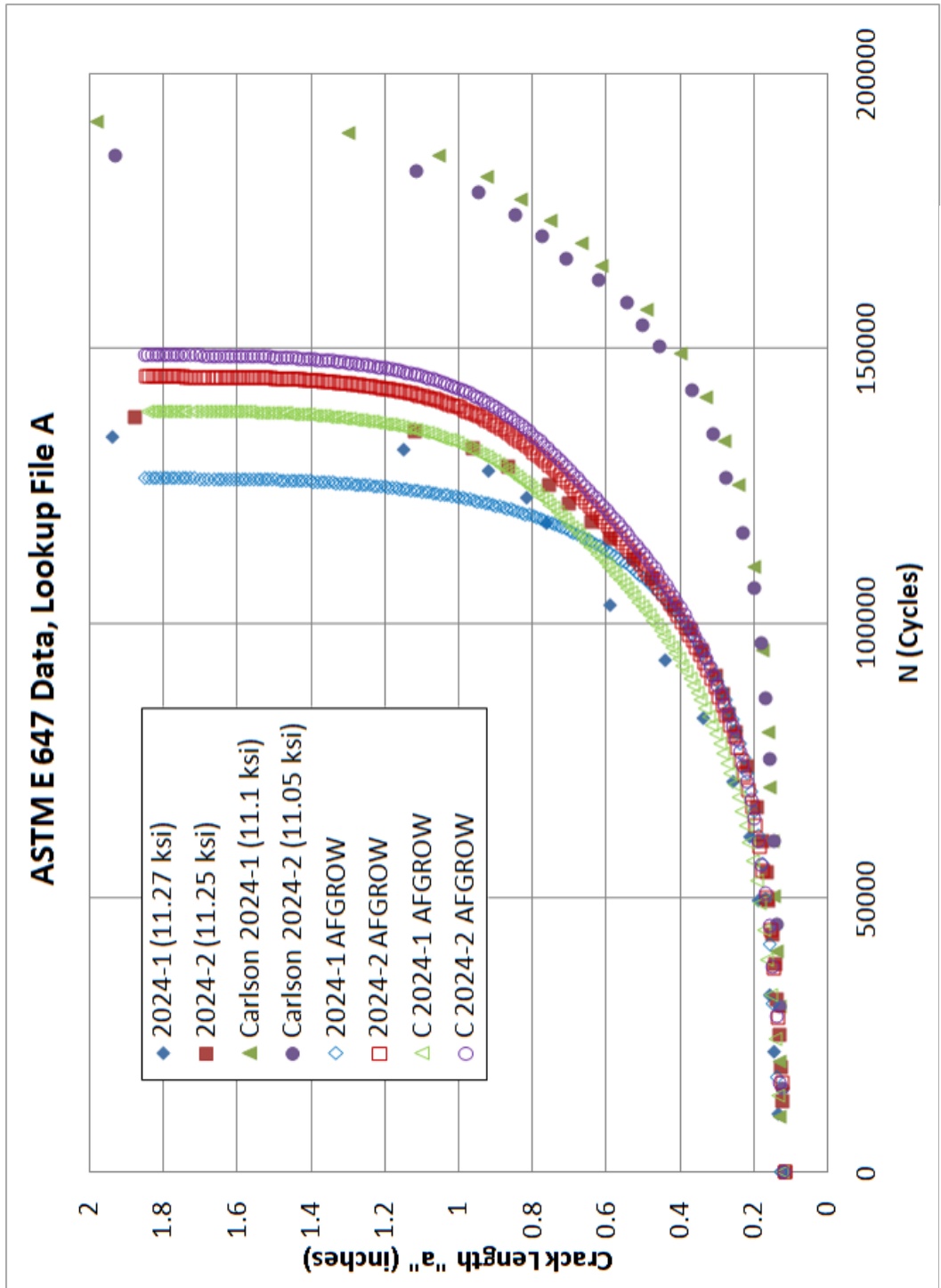


Fig. 34 ASTM E 647 Test Data and AFGROW Predictions Using Lookup File A

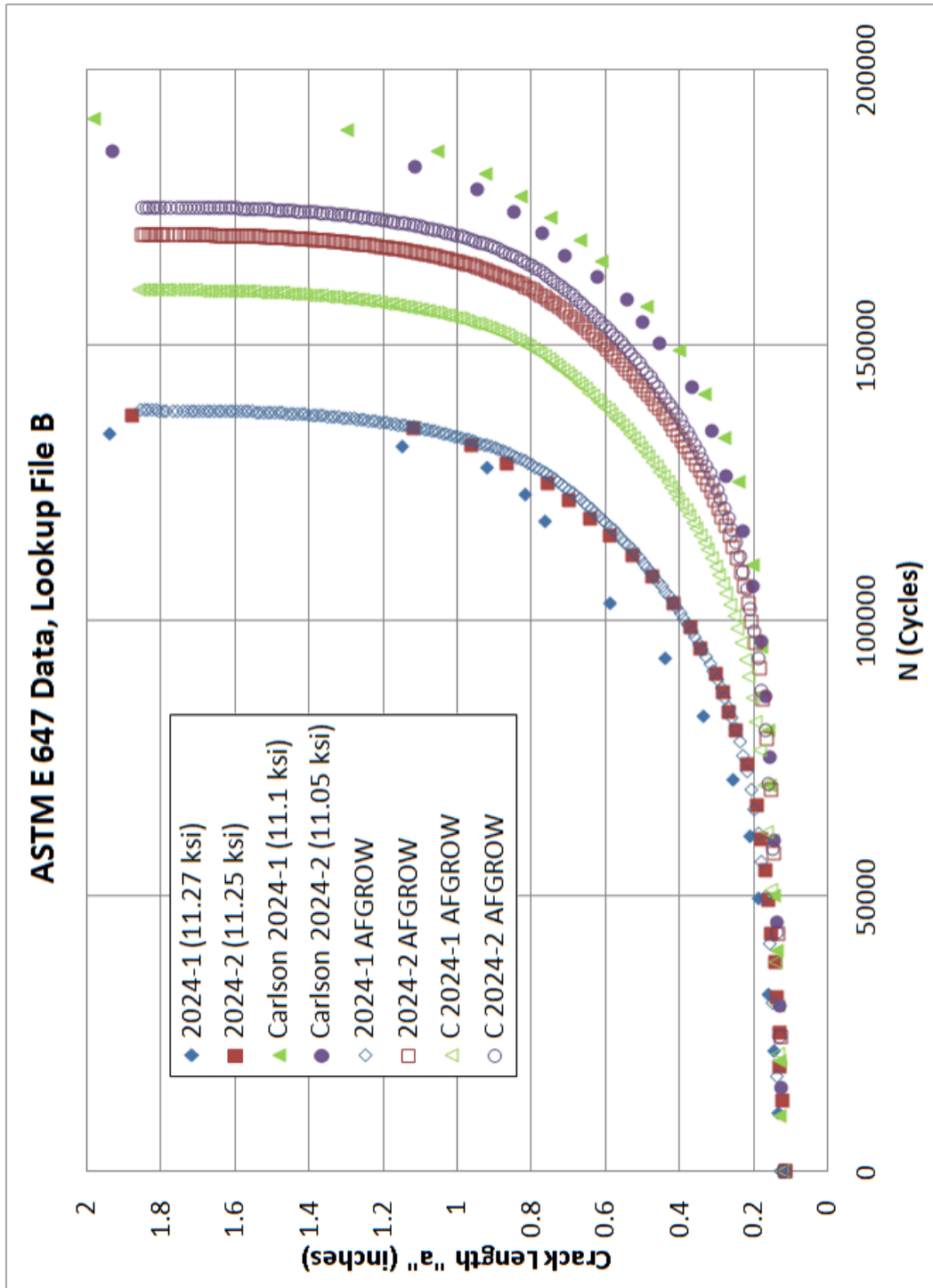
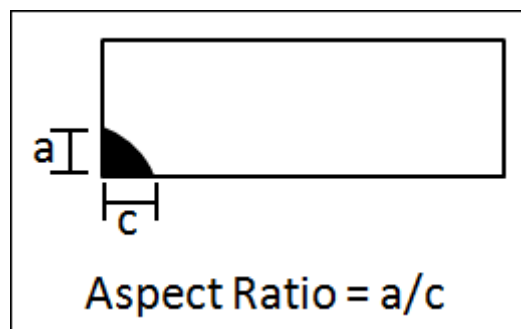


Fig. 35 ASTM E 647 Test Data and AFGROW Predictions Using Lookup File B

Table 3 Tested and Predicted Fatigue Lives for ASTM E 647 Standard Tests

Specimen	Actual Life (cycles)	Lookup File A (cycles)	Percent Disagreement	Lookup File B (cycles)	Percent Disagreement
2024-1	133769	126164	5.69%	138035	-3.19%
2024-2	137224	144693	-5.44%	169908	-23.82%
CC 2024-1	191020	138399	27.55%	159871	16.31%
CC 2024-2	185081	148564	19.73%	174898	5.50%
			11.88%		-1.30%

**Fig. 36 Corner Crack Aspect Ratio Definition****Table 4 AFGROW Baseline Aspect Ratio Analysis Results for Lookup File B**

Specimen ID	Tested Life	Measured Crack Lengths		Averaged Crack Lengths	
		a/c Allowed to Vary	a/c Held Constant	a/c Allowed to Vary	a/c Held Constant
Scott NCX 2024-3	279806	198010	136673	198412	275716
Scott NCX 2024-4	425336	292967	523065	289005	375613
Average Percent Disagreement		30.18%	37.07%	30.57%	6.58%

Table 5 AFGROW SOLR Analysis Results

Specimen ID	SOLR for Lookup file A	SOLR for Lookup File B	SOLR for A-10 Lookup File	Max Stress (ksi)
NCX 2024-4	1.8896	1.829	1.6966	25.00
NCX 2024-5	1.8635	1.8030	1.6727	
NCX 2024-6	1.8852	1.8180	1.6790	
NCX 2024-1	1.7510	1.7100	1.5690	33.00
NCX 2024-2	1.8850	1.8250	1.6600	
NCX 2024-3	1.8478	1.7930	1.6380	
NCX 2024-7	1.9400	1.9000	1.6940	43.25

Table 6 Average AFGROW SOLR Results with Interpolated Values

Specimen ID	Average SOLR for Lookup File A	Average SOLR for Lookup File B	Average SOLR for A-10 Lookup File	Max Stress (ksi)
NCX 2024-4	1.8794	1.8167	1.6828	25.00
NCX 2024-5				
NCX 2024-6				
INTERPOLATED	1.8472	1.7913	1.6450	30.00
NCX 2024-1	1.8279	1.7760	1.6223	33.00
NCX 2024-2				
NCX 2024-3				
NCX 2024-7	1.9400	1.9000	1.6940	43.25

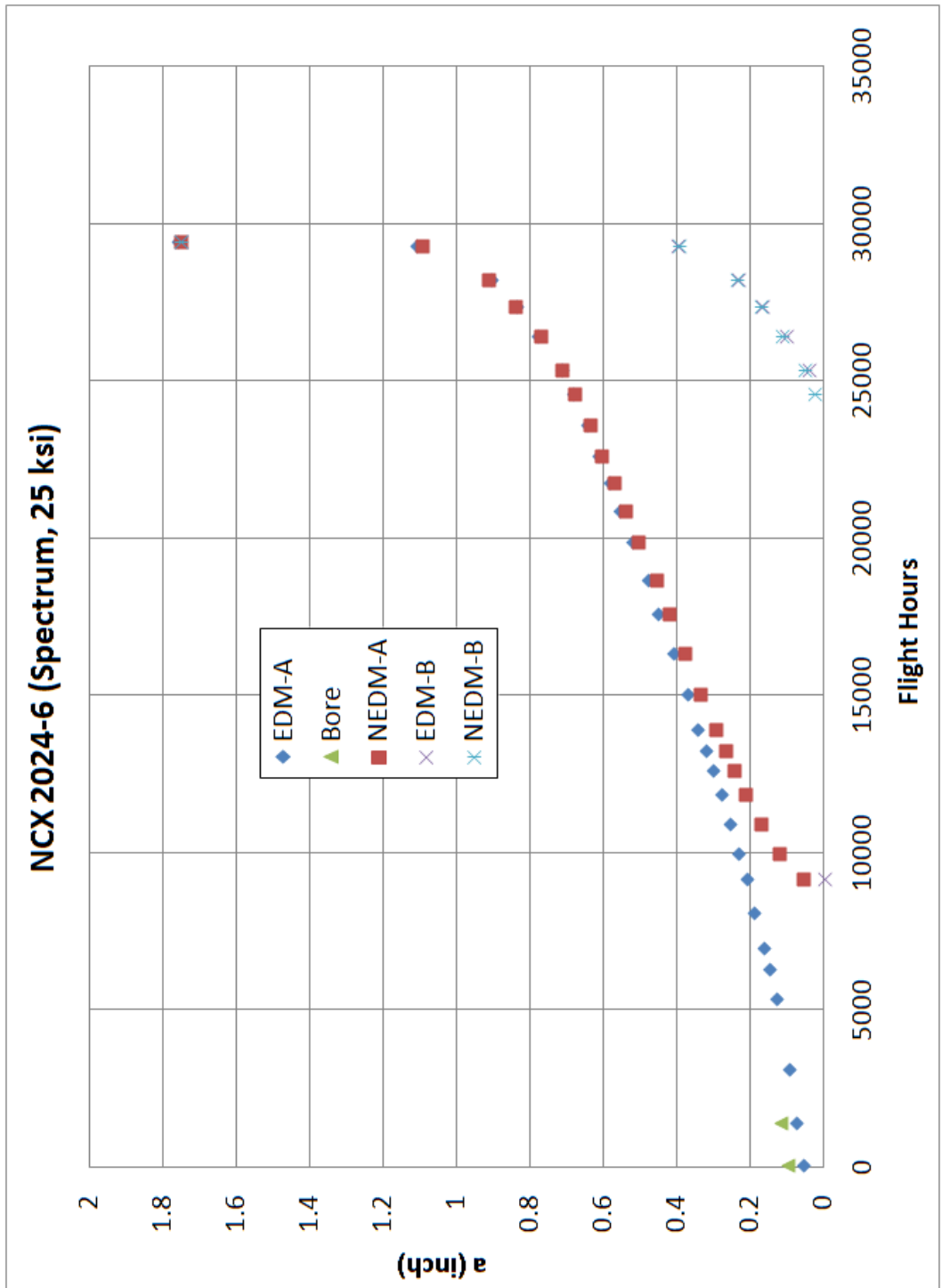


Fig. 37 Curve Fit of Optimum SOLRs for Various Lookup Files

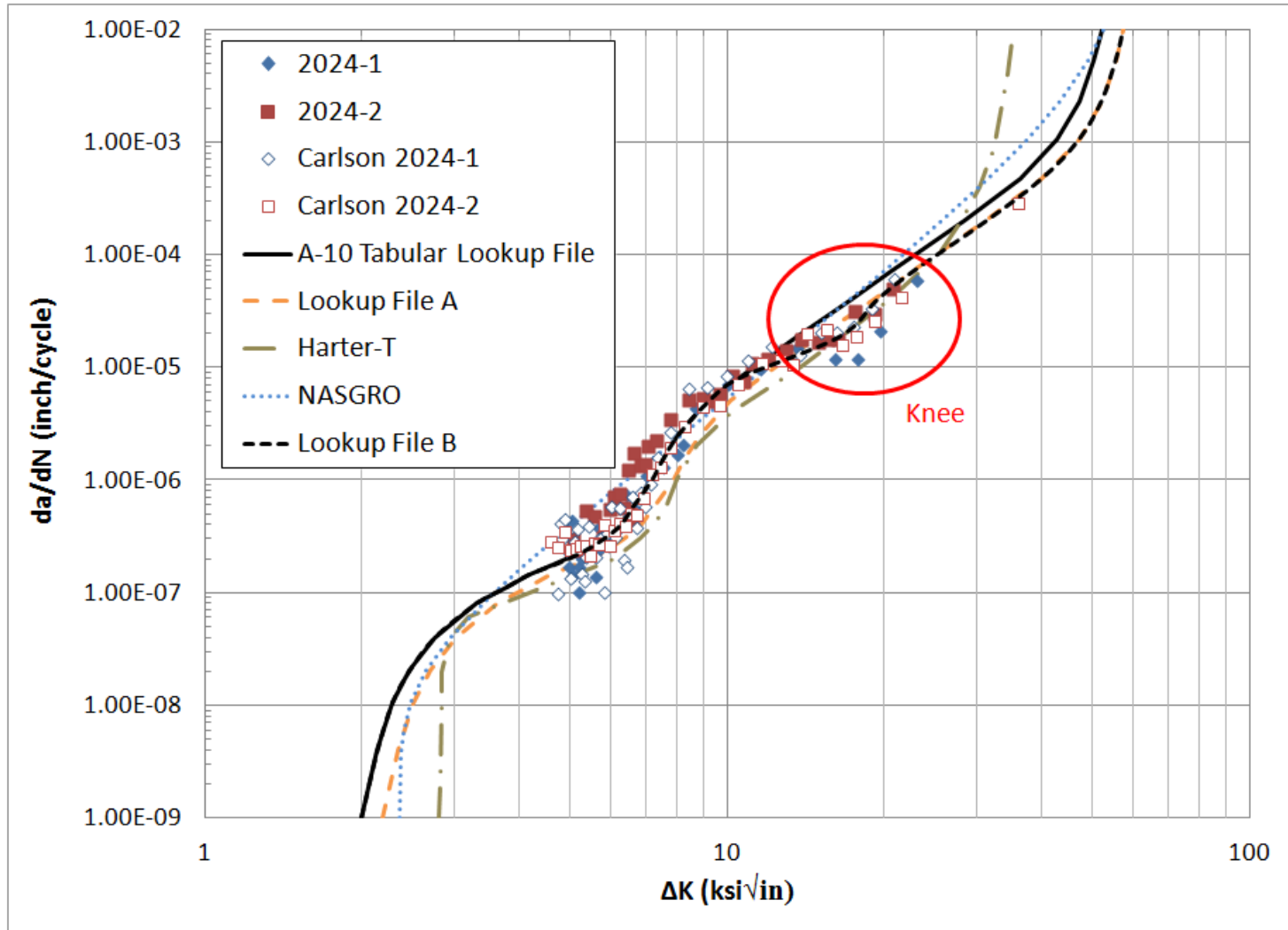


Fig. 38 Upper Knee on da/dN vs. Delta K Curve Captured by Lookup File B

4. RESULTS

A brief summary of all fatigue test results are displayed in Table 7. AFGROW fatigue life predictions using both lookup file A and lookup file B for each of the tests are also included in Table 7. The life benefit due to cold expansion will be displayed as a life improvement factor (LIF). The LIF is the ratio of the cold-expanded life to the non-cold-expanded life as shown below.

$$LIF = \frac{\textit{Cold-Expanded Life}}{\textit{Non-Cold-Expanded Life}} \quad (7)$$

To quantify the amount of scatter between test results a Weibull analysis was performed on the test results for each configuration and loading regime. The β parameter resulting from the Weibull analysis was then used to determine the scatter. The Weibull analysis used employed rank regression in the y direction. For aluminum alloys the amount of scatter among fatigue test results has been found to yield a Weibull β parameter of at least four.³⁹ As this research was an investigative study that incorporated small test sample sizes the Weibull analysis was necessary to demonstrate acceptability of the data scatter. A summary of the Weibull β parameters for each loading condition tested is shown in Table 8.

4.1. Constant Amplitude Loading

The only constant amplitude data generated directly by the author in this work were precracked cold-expanded specimens. The data generated by Scott Carlson was used as the non-cold-expanded baseline for these data.²⁶ Carlson's work also generated data for cracks grown from a previously cold-expanded, or "clean," fastener hole. This data was also used for comparing the fatigue life of a cold-expanded hole with that of a precracked cold-expanded hole.

4.1.1. 20.00 ksi Maximum Stress Tests (Stress Ratio = 0.1)

It should be noted that four tests were conducted at this stress level, and two of those four tests failed prematurely from the grips. An image of the specimen failure in the grip is shown in Fig. 39. The life of these specimens is reported as the life at which the specimen failed in the grip. The specimen identifications for those tests which failed in the grip were PC-CX 2024-14 and PC-CX 2024-17.

The work by Carlson only investigated cold-expanded tests at a maximum stress of 25.00 ksi. Therefore, the only comparison made for constant amplitude loading at the 20.00 ksi stress level was non-cold-expanded life to the precracked cold-expanded life. The average precracked cold-expanded life for this loading was found to be 4,296,067 cycles, yielding an LIF of 90.5. The Weibull β parameter for this stress level was only 1.63, excluding the two tests that failed in the grips. Including the two premature failures would further lower the parameter. The 0.005 inches IFS AFGROW prediction for this stress (20.00 ksi) was 52,645 cycles using lookup file A, and 55,137 cycles using lookup file B. One of the tests conducted by the author, along with the AFGROW predictions

for that test, are plotted in Fig. 40. All other 20.00 ksi max stress, constant amplitude tests are displayed in Appendix C.

A summary of the average tested life for constant amplitude loading, as well as the LIF for each stress level, are reported in Table 9.

4.1.2. 25.00 ksi Maximum Stress Tests (Stress Ratio = 0.1)

At a maximum stress of 25.00 ksi, the average life for the cold-expanded test specimens from Carlson's work was 531,776 cycles, yielding an LIF of 71.4 when compared to the non-cold-expanded specimen tested by Carlson. The average life for the precracked cold-expanded specimens tested by the author at a maximum stress of 25.00 ksi was 452,585 cycles, which yields an LIF of 60.8. The Weibull β parameter for this stress level was 5.989. The AFGROW prediction for the 25.00 ksi max stress tests using an IFS of 0.005 inches was 22,089 cycles using lookup file A, and 23,271 cycles using lookup file B. A plot of one of these precracked cold-expanded tests and the AFGROW predictions done by the author are plotted in Fig. 41. Plots for each of the tests done by the author at this stress level are shown in Appendix C.

4.2. Spectrum Loading

A summary of the averages of the tested and predicted lives for all spectrum loaded tests are shown in Table 10. The table also displays an average LIF for each stress level.

4.2.1. Fatigue Life of Non-Cold-Expanded Specimens

A total of seven non-cold-expanded specimens under spectrum loading were tested at three different stress levels. Three tests were performed with a maximum stress of 25.00 ksi, three tests were performed with a maximum stress of 33.00 ksi, and one test was done at a maximum stress of 43.25 ksi.

4.2.1.1. Maximum Stress of 25.00 ksi

The average life of the non-cold-expanded specimens under spectrum loading with a maximum stress of 25.00 ksi was 31,521 flight hours. The β parameter from the Weibull analysis for this stress level was 15.35. The individual fatigue life for each test under this loading are shown in Table 11.

The non-cold-expanded specimens served as a baseline for the precracked cold-expanded data, as well as an AFGROW baseline to establish the appropriate SOLR for each stress level. The average SOLR for lookup file A was 1.88, and the average SOLR for lookup file B was 1.82. Table 11 presents the AFGROW predictions using the optimum SOLR values for each test as well as the AFGROW prediction using the average SOLR for each test at the 25.00 ksi stress level.

For further evaluation of the validity of the AFGROW predictions using both lookup files and their corresponding SOLR values, the AFGROW predicted growth was plotted with the test data to evaluate how well the AFGROW prediction matched the shape of the crack growth curve. One such plot for a 25.00 ksi maximum stress is shown in Fig. 42. Plots for all other tests are shown in Appendix D.

4.2.1.2. Maximum Stress of 33.00 ksi

The average life for spectrum non-cold-expanded tests with a maximum stress of 33.00 ksi was 12,200 flight hours. The Weibull β parameter at this stress level was 10.84. All individual fatigue lives for the 33.00 ksi stress level are shown in Table 12. A plot of the crack growth for a non-cold-expanded, 33.00 ksi spectrum is shown in Fig. 43. Plots of the crack growth for each test under this loading are shown in Appendix C.

The average SOLR for the 33.00 ksi maximum stress using lookup file A was 1.83, and for lookup file B was 1.78. The optimum SOLRs for each test using both lookup files are displayed in Table 12.

4.2.1.3. Maximum Stress of 43.25 ksi

As the 43.25 ksi stress level was not part of the original test matrix, there was only one non-cold-expanded test performed at the 43.25 ksi stress level. The life of that test was 4657 flight hours. A plot of the crack growth observed is combined with the AFGROW predictions for this test in Fig. 44. The optimum SOLRs observed for this test were 1.94 for lookup file A, and 1.9 for lookup file B. A summary of all the results for this loading is shown in Table 13.

4.2.2. Fatigue Life of Precracked Cold-Expanded Specimens

Ten tests were precracked cold-expanded and tested under spectrum loading conditions. One of these tests was conducted at a maximum stress of 25.00 ksi, three were tested at maximum stresses of 30, 33, and 43.25 ksi.

4.2.2.1. Maximum Stress of 25.00 ksi

One spectrum test was conducted at a maximum stress of 25.00 ksi. This specimen failed in the grip after 704,450 flight hours. The LIF based off of the average life from the three non-cold-expanded specimens is 22.35. After the grip failure, the specimen was removed from the test frame, and the bonded tabs were cut off of the specimen. The specimen was then put back into the test frame, and the test was continued to failure from the hole. The total tested life to failure of the hole was 831,641 flight hours, yielding an LIF of 26.38. The AFGROW predictions for this test were 86,611 flight hours using lookup file A, and 75,729 flight hours using lookup file B. A plot of the test data and the AFGROW predictions is displayed in Fig. 45.

4.2.2.2. Maximum Stress of 30.00 ksi

The average life of the precracked cold-expanded specimens tested under spectrum loading with a max stress of 30.00 ksi was 194,950 flight hours. The Weibull β parameter at this stress level was 7.35. As there were not any non-cold-expanded baseline tests done at this stress level, the average tested life was compared with the AFGROW predicted life of a non-cold-expanded test using an SOLR which was interpolated from those optimized for the 25.00 ksi and 33.00 ksi tests. The interpolated SOLR was 1.79 for lookup file B, which predicted a life of 19,742 flight hours, yielding an LIF of 9.87. A plot of the test and prediction data is displayed in Fig. 46.

The cold-expanded predictions from AFGROW, assuming the 0.005 inch IFS, predicted a life of 43,923 flight hours for lookup file A and 50,197 flight hours for lookup file B.

4.2.2.3. Maximum Stress of 33.00 ksi

The average tested life at the 33.00 ksi maximum stress was 80220 flight hours, which indicates an LIF of 6.57. The Weibull β parameter for this stress level was 8.69. The AFGROW predictions for a 0.005 inch IFS were 32,677 flight hours for lookup file A, and 37,277 flight hours for lookup file B. A plot of the tested and predicted crack growths is shown in Fig. 47.

4.2.2.4. Maximum Stress of 43.25 ksi

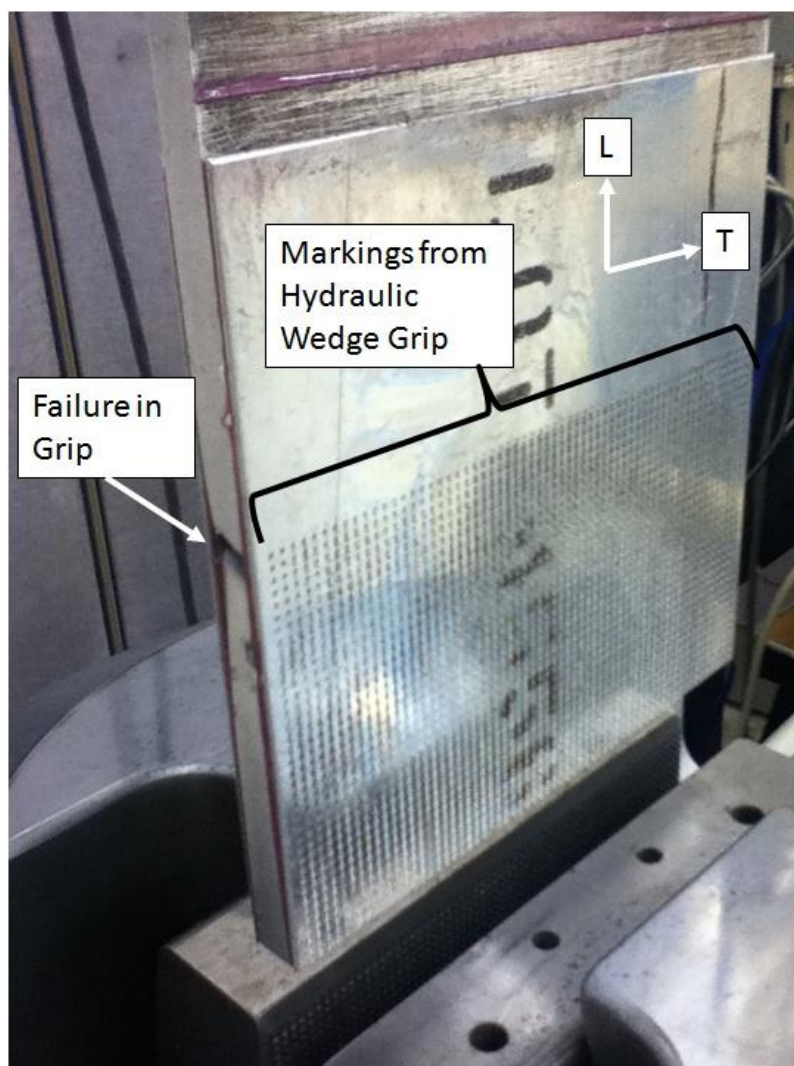
At a maximum stress of 43.25 ksi the average test life was 6,201 flight hours, which yielded an average LIF of 1.33. The Weibull β parameter for the three tests conducted at this stress level was 18.71. The average AFGROW predictions for these tests, assuming the 0.005 inch IFS, were 9,357 flight hours for lookup file A and 10,032 flight hours for lookup file B. A plot of the crack growth for one of the tests and predictions at this stress state is shown in Fig. 48.

Table 7 Test Data Summary

CX/ NCX	CA or Spectrum	Peak Stress (ksi)	Specimen ID	Tested Life (cycles or hours)	AFGROW-A (cycles or hours)	AFGROW-B (cycles or hours)	Notes
NON-CX	CA (ASTM E647)	11.25	2024-1	133769	118175	129955	
			2024-2	137224	136560	158418	
		11.07	CC 2024-1	191020	138399	159871	
			CC 2024-2	185081	148564	174898	
	CA	25.00	Scott NCX 2024-1	7443	7832	7087	
		20.00	Scott NCX 2024-2	47443	23698	20151	
	Spectrum	25.00	NCX 2024-4	32215	32837	33179	
			NCX 2024-5	32978	31755	31900	
			NCX 2024-6	29378	29689	29477	
		33.00	NCX 2024-1	12169	10143	10247	
			NCX 2024-2	11138	12607	12578	
			NCX 2024-3	13298	13933	13933	
	43.25	NCX 2024-7	4658	4658	4658		
CX	CA	20.00	PC-CX 2024-14	5688476	52606	55099	Failed in Grip
			PC-CX 2024-15	1403233	52669	55159	
			PC-CX 2024-16	3050999	52659	55151	
			PC-CX 2024-17	7041458	52645	55137	Failed in Grip
		25.00	PC-CX 2024-9	508291	22097	23277	
			PC-CX 2024-10	473555	22084	23267	
	PC-CX 2024-11		375910	22086	23269		
	Spectrum	25.00	PC-CX 2024-5	704498	86612	75729	Failed in Grip
		30.00	PC-CX 2024-4	187495	43931	50173	
			PC-CX 2024-12	181538	43933	50228	
			PC-CX 2024-13	215858	43907	38170	
		33.00	PC-CX 2024-1	72169	32678	37278	
			PC-CX 2024-2	89618	32678	37278	
			PC-CX 2024-3	78889	32678	37278	
		43.25	PC-CX 2024-6	6409	9357	10009	
PC-CX 2024-7			5858	9357	10009		
PC-CX 2024-8	6338		9357	10077			

Table 8 Weibull β Parameter

Loading	Max Stress (ksi)	NCX β Parameter	CX β Parameter
Constant Amplitude	20.00	N/A	1.63
	25.00	N/A	5.99
Spectrum	25.00	15.35	N/A
	30.00	N/A	7.35
	33.00	10.84	8.69
	43.25	N/A	18.71

**Fig. 39 Premature Specimen Failure in Grip**

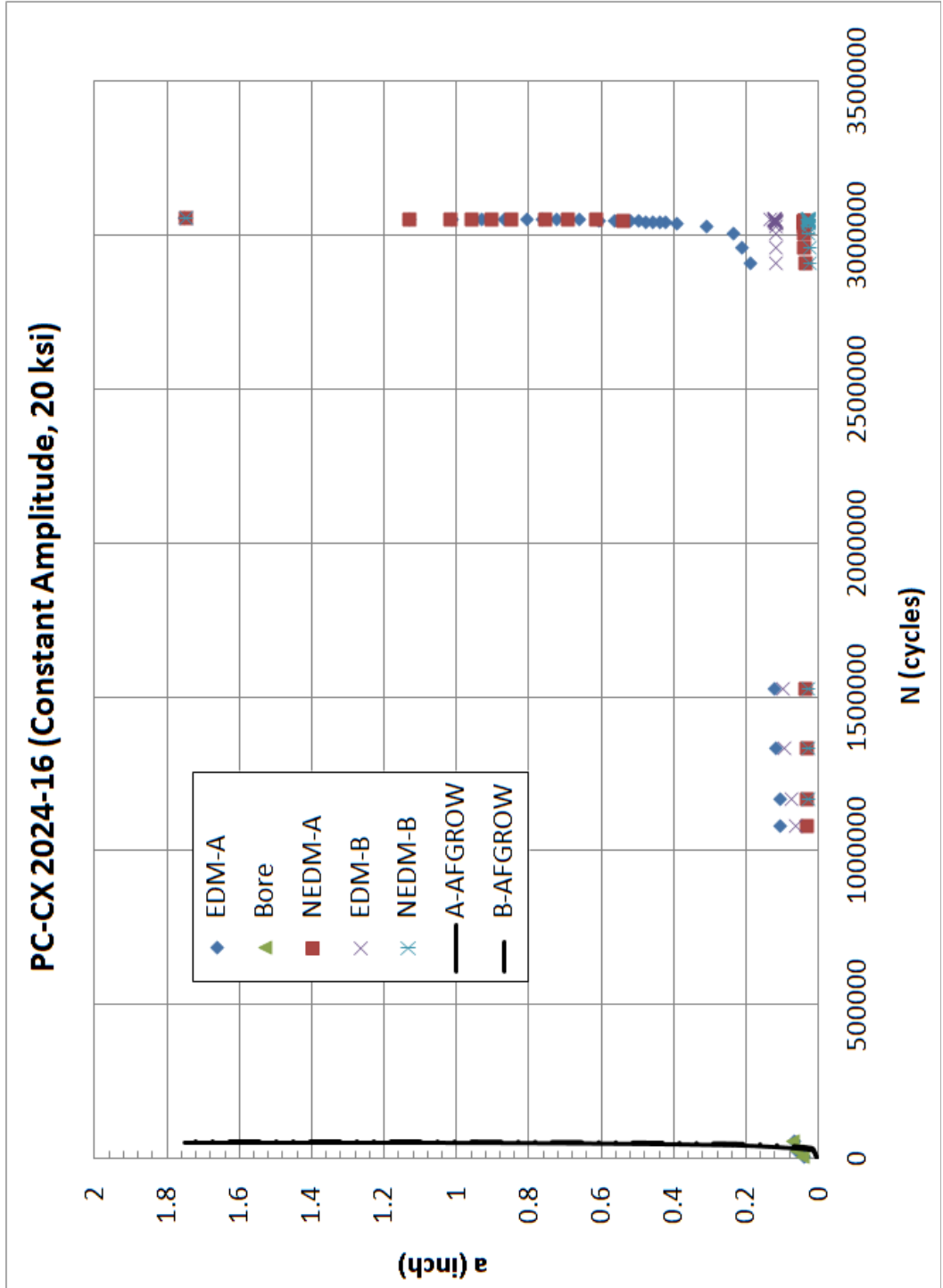


Fig. 40 Crack Growth for 20.00 ksi Constant Amplitude Precracked Cold-Expanded Test

Table 9 Constant Amplitude Test and Prediction Averages

Max Stress (ksi)	Non-CX Life (cycles)	AFGROW Non-CX (cycles)	CX Life (cycles)	LIF NCX to CX	PC-CX Life (cycles)	LIF NCX to PC-CX	AFGROW File A 0.005" IFS (cycles)	AFGROW File B 0.005" IFS (cycles)
20.00	47443	20151	N/A	N/A	4296067	90.6	52645	55137
25.00	7443	7087	531776	71	452585	60.8	22089	23271

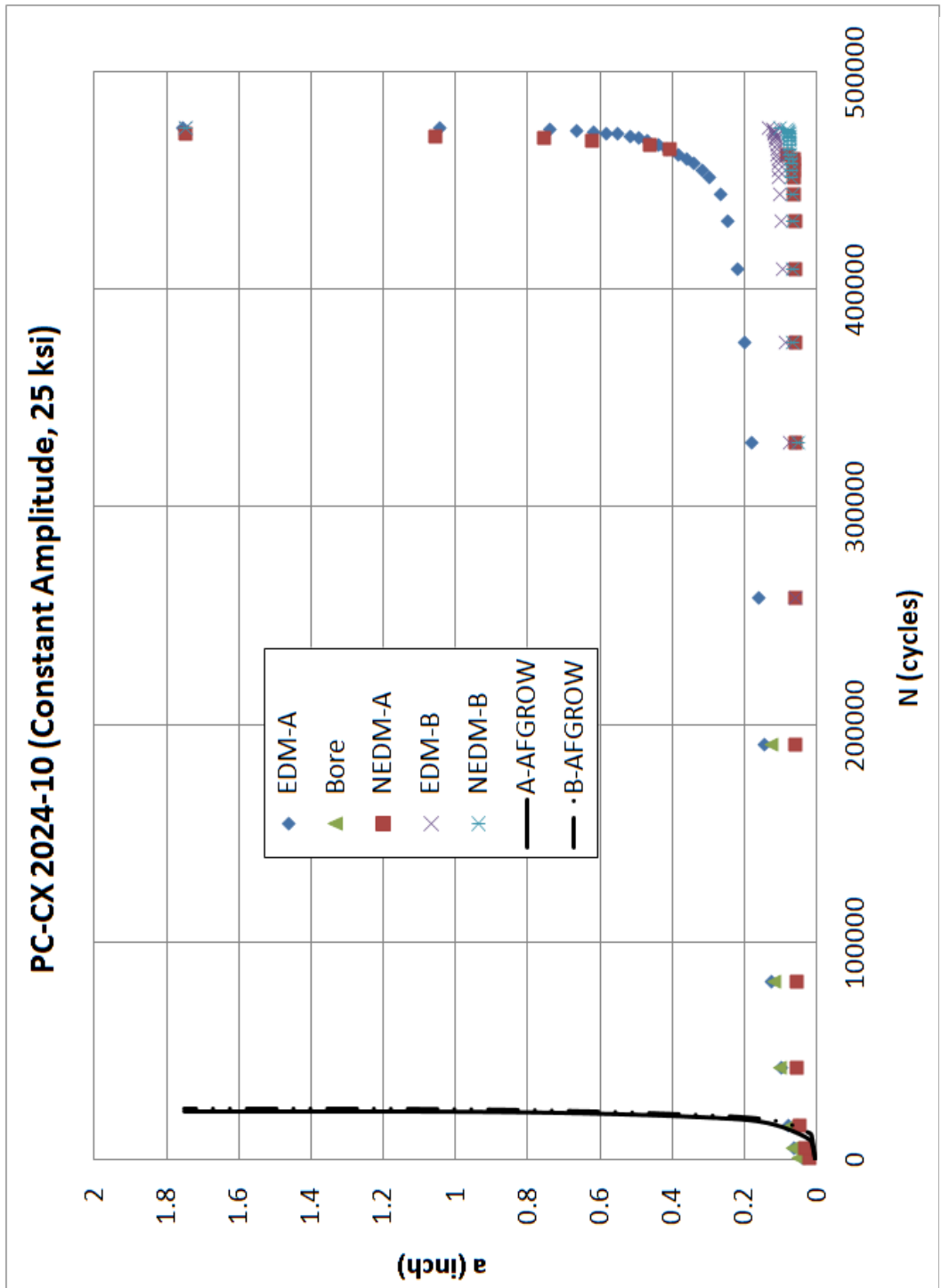


Fig. 41 Crack Growth for 25 ksi Constant Amplitude Precracked Cold-Expanded Test

Table 10 Spectrum Test and Prediction Averages

Max Stress (ksi)	Non-CX Life (cycles)	AFGROW Non-CX (cycles)	PC-CX Life (cycles)	LIF NCX to PC-CX	AFGROW File A 0.005" IFS (cycles)	AFGROW File B 0.005" IFS (cycles)
25.00	31521	31519	704450	22.3	86612	75729
30.00	N/A	18957	194950	10.3	43923	50198
33.00	12201	12253	80220	6.6	32678	37278
43.00	4658	4658	6201	1.3	9357	10032

Table 11 Test and Prediction Results for 25.00 ksi Spectrum

Specimen ID	Tested Life (hours)	Lookup File A				Lookup File B			
		Individual SOLR	Individual SOLR (hours)	Average SOLR	AFGROW for Average SOLR (hours)	Individual SOLR	Individual SOLR (hours)	Average SOLR	AFGROW for Average SOLR (hours)
NCX 2024-4	32213	1.8896	32215	1.8794	32837	1.8290	32223	1.8167	33179
NCX 2024-5	32976	1.8635	32978		31755	1.8030	32978		31900
NCX 2024-6	29376	1.8852	29378		29689	1.8180	29373		29477

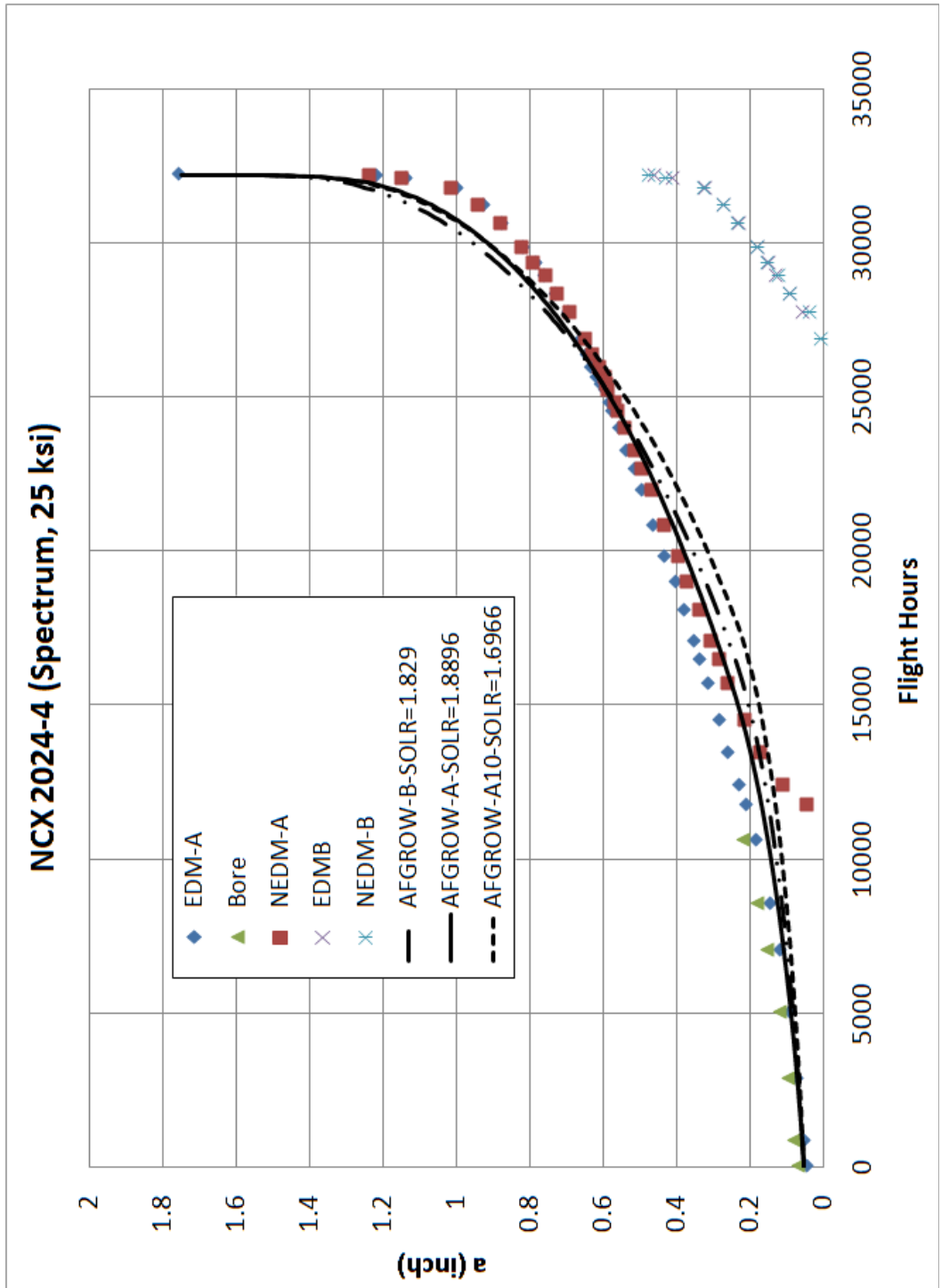


Fig. 42 Crack Growth for 25 ksi Spectrum Non-Cold-Expanded Test

Table 12 Test and Prediction Results for 33.00 ksi Spectrum

Specimen ID	Tested Life (hours)	Lookup File A				Lookup File B			
		Individual SOLR	Individual SOLR (hours)	Average SOLR	AFGROW for Average SOLR (hours)	Individual SOLR	Individual SOLR (hours)	Average SOLR	AFGROW for Average SOLR (hours)
NCX 2024-1	12168	1.7510	12169	1.8279	10143	1.7100	12167	1.7760	10247
NCX 2024-2	11137	1.8850	11138		12607	1.8250	11138		12578
NCX 2024-3	13297	1.8478	13298		13933	1.7930	13298		13933

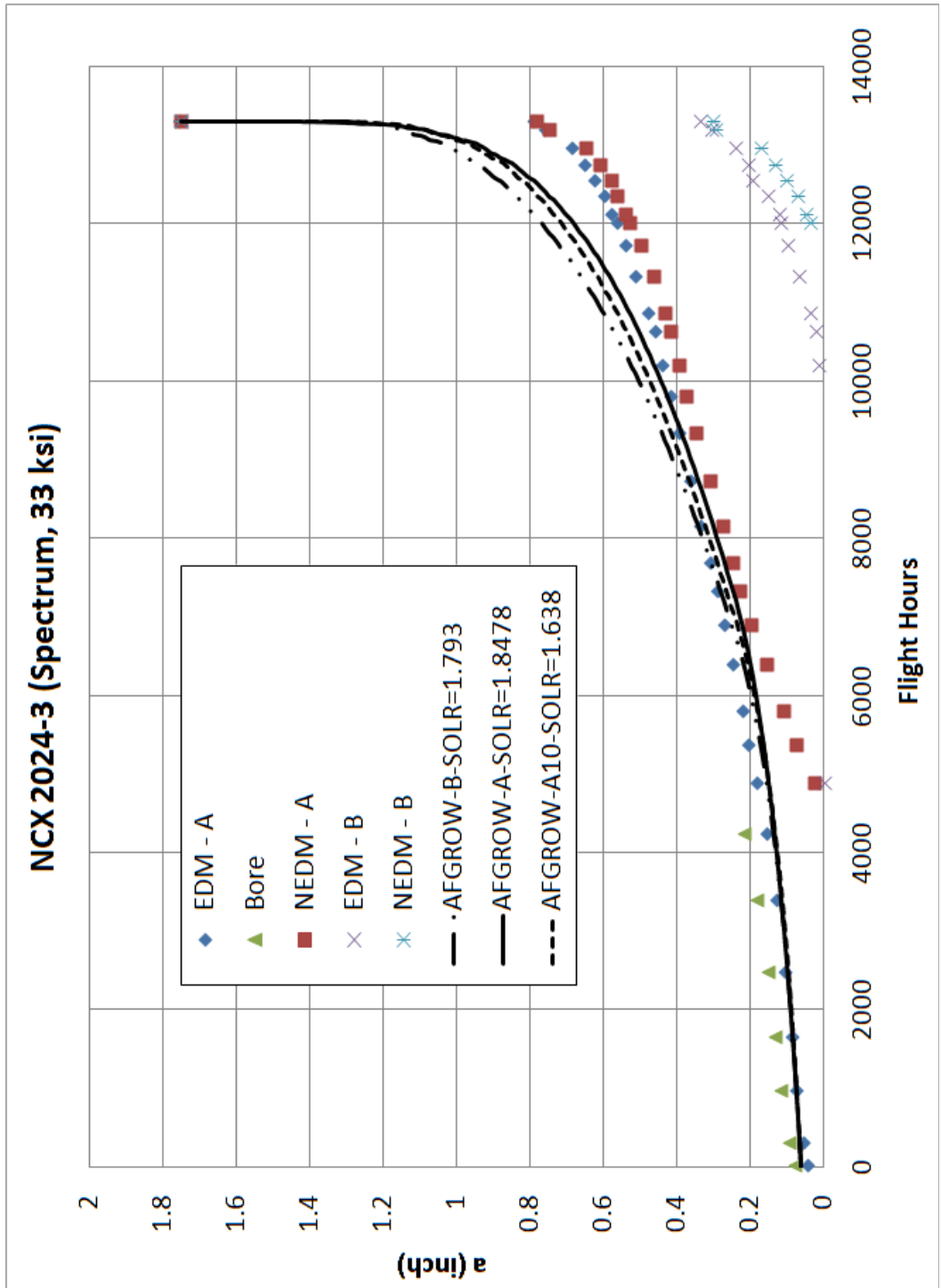


Fig. 43 Crack Growth for 33.00 ksi Spectrum Non-Cold-Expanded Test

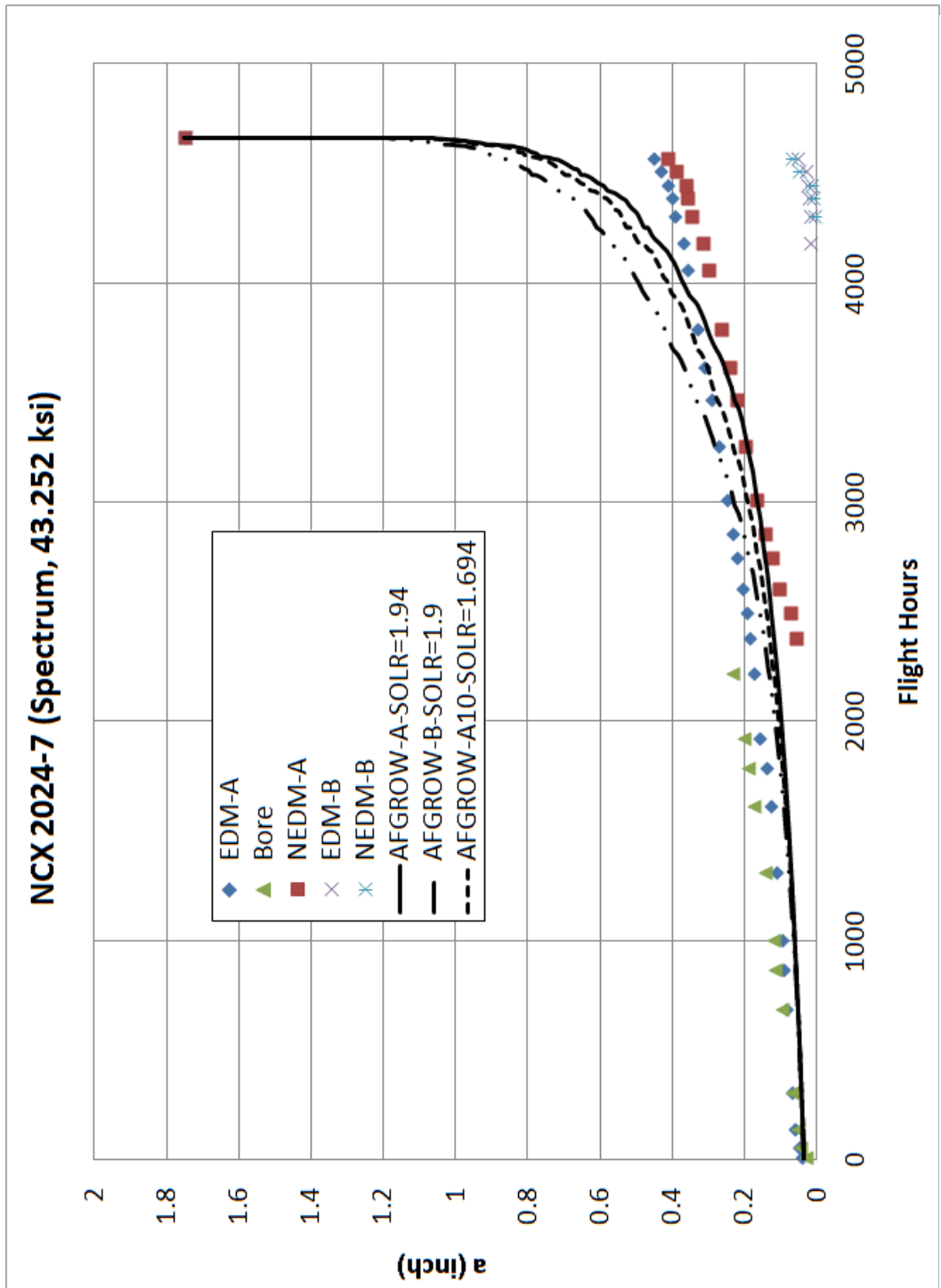


Fig. 44 Crack Growth for 43.25 ksi Spectrum Non-Cold-Expanded Test

Table 13 Test and Prediction Results for NCX 43.25 ksi Spectrum

Specimen ID	Tested Life (hours)	Lookup File A				Lookup File B			
		Individual SOLR	Individual SOLR (hours)	Average SOLR	Average SOLR (hours)	Individual SOLR	Individual SOLR (hours)	Average SOLR	Average SOLR (hours)
NCX 2024-7	4658	1.9400	4658	1.9400	4658	1.9000	4658	1.9000	4658

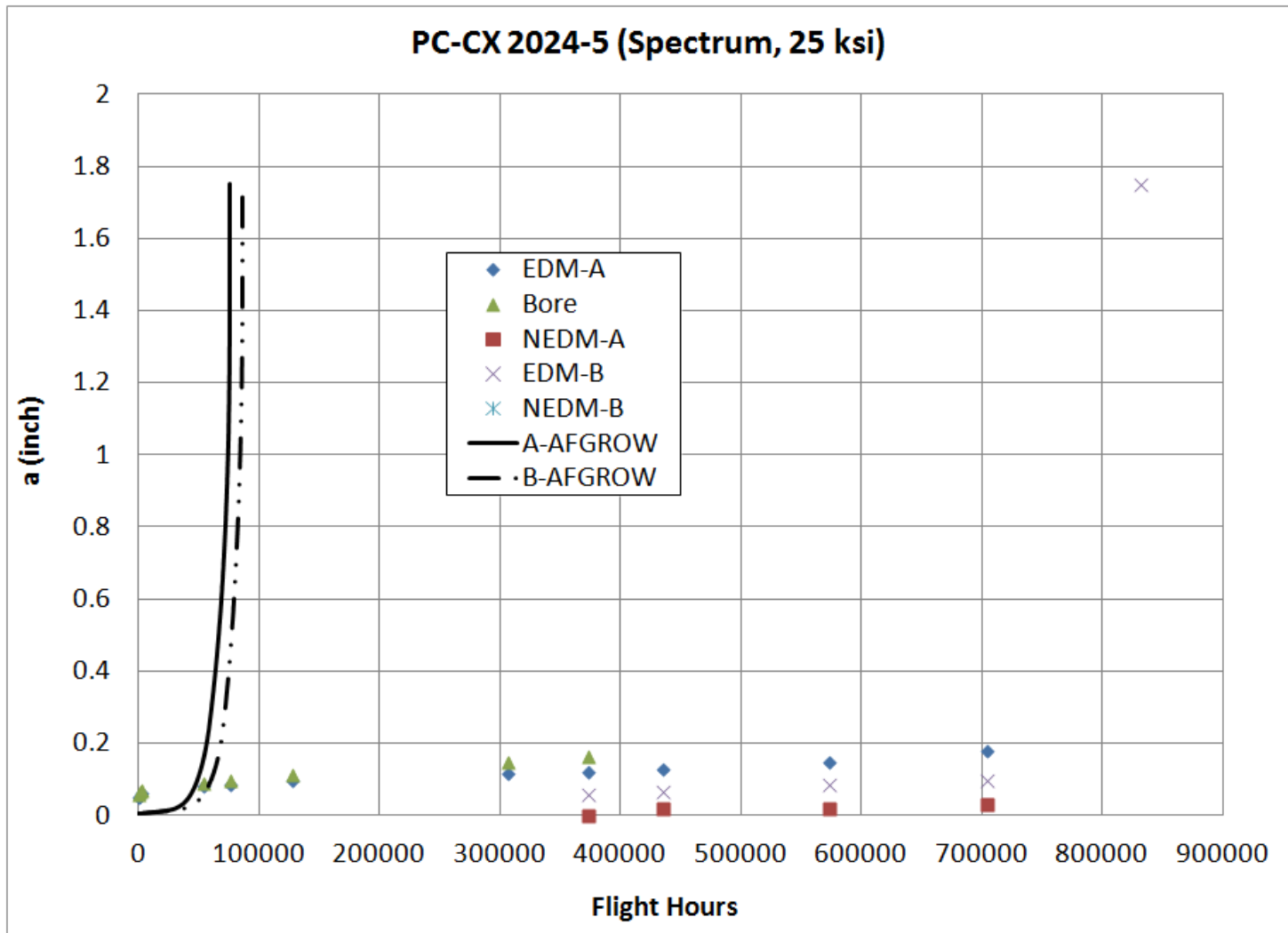


Fig. 45 Crack Growth for 25 ksi Spectrum Precracked Cold-Expanded Test

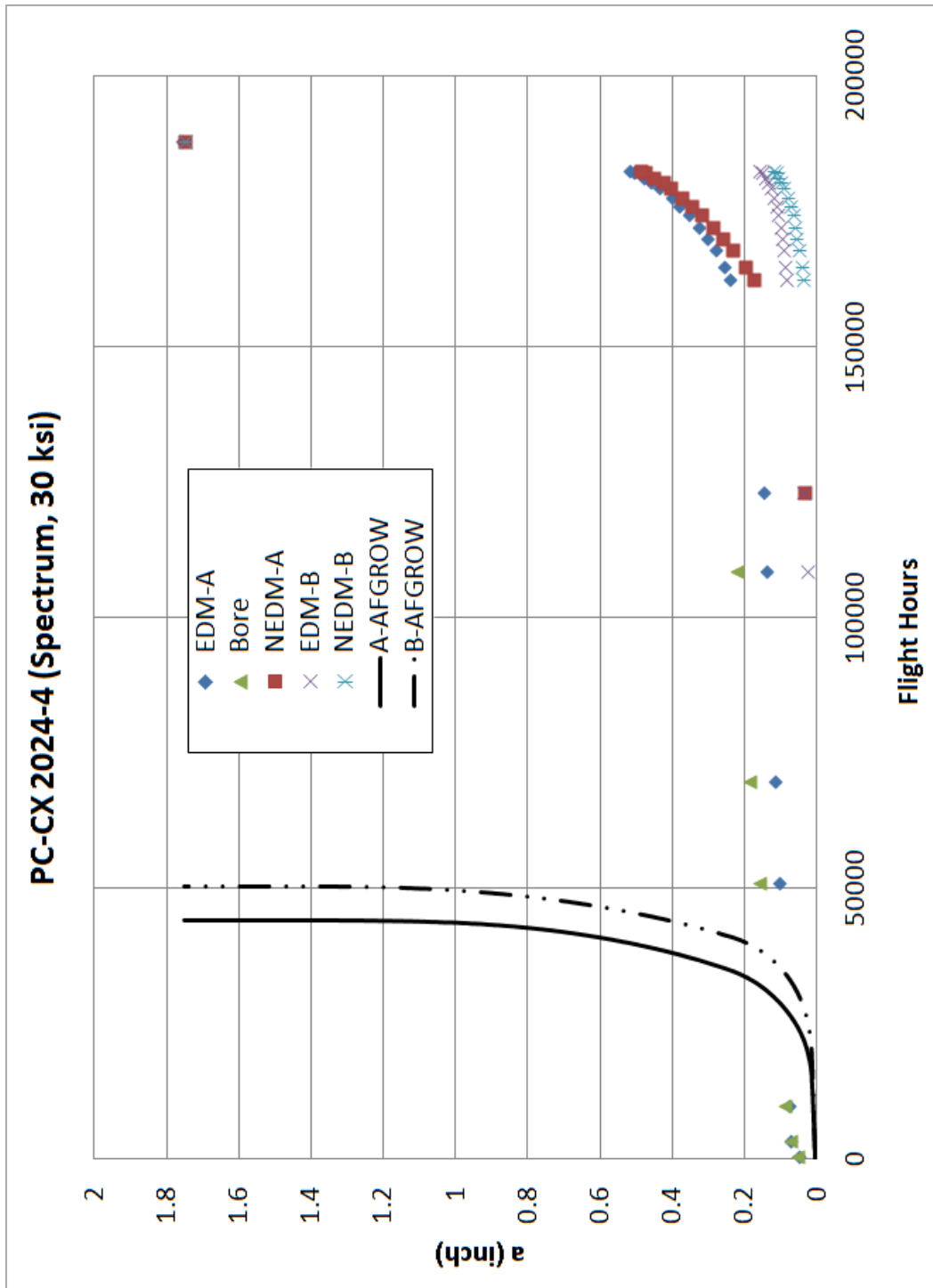


Fig. 46 Crack Growth for 30.00 ksi Spectrum Precracked Cold-Expanded Test

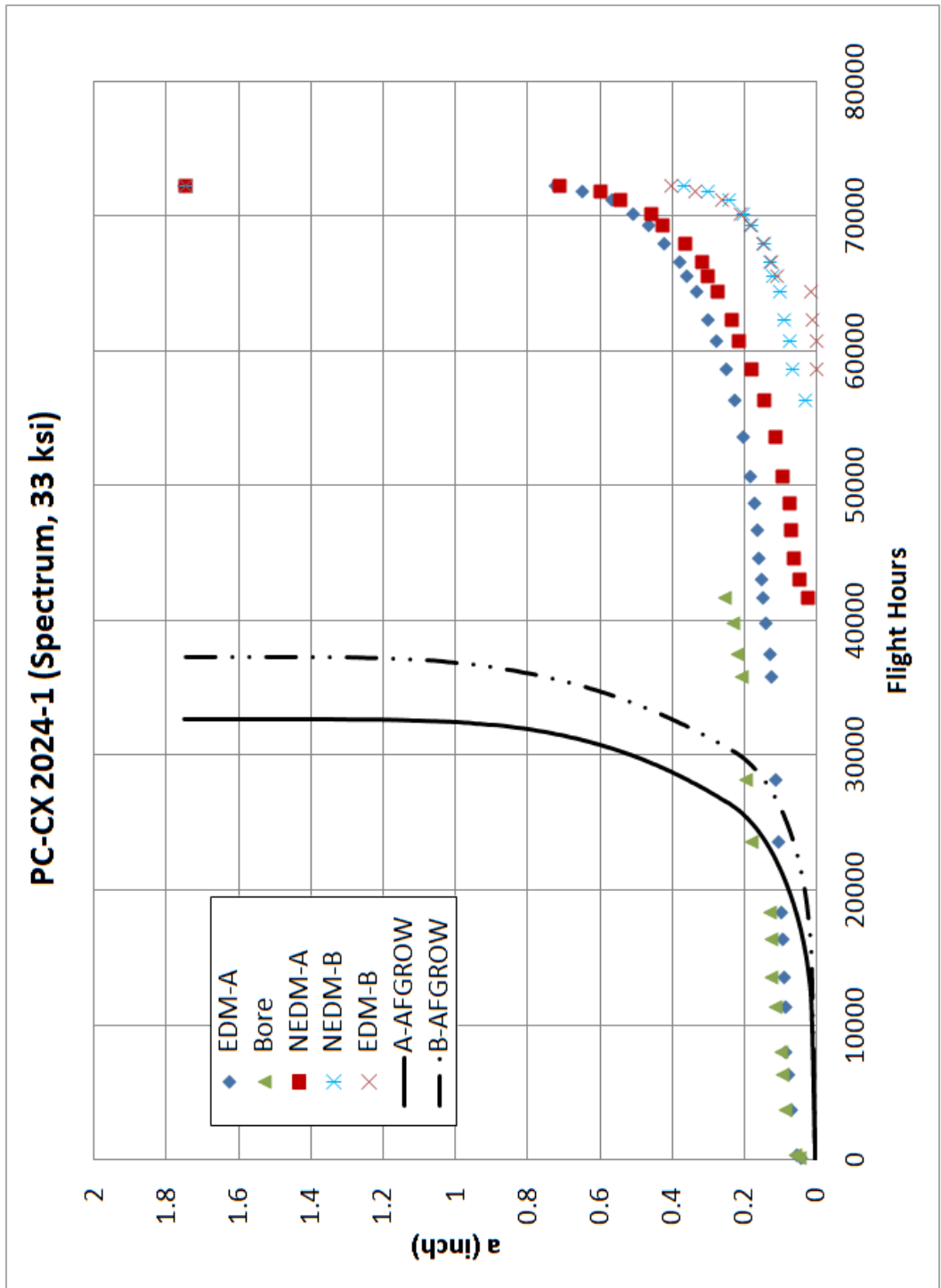


Fig. 47 Crack Growth for 33.00 ksi Spectrum Precracked Cold-Expanded Test

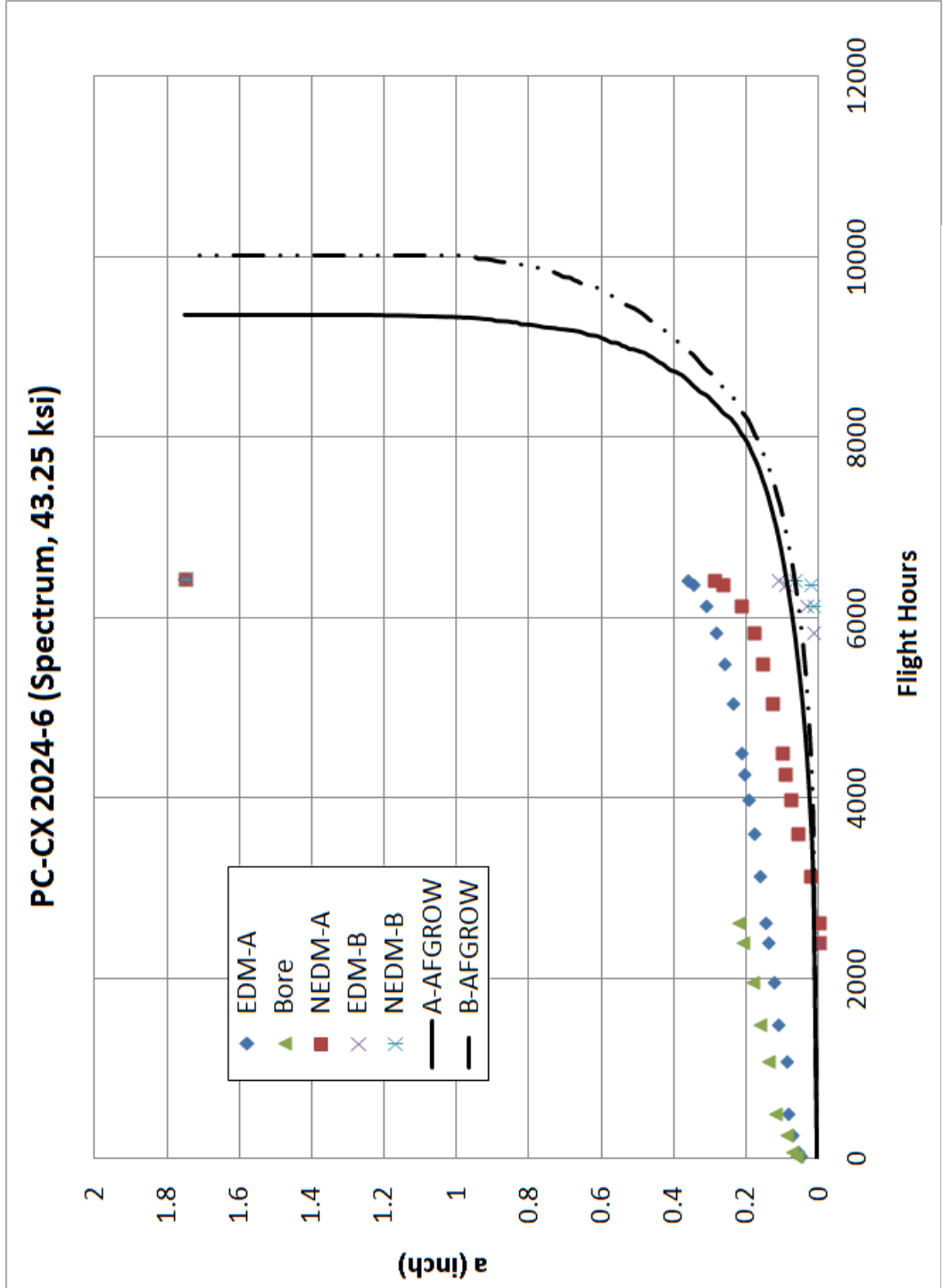


Fig. 48 Crack Growth for 43.25 ksi Spectrum Precracked Cold-Expanded Test

5. DISCUSSION

5.1. Cold-Expanded Holes and Precracked Cold-Expanded Holes

From the testing performed by Scott Carlson, the LIF for cold expansion from a clean fastener hole was found to be 71.4 for a stress ratio of 0.1 and with a maximum stress of 25.00 ksi.²⁶ The research conducted herein found that cold expansion of a precracked hole under the same loading yielded a LIF of only 60.8. This implies that the benefit of cold expansion is reduced by 15% for a hole that has a preexisting crack of 0.05 inches compared to a hole that has no detectable cracks prior to cold expansion.

It was expected that the existence of a 0.05 inch crack before cold expansion would cause a decrease in the life benefit due to cold expansion, and it was one of the goals of this research to quantify that decrease. However, some previous research indicated that for other 7075-T7351 aluminum alloy pre cracks on the order of 1 mm (0.039 inches) increase the benefit of cold expansion compared to the cold expansion of a hole without any detectable crack.²²

5.2. Benefit of Cold Expansion on Precracked Holes

The crack lengths of some specimens were measured after cold expansion and before final reaming to quantify the amount of crack extension due to the cold expansion process. The average crack growth along the surface was found to be 0.0014 inches and

the average crack growth observed down the bore was 0.003 inches. The crack extension due to cold expansion of all specimens is shown in Table 14 along with the applied and residual percent cold expansion for each specimen. It was noted that the applied and residual percent cold expansion was fairly consistent, and no obvious correlations between percent cold expansion and fatigue life were noticed.

5.2.1. Constant Amplitude Loading

At a maximum stress of 20.00 ksi, the average LIF for precracked cold-expanded holes was found to be 90.5. For a maximum stress of 25.00 ksi, the average LIF was found to be 60.8.

Although the data appear reasonable, a number of variables may have affected LIF of the constant amplitude tests. Primarily, the non-cold-expanded baseline that is being used for comparison was taken from the research done by Carlson in 2008.²⁶ The material used in Carlson's research was a different batch of aluminum than the tests done by the author. The material report for the aluminum used in Carlson's research demonstrated showed a yield strength 0.6 ksi lower than the material report of the aluminum used for this research.²⁶ The test specimens were also manufactured at different companies in different locations. The specimens in Carlson's research were manufactured (cut, drilled, etc.) by the Center for Aircraft Structural Life Extension (CAStLE) in Colorado, while the specimens for this research were manufactured by the Southwest Research Institute (SwRI) in San Antonio, Texas.

In addition to the different material batches, it was observed that the crack growth rate for the non-cold-expanded specimens tested by Carlson were an order of magnitude

higher than the crack growth rates measured by Carlson and the author for each of their ASTM standard E 647 specimens. These factors, however, were assumed to be of negligible significance as similar tolerances were specified for the manufacture of both sets of specimens, and lot variability for aluminum is generally small as it typically yields a Weibull β parameter greater than four.³⁹

5.2.2. Spectrum Loading

For spectrum loading, both the non-cold-expanded baseline and the precracked cold-expanded tests were performed by the author and the specimens came from the same batch of material. Therefore, none of the variables discussed for constant amplitude loading are applicable here. Rather, the primary variables for the spectrum loaded specimens were premature specimen failures in the grips, and an insufficient number of non-cold-expanded specimens to establish a confident baseline. The small number of non-cold-expanded specimens resulted in only one non-cold-expanded baseline test for the 43.25 ksi stress level, and no tests at a 30.00 ksi max stress. As a result the non-cold-expanded baseline for the 30.00 ksi stress level was an AFGROW prediction which used an interpolated SOLR from the SOLR values derived in this research for maximum stresses of 25.00 ksi and 33.00 ksi.

The average LIFs found in this research for precracked cold-expanded holes spectrum loaded with max stresses of 25, 30, 33, and 43.25 ksi were 22.35, 10.28, 6.57, and 1.33, respectively. (The LIF for the hole failure of the 25.00 ksi test was 26.38. This LIF, however, was not reported in the charts because the specimen was removed from the test frame, and reinserted in the test frame later. The author could not prove that stress

relaxation did not affect the test results, therefore the conservative LIF for the grip failure was used.) This clearly shows a decrease in cold expansion benefit for an increase in max stress as shown in Fig. 49. The decrease in LIF with an increase in max stress is likely due to the fact that cold expansion causes some finite residual compressive stress in the material. The stress applied to the specimen, then, must first overcome the compressive residual stress from cold expansion before inducing a tensile stress at the crack tip. At low stress levels the residual compressive stress from cold expansion prevents the crack tip from experiencing high tensile stresses causing significant fatigue life benefits. However, as the applied stress is increased, the residual compressive stress from cold expansion has a diminishing effect of decreasing the tensile stress at the crack tip.

Of particular importance here is the LIF for the 43.25 ksi max stress level. The LIF of only 1.33 gives a fatigue life that is less than two-thirds of the AFGROW predicted life assuming a 0.005 inch IFS. This indicates that the current USAF approach to account for cold expansion at a hole in analysis is nonconservative at some stress levels.

5.3. AFGROW Predictions

5.3.1. Lookup Files

The AFGROW predictions for the ASTM E 647 standard tests agreed with the tested life within an average of 15% using lookup file A, and agreed within 10 % using lookup file B. Lookup file B was created specifically to increase the agreement of the predicted life with the tested life for the ASTM E 647 standard tests. The primary

difference between these two lookup files is that lookup file A has a slightly lower crack growth rate for stress intensity factor ranges near 20 ksi $\sqrt{\text{in}}$ as shown in Fig. 38. This difference causes lookup file B to predict greater fatigue lives, even nonconservative fatigue lives as is the case for test 2024-2, than lookup file A. Therefore, AFGROW predictions that used lookup file B generally yielded greater fatigue lives than predictions that used lookup file A.

The primary motivation for using both lookup files was to observe the difference in predicted life from using a conservative lookup file to using a more liberal lookup file. To analyze the difference in life predictions of the two lookup files for precracked cold-expanded tests Table 15 was created. The table demonstrates that the difference in life prediction from the two lookup files for constant amplitude loading is less than 1% at both max stresses of 20.00 and 25.00 ksi. For spectrum loading, the average difference in agreement between the two lookup files is less than 6% for max stress levels less than 33.00 ksi. However, at the max stress of 43.25 ksi the difference in agreement raises to 11 % with lookup file A yielding the prediction with greater agreement. This is because at the 43.25 ksi max stress the assumed 0.005 inch IFS is no longer conservative, thus the more conservative lookup file yielded a prediction with greater agreement.

5.3.2. Precracked Cold-Expanded Predictions

The assumed benefit from cold expansion of a 0.005 inch IFS was selected by the USAF to ensure a conservative prediction in all cases.³⁵ To easily quantify and discuss the degree of conservation in the prediction models, a ratio of the predicted life and the tested life will be compared. These ratios for all loading conditions are provided in Table

16. From Table 16 it was noticed that the ratio of tested life to predicted life was far greater for the constant amplitude tests than for spectrum tests. This is likely related to the reason that greater cold expansion benefits have been observed for constant amplitude loading than for spectrum loading.²⁵ It was also observed from Table 16 that the AFGROW predictions grew increasingly less conservative as the stress increased. This is the same effect shown in Fig. 49.

5.3.3. Nonconservative Predictions Assuming 0.005 inch IFS

Until recently it has generally been assumed that changing the IFS in analysis to 0.005 inches to incorporate the benefit of a cold-expanded hole would always yield a conservative life prediction. The work of Andrew recently demonstrated that the 0.005 inch IFS approach yields nonconservative fatigue life predictions for short edge margin holes.²⁵ This research has demonstrated that at stresses above 43.25 ksi, the prediction is also nonconservative. For the spectrum file used at a max stress of 43.25 ksi the average stress is 11 ksi, the root mean square stress is 13 ksi, and the third quartile stress is 15.3 ksi. The yield stress for this batch was 48.1 ksi. Assuming a stress concentration factor of three due to the hole implies that any stress above 16 ksi causes plastic deformation at the hole. Thus, most loads in the upper quartile of the spectrum file for a max stress of 43.25 ksi are above yield and, therefore, cause plastic deformation at the hole. The root mean square, average, and third quartile stresses for each stress level investigated is provided in Table 17.

It should be noted that the tests carried out for this research were open hole tests, and most applications have some sort of fastener in the hole which reduce deformation,

stress and stress intensity at the crack tip. However, this does not affect the unconservative nature of the AFGROW prediction model approach, as the AFGROW predictions did not incorporate any fastener for crack retardation either.

The primary cause of so much variation in the 0.005 inch IFS approach is that it is not a physics based approach. Hoepfner has emphasized the importance and criticality of applying physics based models.^{40,41} Physics based models accurately account for any retardation effects, rather than making an assumption to modify the model predictions. There are a number of physics based approaches available to the USAF, even inside the AFGROW software package. AFGROW has some residual stress models that can be applied to account for the residual compression field of a cold-expanded hole. Other research has been successful at predicting the fatigue life of cold-expanded holes using such methods.^{19,20,28,29} A number of sources have indicated that cold expansion has little or no effect for crack lengths less than 0.039 inches.^{16,17,20,22} Yet, the method assumes a crack size smaller than that to account for the cold expansion benefits.

These two situations identified (short edge margins and high stresses) at which the 0.005 inch IFS is not conservative may not be the only scenarios at which the 0.005 inch IFS is nonconservative. The only way to confidently predict the fatigue life of cold-expanded holes will be to incorporate a physics based model that accounts for the effects of cold expansion, as was done by the researchers listed in the previous paragraph.

5.4. Error in Spectrum Loading

The Instron Random Loading software used to conduct the spectrum tests uses the Fatigue Research Advisory Group (FRAG) error verification system that tracks the

percent error for each load in the test and records the data for each point with error greater than a specified amount to a log file. The author performed all tests with the FRAG system set to record all loads with 2% error or greater, and it was observed that all errors recorded in the log files were less than 3%. Near completion of the testing, it was discovered that the error calculated by the FRAG system is the system error, rather than the absolute error of the current data point. (System error is the difference of command and feedback divided by the max range for the test. Absolute error is the difference in magnitude of command and feedback divided by the command load). The author then calculated the error for each point and found the average error from those points recorded in the test logs to be 2.69%, and the maximum error to be 10.38%. The maximum and average error percentages are summarized in Table 18. It should be noted that there were two error sets excluded from Table 18. One was the max error from test PC-CX 2024-1 was actually 38.21%, which was excluded because that occurred due to an operator error. The other excluded error was from the PC-CX 2024-5 test which actually had a maximum error of 17.27% and was excluded because this occurred due to the hydraulic pump overheating and shutting down.

While this information from the log files is informative it does not represent the accuracy of the entire test, as the log files only contained data points with system error greater than or equal to 2%. Therefore, in an attempt to further validate the accuracy of the spectrum loading, an error test was conducted. This error test ran through the spectrum file five times, and adjusted the controller settings to record every data point with system error greater than or equal to 0.01% (this was changed to 0% for some tests) in an attempt to capture every data point.

This error testing was conducted at three load rates, namely 100,000 lbs/sec, 200,000 lbs/sec, and 500,000 lbs/sec. The different load rates were investigated to assess whether a slower load rate would have improved the accuracy of the test data. The testing was also conducted at each of the max stress levels tested in this work, although incomplete data was obtained for the max stress of 43.25 ksi as the test specimen failed during this testing.

The results of this error testing indicated the average percent error for the testing conducted herein was always less than or equal to 2.1%. The max error observed was 21,881%, but it should be noted that the spectrum value at which this percent error was recorded was 0.00317, which is a load of less than 80 lbs. At loads this low small differences in applied load can cause large percent error. Thus, a large percent error at a point with a max load of 80 lbs is not of concern, as the percentage is not indicative of a large difference between command and feedback load.

A more useful indicator of the accuracy of a spectrum loading test than the percent error of each point is the damage parameter at each point. The damage parameter, Γ , is the ratio of the actual load applied to the command load raised to a power equal to the slope of the Paris equation, m , as shown.⁴²

$$\text{Damage Parameter} = \Gamma = \left(\frac{P_{\text{actual}}}{P_{\text{command}}} \right)^m \quad (8)$$

This damage parameter was introduced by McKeighan, and is a good indicator of how well loads are being reached throughout a spectrum file.⁴³ The exponent used for the calculation of the damage parameters for the tests conducted herein was 3, because it is a common value for the Paris equation. McKeighan explains that the damage

parameter indicates a percentage of actual flight represented by the test.⁴³ For example, a damage parameter of 0.8 indicates that if the test ran for 100 hours, the test is representative of 80 actual hours.

The average damage parameter value for this error testing was 1.00, indicating that the spectrum loads were achieved with sufficient accuracy to be representative of the spectrum file being used. The percent error and damage parameter for each of the conditions tested are presented in Table 19.

Table 14 Crack Extension from Cold Expansion and Percent Cold Expansion

Specimen ID's	Post Pre-Crack Diameter (inches)	Applied Percent Cold Expansion	Residual Percent Cold Expansion	Post Cold Expansion Diameter (inches)	Surface Crack Growth from Cold Expansion (inches)	Bore Crack Growth from Cold Expansion (inches)	LIF	CA or Spectrum	Max Stress (ksi)
PC-CX 2024-1	0.476945	3.47%	2.24%	0.48787	N/A	N/A	5.91	Spectrum	33.00
PC-CX 2024-2	0.476695	3.53%	2.48%	0.488795	N/A	N/A	7.34	Spectrum	33.00
PC-CX 2024-3	0.476595	3.55%	2.49%	0.48877	N/A	N/A	6.47	Spectrum	33.00
PC-CX 2024-4	0.47682	3.50%	2.43%	0.488695	N/A	N/A	9.89	Spectrum	30.00
PC-CX 2024-5	0.476495	3.57%	2.51%	0.488745	N/A	N/A	22.35	Spectrum	25.00
PC-CX 2024-6	0.477045	3.45%	2.41%	0.488845	N/A	N/A	1.38	Spectrum	43.25
PC-CX 2024-7	0.47657	3.55%	2.52%	0.488895	N/A	N/A	1.26	Spectrum	43.25
PC-CX 2024-8	0.47657	3.55%	2.51%	0.48882	N/A	N/A	1.36	Spectrum	43.25
PC-CX 2024-9	0.47555	3.77%	2.68%	0.48865	0.00086	0.00343	68.29	CA	25.00
PC-CX 2024-10	0.47555	3.77%	2.68%	0.48865	0.00480	None Observed	63.62	CA	25.00
PC-CX 2024-11	0.4757	3.74%	2.74%	0.4891	0.00172	None Observed	50.51	CA	25.00
PC-CX 2024-12	0.475675	3.75%	2.60%	0.488375	0.00200	None Observed	9.58	Spectrum	30.00
PC-CX 2024-13	0.4757	3.74%	2.61%	0.48845	0.00238	0.00532	11.39	Spectrum	30.00
PC-CX 2024-14	0.475625	3.76%	2.60%	0.488325	None Observed	0.00267	119.90	CA	20.00
PC-CX 2024-15	0.47575	3.73%	2.60%	0.48845	None Observed	None Observed	29.58	CA	20.00
PC-CX 2024-16	0.47585	3.71%	2.58%	0.488475	0.00078	None Observed	64.31	CA	20.00
PC-CX 2024-17	0.47575	3.73%	2.62%	0.48855	0.00014	0.01644	148.42	CA	20.00

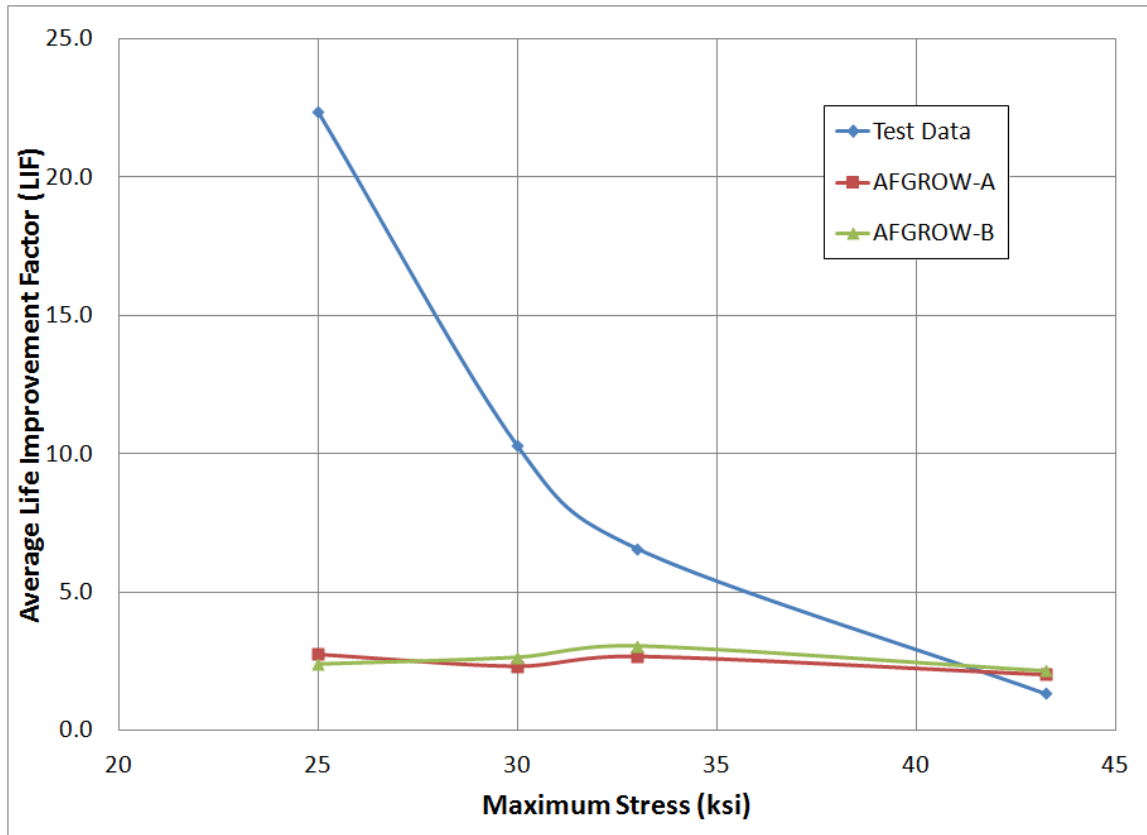


Fig. 49 Life Improvement Factor and Maximum Stress Correlation

Table 15 AFGROW Prediction Average Percent Disagreement for Precracked Cold-Expanded Tests

Loading	Max Stress (ksi)	Average Percent Disagreement Lookup File A	Average Percent Disagreement Lookup File B
Constant Amplitude	20.00	98.21%	98.13%
	25.00	95.04%	94.77%
Spectrum	25.00	87.71%	89.25%
	30.00	77.34%	74.10%
	33.00	58.94%	53.16%
	43.25	-51.13%	-62.02%

Table 16 Ratios of Tested Life to AFGROW Predicted Life for Precracked Cold-Expanded Tests

Loading	Max Stress (ksi)	Average Ratio of Tested Life to Predicted Life Lookup File A	Average Ratio of Tested Life to Predicted Life Lookup File B
Constant Amplitude	20.00	81.60	77.92
	25.00	20.49	19.45
Spectrum	25.00	8.13	9.30
	30.00	4.44	3.88
	33.00	2.45	2.15
	43.00	0.66	0.62

Table 17 Spectrum Stress Distributions

Max Stress (ksi)	Average Stress	RMS Stress	3rd Quartile Stress
25.00	6.31	7.49	8.85
30.00	7.58	8.99	10.62
33.00	8.33	9.87	11.68
43.25	10.92	12.96	15.31

Table 18 Maximum and Average Error Calculated from FRAG Log Files

Specimen ID	Max Stress (ksi)	Max Error	Average Error
NCX 2024-1	33.00	0.00%	0.00%
NCX 2024-2	33.00	7.14%	3.26%
NCX 2024-3	33.00	5.83%	2.91%
NCX 2024-4	25.00	6.78%	2.48%
NCX 2024-5	25.00	6.81%	2.39%
NCX 2024-6	25.00	6.93%	2.43%
NCX 2024-7	43.25	7.04%	4.49%
PC-CX 2024-1	33.00	5.01%	2.29%
PC-CX 2024-2	33.00	8.03%	2.27%
PC-CX 2024-3	33.00	9.08%	2.38%
PC-CX 2024-4	30.00	8.24%	2.41%
PC-CX 2024-5	25.00	8.87%	2.48%
PC-CX 2024-6	43.25	7.53%	4.57%
PC-CX 2024-7	43.25	7.15%	4.51%
PC-CX 2024-8	43.25	6.67%	4.37%
PC-CX 2024-12	30.00	10.38%	2.53%
PC-CX 2024-13	30.00	0.06%	0.02%
Overall Max:			10.38%
Overall Average:			2.69%

Table 19 Spectrum Loading Validation Tests

Max Stress (ksi)	Load Rate (kip/sec)	Average Absolute Percent Error	Average Damage Parameter
43.25	500	1.18%	1.04
33.00	500	1.66%	1.05
	200	2.50%	1.01
	100	2.50%	0.97
30.00	500	1.52%	1.00
	200	1.35%	0.98
	100	1.81%	0.97
25.00	500	2.10%	1.00
	200	1.56%	0.99
	100	2.02%	0.97

6. SUMMARY

6.1. Conclusions

6.1.1. ASTM E 647 Standard Tests

The ASTM E 647 standard tests performed in this research demonstrated the equipment, techniques, operators, and methods used for the material testing performed in this research is consistent with ASTM standard requirements. Furthermore, the data generated from the ASTM E 647 tests were consistent with the data generated by Carlson in his research on cold-expanded holes in the 2024-T351 aluminum alloy.²⁶

6.1.2. Spectrum Fatigue Life

The average fatigue life for the tested geometry and A-10 spectrum loading was 31,518.78 flight hours for a max stress of 25.00 ksi, 12,252 flight hours for a max stress of 33.00 ksi, and 4,657 flight hours. These fatigue lives matched reasonably with AFGROW predictions using standard A-10 lookup files and SOLRs.

6.1.3. Precracked Cold Expansion Benefit under

Constant Amplitude Loading

The average precracked cold-expanded fatigue life for the tested geometry under constant amplitude loading with a stress ratio of 0.1 was 4,296,067 cycles for a max

stress of 20.00 ksi, and 452,585 cycles for a max stress of 25.00 ksi. That yields a LIF of 90.5 and 60.8 for the max stress of 20.00 ksi and 25.00 ksi, respectively when compared against the constant amplitude data from Carlson as a baseline. This benefit is approximately 15% less than the benefit of the cold-expanded specimens tested by Carlson with no crack detected before cold expansion.²⁶

6.1.4. Precracked Cold Expansion Benefit under Spectrum Loading

The average fatigue lives of precracked cold-expanded specimens under spectrum loading were 704,450 flight hours for a max stress of 25.00 ksi, 194,950 flight hours for a max stress of 30.00 ksi, 80,220 flight hours for a max stress of 33.00 ksi, and 6,201 flight hours for a max stress of 43.25 ksi. These average fatigue lives indicate LIFs of 22.35, 10.28, 6.57, and 1.33 for the max stresses of 25, 30, 33, and 43.25 ksi, respectively.

6.1.5. AFGROW 0.005 inch IFS Assumption

The 0.005 inch IFS assumption to account for the benefit of cold expansion predicted lives nine times shorter than the tested life at 25.00 ksi max stress, and one and a half times greater than the tested life at 43.25 ksi max stress. The 0.005 inch IFS assumption is prone to be extremely conservative at some stress levels, and unconservative at other stress levels. The 0.005 inch IFS yields an LIF of approximately two for all stress levels.

6.2. Recommendations

The observations and conclusions obtained from this research project provide useful information on the implementation of cold expansion. Based on the conclusions

from this research some recommendations have been made for fatigue design and prediction of cold-expanded holes:

1. Employ a physics based model to account for cold expansion benefits in fatigue life predictions.
2. Investigate residual stress models in AFGROW to determine if one could be a suitable model for analyzing cold expansion effects on fatigue life.
3. Perform further research to validate cold expansion of a gouged or otherwise damaged hole to assess when a hole can be cold-expanded rather than oversized.
4. Continue to cold-expand critical fastener holes, as the life benefit was observed to be up to a factor of 90.5 for a maximum stress of 25.00 ksi.
5. When using a 0.005 inch IFS model in AFGROW, investigate running a separate model in AFGROW using the physics based residual stress models for cold expansion, and verify that the 0.005 inch IFS prediction is conservative compared to the residual stress model before recommending an inspection interval.

6.3. Further Research Possibilities

The conclusions of this research are informative and useful. They have also brought to light further questions that should be tested and researched for further understanding of the effects of cold expansion:

1. Test precracked cold-expanded specimens at varying stress levels to identify the stress at which the 0.005 inch IFS assumption yields nonconservative predictions.
2. Test cold-expanded and precracked cold-expanded specimens with various edge margins to establish the decreasing benefit with the approaching free edge.
3. Test the effects of various fasteners in the hole for cold-expanded and precracked cold-expanded specimens under spectrum loading.
4. Test the effects of corrosion pits and a corrosive environment on the fatigue benefit of cold-expanded and precracked cold-expanded specimens under spectrum loading.
5. Quantify the residual stress from cold expansion at crack tips, corrosion pits, or other defects that may be present in the fastener hole.

6. Test the effects of gouges or other organic damage induced before and after cold expansion.
7. Conduct further testing to evaluate the da/dN vs. ΔK curve and investigate modifications to the current A-10 tabular lookup file to capture effects observed in this research.

APPENDIX A

MATERIAL CERTIFICATION SHEET



CERTIFIED TEST REPORT
<http://Certs.KaiserAluminum.com>

Kaiser Aluminum
 Trentwood Works
 Spokane, WA 99205-5108
 (800) 367-2586

CUSTOMER PO NUMBER: 5400078947-0010		WORK PACKAGE:	CUSTOMER PART NUMBER: ALFLR00822-48.5		PRODUCT DESCRIPTION: Sawed Plate
KAISER ORDER NUMBER: 1105438	LINE ITEM: 1	SHIP DATE: 11/12/2010	ALLOY: 2024	CLAD: BARE	TEMPER: T351
WEIGHT SHIPPED: 4172 LB	QUANTITY: 23 PCS EST.	B/L NUMBER: 2029605	GAUGE: 0.2500 IN	WIDTH: 48.500 IN	LENGTH: 144.500 IN
SHIP TO: COPPER & BRASS SALES 5450 EAST HOME FRESNO, CA 93727 US			SOLD TO: COPPER & BRASS SALES ATTN: ACCOUNTS PAYABLE P.O. Box 5116 SOUTHFIELD, MI 48086 US		

Certified Specifications

AMS 4037/RevN AMS-QQ-A-250/4/RevA ASTM B 209/Rev07 CMMP 025/RevT

Test Code: 1504

Test Results:

LOT: 521928A2 CAST: 513 DROP: 05 INGOT: 3

(ASTM E8/B557)
 (EN 2002-1)

Tensile: Temper	Dir/#Tests	Ultimate KSI (MPA)	Yield KSI (MPA)	Elongation %
T351	LT / 02 (Min:Max)	68.4 : 69.0 (472 : 476)	48.1 : 48.6 (332 : 335)	17.4 : 17.6

(ASTM E1251)

Chemistry:	SI	FE	CU	MN	MG	CR	ZN	TI	V	ZR	OTHER
Actual	0.08	0.20	4.4	0.56	1.3	0.01	0.16	0.02	0.01	0.00	TOT 0.03

Chemistry:	SI	FE	CU	MN	MG	CR	ZN	TI	V	ZR	OTHER
2024	MIN 0.00	0.00	3.8	0.30	1.2	0.00	0.00	0.00	0.00	0.00	MAX 0.05
	MAX 0.50	0.50	4.9	0.9	1.8	0.10	0.25	0.15	0.05	0.05	TOT 0.15

Aluminum Remainder

CERTIFICATION

Kaiser Aluminum Fabricated Product, LLC (Kaiser) hereby certifies that metal shipped under this order was melted in the United States of America or a qualifying country per DFARS 225.872-1(a), was manufactured in the United States of America, and meets the requirements of DFARS 252.225 for domestic content. This material has been inspected, tested and found in conformance with the requirements of the applicable specifications as indicated herein. All metal which is solution heat treated complies with AMS 2772. Any warranty is limited to that shown on Kaiser's standard general terms and conditions of sale. Test reports are on file, subject to examination. Test reports shall not be reproduced except in full, without the written approval of Kaiser Aluminum Fabricated Products, LLC laboratory. The recording of false, fictitious or fraudulent statements or entries on the certificate may be punished as a felony under federal law. ISO-9001:2000 certified.

BILL POYNOR, LABORATORIES SUPERVISOR

Plant Serial: 4210062

Kaiser Order Number: 1105438

Fig. 50 Material Certification Data Sheet

APPENDIX B

FATIGUE CRACK GROWTH TEST DATA SHEETS

2024-1 Fatigue Crack Growth Data Sheet

Width: 3.9995 in. Thick: 0.253 in. Area: 1.0118 in²

Precrack Information

Precrack Date: 17-Jul-11 Loading Condition: Constant Amplitude R=0.1
 Frequency: 20 Hz Hole Diameter: 0.10094 in. Peak Stress: 11.1 ksi
 Surface EDM Length: 0.02034 in.

Testing Information

Test Date: 17-Jul-11 Loading Condition: Constant Amplitude R= 0.1
 Frequency: 20 Hz Hole Diameter: N/A in.
 Peak Stress: 11.4 ksi Surface EDM Length: N/A in. Bore EDM Length: N/A in.

Total Cycles	Measured Crack Length (inches)				Comments
	EDM		NEDM		
	A	B	A	B	
32377	0.07081	0.07069	0.07025	0.07208	Test Started 17-Jul-2011
34445	0.07601	0.07069	0.07443	0.07559	
38449	0.07601	0.07069	0.07537	0.07745	
43495	0.07611	0.07599	0.07661	0.07771	
48511	0.07779	0.07599	0.07753	0.07851	
53534	0.07997	0.07929	0.07995	0.07943	
58661	0.07997	0.07937	0.08029	0.08189	
64545	0.08337	0.08069	0.08143	0.08243	
69875	0.08337	0.08201	0.08291	0.08319	
75020	0.08337	0.08271	0.08539	0.08483	
80218	0.08357	0.08343	0.08617	0.08521	
87017	0.08423	0.08595	0.08787	0.08647	
97037	0.08781	0.08885	0.08859	0.08719	
107114	0.09711	0.09399	0.09145	0.09029	
117279	0.09711	0.09583	0.09177	0.09379	
127584	0.09939	0.09841	0.09417	0.09595	
138158	0.10069	0.10585	0.09549	0.10199	
148460	0.10675	0.10585	0.09905	0.10507	
159668	0.11349	0.10757	0.10185	0.10637	
170666	0.11971	0.11091	0.10667	0.10777	
181832	0.11995	0.11841	0.11331	0.11109	
192917	0.13429	0.12611	0.12083	0.11391	Pre Crack Ends

2024-1 Test Data (Continued)

Total Cycles	Measured Crack Length (inches)				Comments
	EDM		NEDM		
	A	B	A	B	
0	0.13801	0.13174	0.13105	0.11949	
10513	0.13937	0.13723	0.13899	0.12677	
21679	0.16333	0.14851	0.14845	0.13123	
32032	0.18715	0.16017	0.15513	0.14223	
49292	0.20695	0.20173	0.18995	0.16069	
60775	0.20713	0.23009	0.22367	0.19367	
70881	0.25655	0.27187	0.26477	0.23817	
82413	0.34971	0.34601	0.35043	0.31399	
93109	0.44355	0.45075	0.45687	0.42039	
103138	0.60947	0.59103	0.56719	0.59803	
118006	0.76685	0.72827	0.77927	0.78387	
122719	0.82993	0.78475	0.83467	0.82915	
127530	0.98797	0.79053	0.97493	0.93291	
131498	1.18945	1.11911	1.20837	1.09105	
133769	1.93911	1.93917	1.93939	1.93866	Failure

2024-2 Fatigue Crack Growth Data Sheet

Width: 3.9985 in. Thick: 0.2535 in. Area: 1.0136 in²

Precrack Information

Precrack Date: 18-Jul-11 Loading Condition: Constant Amplitude R=0.1
 Frequency: 20 Hz Hole Diameter: 0.10197 in. Peak Stress: 11.4 ksi
 Surface EDM Length: 0.01934 in.

Testing Information

Test Date: 18-Jul-11 Loading Condition: Constant Amplitude R= 0.1
 Frequency: 20 Hz Hole Diameter: N/A in.
 Peak Stress: 11.4 ksi Surface EDM Length: N/A in. Bore EDM Length: N/A in.

Total Cycles	Measured Crack Lengths (inches)				Comments
	EDM		NEDM		
	A	B	A	B	
29214	0.06954	0.07156	0.07634	0.07694	Started Test 18-Jul-2011
34252	0.06954	0.0763	0.07482	0.07904	
48725	0.07776	0.08292	0.07864	0.08104	
63741	0.08264	0.09144	0.08066	0.0835	
78904	0.08584	0.0982	0.08104	0.08742	
94156	0.0925	0.10396	0.09482	0.09388	
109197	0.1009	0.10868	0.10368	0.10036	
125280	0.10722	0.11232	0.1112	0.10282	
140572	0.11224	0.11968	0.12286	0.11242	Pre Crack Ends
153304	0.1174	0.12656	0.13406	0.1254	
159403	0.12296	0.12678	0.13494	0.13694	
165556	0.12612	0.12976	0.1411	0.13844	
171937	0.13396	0.13766	0.15132	0.1436	
178403	0.13408	0.14026	0.15876	0.14458	
183660	0.1385	0.14702	0.16518	0.16282	
189832	0.1488	0.15136	0.1731	0.17332	
195005	0.14924	0.1582	0.18698	0.18012	
200679	0.15894	0.16906	0.1971	0.19448	
206926	0.1725	0.18198	0.21034	0.2113	
214395	0.19922	0.1986	0.23918	0.24024	
220580	0.23736	0.23108	0.26422	0.27158	
223933	0.25404	0.2469	0.27772	0.2959	

2024-2 Test Data (Continued)

Total Cycles	Measured Crack Lengths (inches)				Comments
	EDM		NEDM		
	A	B	A	B	
227382	0.27516	0.2702	0.28926	0.3082	
230806	0.29654	0.28994	0.31146	0.32274	
235481	0.33448	0.33954	0.35152	0.35224	
239282	0.36114	0.3669	0.38492	0.37736	
243510	0.38474	0.41496	0.43502	0.43864	
248469	0.45812	0.45746	0.48056	0.50774	
252237	0.50696	0.53096	0.52586	0.55066	
255787	0.58754	0.59294	0.47546	0.61206	
258925	0.63856	0.63492	0.62136	0.67688	
262260	0.67734	0.67428	0.70054	0.75462	
265444	0.72668	0.71916	0.75492	0.82968	
268994	0.84146	0.90338	0.8271	0.89978	
272272	0.91728	1.0229	0.90172	1.0194	
275452	1.02942	1.19266	1.06354	1.20262	
277796	2	2	2	2	Failure

NCX 2024-1 Fatigue Crack Growth Data Sheet

Width: 3.9911 in. Thick: 0.2535 in. Area: 1.0117 in²

Precrack Information

Precrack Date: 1-Aug-11 Loading Condition: Constant Amplitude R=0.1
 Frequency: 20 Hz Hole Diameter: 0.47717 in. Peak Stress: 9 ksi
 Surface EDM Length: 0.01402 in.

Testing Information

Test Date: 13-Oct-11 Loading Condition: Spectrum
 Loading Rate: 500,000 lbs/s Hole Diameter: 0.497695 in.
 Peak Stress: 33 ksi Surface EDM Length: 0.0067 in. Bore EDM Length: 0.0044 in.

Flight Hours	Measured Crack Length (inches)				Comments	
	EDM		NEDM			Bore
	A	B	A	B		
52	0.0644				0.086793	Tuning cycles;
20	0.10888				0.132532	load rate 80,000 lbs/sec
239	0.12286				0.151978	load rate 200,000 lbs/sec
478	0.12964				0.169294	
718	0.13428				0.174833	
958	0.13996				0.185241	
1198	0.14342				0.195801	pped to 450,000 lbs/sec
1678	0.15472				0.211717	
2158	0.1696				0.231832	
2638	0.18328		0.02854			
3118	0.2013		0.07048			
3598	0.21982		0.10354			
4078	0.23722		0.13852			
4556	0.25836		0.16744			
5037	0.27908		0.19792			pped to 500,000 lbs/sec
5357	0.29232		0.2224			pped to 550,000 lbs/sec
5828	0.31388		0.24636			ropped to 500,000 lbs/sec
6359	0.33236		0.27576			
6706	0.35014		0.29926			

NCX 2024-1 Test Data (Continued)

Flight Hours	Measured Crack Length (inches)					Comments
	EDM		NEDM		Bore	
	A	B	A	B		
7206	0.3713		0.32114			
7707	0.39216		0.34724			
8402	0.4175		0.38744			
9117	0.44622		0.4147			
9610	0.47066		0.45198			
10013	0.4995		0.47964			
10452	0.52942		0.51438			
10797	0.5675		0.55048			
11148	0.59722	0.13956	0.58166	0.16134		
11517	0.65098	0.19144	0.6343	0.213		
11997	0.7419	0.29002	0.72872	0.3059		
12168	1.7534025	1.746703	1.746703	1.746703		Failure

NCX 2024-2 Fatigue Crack Growth Data Sheet

Width: 3.998 in. Thick: 0.254 in. Area: 1.0154 in²

Precrack Information

Precrack Date: 1-Aug-11 Loading Condition: Constant Amplitude R=0.1
 Frequency: 20 Hz Hole Diameter: 0.476995 in. Peak Stress: 9 ksi
 Surface EDM Length: 0.01988 in.

Testing Information

Test Date: 14-Oct-11 Loading Condition: Spectrum
 Loading Rate: 500,000 lbs/s Hole Diameter: 0.496895 in.
 Peak Stress: 33 ksi Surface EDM Length: 0.0102 in. Bore EDM Length: 0.0078 in.

Flight Hours	Actual Flaw Length (inches)				Bore	Comments
	Surface of Hole					
	EDM		NEDM			
	A	B	A	B		
48	0.06758				0.094501	Tuning
267	0.08712				0.11586	
845	0.10952				0.14249	
1198	0.12164				0.157129	
1678	0.13454				0.178712	
2158	0.15164				0.199709	
2638	0.17252				0.218977	
3118	0.19582		0.01512			
3598	0.21312		0.07352			
4078	0.23552		0.11344			
4557	0.25728		0.1521			
5037	0.28216		0.19612			
5517	0.3044		0.22542			
5997	0.32566		0.2578			
6477	0.35196		0.29054			
6957	0.37702		0.31802			
7437	0.40362		0.35006			
7917	0.4256		0.3693			
8397	0.45628		0.41018			
8877	0.47904		0.43618			

NCX 2024-2 Test Data (Continued)

Flight Hours	Actual Flaw Length (inches)				Bore	Comments
	Surface of Hole					
	EDM		NEDM			
	A	B	A	B		
9357	0.50486		0.4729			
9837	0.5458	0.04328	0.50182	0.06166		
10317	0.6003	0.12978	0.56208	0.13144		
10557	0.63706	0.16778	0.60622	0.17636		EC=34; N-EDM-A branching
10797	0.68332	0.20938	0.66094	0.21558		
11037	0.75752	0.29086	0.75284	0.30294		
11137	1.7602	1.75	1.75	1.75		Failure

NCX 2024-3 Fatigue Crack Growth Data Sheet

Width: 4.0015 in. Thick: 0.2535 in. Area: 1.0143 in²

Precrack Information

Precrack Date: 2-Aug-11 Loading Condition: Constant Amplitude R=0.1
 Frequency: 20 Hz Hole Diameter: 0.47632 in. Peak Stress: 7.5 ksi
 Surface EDM Length: 0.01362 in.

Testing Information

Test Date: 1-Nov-11 Loading Condition: Spectrum
 Loading Rate: 500,000 lbs/s Hole Diameter: 0.49872 in.
 Peak Stress: 33 ksi Surface EDM Length: 0.00466 in. Bore EDM Length: 0.0029 in.

Flight Hours	Actual Crack Length (inches)				Bore	Comments
	Surface of Hole					
	EDM		NEDM			
	A	B	A	B		
0	0.0465				0.080706	
294	0.0573				0.095581	
953	0.07422				0.11847	
1648	0.08824				0.132628	
2471	0.10556				0.153959	
3372	0.1293				0.182274	
4231	0.1578				0.21901	
4877	0.18254		0.02396			
5362	0.20434		0.07372			
5791	0.22302		0.11194			
6377	0.2491		0.15774			
6885	0.27102		0.19768			
7306	0.2921		0.23078			
7678	0.31136		0.24884			
8140	0.33554		0.27718			
8704	0.36246		0.3083			
9331	0.3933		0.34946			
9796	0.41784		0.37452			
10191	0.43922	0.01538	0.39486			
10614	0.46064	0.02154	0.41868			
10846	0.47906	0.03678	0.43414			
11315	0.51306	0.06692	0.46238			

NCX 2024-3 Test Data (Continued)

Flight Hours	Actual Crack Length (inches)				Bore	Comments
	Surface of Hole					
	EDM		NEDM			
	A	B	A	B		
11710	0.54014	0.09662	0.49722			
11991	0.56478	0.11884	0.5296	0.03616		
12105	0.57966	0.12308	0.54086	0.04682		
12340	0.59792	0.15164	0.56192	0.07316		
12539	0.62368	0.19352	0.58072	0.10148		
12740	0.65118	0.20448	0.611	0.13218		
12942	0.68608	0.23948	0.64942	0.17198		
13176	0.76084	0.30644	0.74712	0.29362		
13289	0.79096	0.33642	0.78322	0.3016		
13297	1.75605	1.75139	1.75139	1.75139	Failure	

NCX 2024-4 Fatigue Crack Growth Data Sheet

Width: 3.9975 in. Thick: 0.253 in. Area: 1.0113 in²

Precrack Information

Precrack Date: 3-Aug-11 Loading Condition: Constant Amplitude R=0.1
 Frequency: 20 Hz Hole Diameter: 0.36897 in. Peak Stress: 7.5 ksi
 Surface EDM Length: 0.01522 in.

Testing Information

Test Date: 3-Nov-11 Loading Condition: Spectrum
 Loading Rate: 500,000 lbs/s Hole Diameter: 0.49852 in.
 Peak Stress: 25 ksi Surface EDM Length: 0.00738 in. Bore EDM Length: 0.0042 in.

Flight Hours	Actual Crack Length (inches)				Bore	Comments
	Surface of Hole					
	EDM		NEDM			
	A	B	A	B		
0	0.0471				0.071429	
827	0.05716				0.084993	
2860	0.07594				0.099401	
4990	0.09502				0.122949	
7020	0.1208				0.155578	
8538	0.1469				0.184744	
10596	0.18758				0.220458	
11738	0.21462		0.04944			
12389	0.2314		0.1125			
13455	0.2621		0.1741			
14478	0.28594		0.21762			
15707	0.31714		0.26438			
16481	0.34258		0.28848			
17055	0.3562		0.30836			
18059	0.38226		0.34252			
18987	0.4067		0.37688			
19799	0.43584		0.39844			
20830	0.46756		0.43578			
21954	0.49684		0.4727			
22635	0.51868		0.49942			

NCX 2024-4 Test Data (Continued)

Flight Hours	Actual Crack Length (inches)				Bore	Comments
	Surface of Hole					
	EDM		NEDM			
	A	B	A	B		
23270	0.53902		0.51774			
23968	0.56114		0.5451			
24531	0.57888		0.56236			
24798	0.58738		0.5715			
25217	0.59806		0.58914			
25413	0.61032		0.59492			Stopped: 5:15, 3-Nov-2011
25615	0.62194		0.59966			Started: 11:00, 4-Nov-2011
25959	0.63702		0.61436			
26383	0.64864		0.632			
26848	0.66512		0.6528	0.01056		
27738	0.69808	0.0602	0.69478	0.0412		
28340	0.73108	0.09476	0.72924	0.09306		
28918	0.76202	0.1316	0.75988	0.12568		
29364	0.78484	0.15356	0.79292	0.15638		
29854	0.82224	0.18344	0.82336	0.18234		
30643	0.87762	0.23268	0.88406	0.23616		
31211	0.92824	0.27346	0.94568	0.27694		
31790	1.00284	0.32374	1.0174	0.32954		
32109	1.1414	0.41528	1.15196	0.43182		
32181	1.22152	0.46524	1.23996	0.47796		
32213	1.75738	1.75	1.75	1.75		Failure

NCX 2024-5 Fatigue Crack Growth Data Sheet

Width: 3.9995 in. Thick: 0.253 in. Area: 1.0118 in²

Precrack Information

Precrack Date: 3-Aug-11 Loading Condition: Constant Amplitude R=0.1
 Frequency: 20 Hz Hole Diameter: 0.47652 in. Peak Stress: 7.5 ksi
 Surface EDM Length: 0.01296 in.

Testing Information

Test Date: 8-Nov-11 Loading Condition: Spectrum
 Loading Rate: 500,000 lbs/s Hole Diameter: 0.497145 in.
 Peak Stress: 25 ksi Surface EDM Length: 0.00838 in. Bore EDM Length: 0.0079 in.

Flight Hours	Actual Crack Length (inches)				Bore	Comments
	Surface of Hole					
	EDM		NEDM			
	A	B	A	B		
0	0.0498				0.07489	Started 9:00, 8-Nov-2011
814	0.05752				0.087474	
2443	0.0747				0.10271	
4525	0.09434				0.1223	
6321	0.11886				0.147467	
8468	0.15686				0.183178	
9569	0.17842				0.204196	
11489	0.22896		0.07372			
12920	0.2626		0.18088			
13934	0.28698		0.2153			
14733	0.31356		0.24396			
15561	0.33658		0.27772			
16621	0.35964		0.31554			
17447	0.381		0.34536			
18392	0.40272		0.37714			
19395	0.4415		0.41518			
20506	0.47202		0.45246			
21567	0.51054		0.4883			
22123	0.52624		0.50196			Stopped 5:30

NCX 2024-5 Test Data (Continued)

Flight Hours	Actual Crack Length (inches)				Bore	Comments
	Surface of Hole					
	EDM		NEDM			
	A	B	A	B		
22752	0.5466		0.52812			Started 6:45, 10-Nov-2011
23656	0.57904		0.55868			
24507	0.60528		0.58498			
25528	0.63794		0.61868			
26180	0.65992		0.6475			
27138	0.69764		0.6812			
27987	0.72596		0.71492			
28667	0.75154		0.74702			
29483	0.79324		0.7903			
30148	0.82996		0.832			
31108	0.88188		0.8838	0.21744		
31786	0.92686	0.24768	0.93374	0.2639		
32589	1.023	0.32948	1.02342	0.33988		
32736	1.04438	0.34504	1.04142	0.36184		
32976	1.75838	1.75	1.75	1.75		Failure

NCX 2024-6 Fatigue Crack Growth Data Sheet

Width: 4.006 in. Thick: 0.253 in. Area: 1.0135 in²

Precrack Information

Precrack Date: 4-Aug-11 Loading Condition: Constant Amplitude R=0.1
 Frequency: 20 Hz Hole Diameter: 0.47692 in. Peak Stress: 9 ksi
 Surface EDM Length: 0.01312 in.

Testing Information

Test Date: 22-Nov-11 Loading Condition: Spectrum
 Loading Rate: 500,000 lbs/s Hole Diameter: 0.498745 in.
 Peak Stress: 25 ksi Surface EDM Length: 0.00742 in. Bore EDM Length: 0.0043 in.

Flight Hours	Actual Crack Length (inches)				Bore	Comments
	Surface of Hole					
	EDM		NEDM			
	A	B	A	B		
0	0.05468				0.096736	
1361	0.07536				0.117467	
3062	0.09506				0.133855	
5317	0.13018				0.162196	
6244	0.1468				0.18083	
6926	0.16338				0.194072	
8057	0.1903				0.216331	
9126	0.21182		0.055572			
9910	0.23228		0.12188			
10890	0.25448		0.17342			
11807	0.27926		0.21324			
12590	0.303		0.2461			
13219	0.32234		0.26928			
13877	0.34376		0.29558			
14989	0.37196		0.33636			
16281	0.41		0.38082			
17558	0.45104		0.4233			
18605	0.47946		0.45784			
19840	0.52198		0.50428			
20841	0.55504		0.54136			

NCX 2024-6 Test Data (Continued)

Flight Hours	Actual Crack Length (inches)				Bore	Comments
	Surface of Hole					
	EDM		NEDM			
	A	B	A	B		
21699	0.58274		0.56988			
22573	0.61386		0.60422			
23559	0.64424		0.63854			
24567	0.68212		0.67946	0.02622		
25295	0.71326	0.0426	0.71196	0.0532		
26362	0.7778	0.10264	0.77266	0.11222		
27334	0.83706	0.16628	0.84082	0.1732		
28159	0.9061	0.23398	0.9144	0.23736		
29261	1.10772	0.3966	1.0954	0.39618		
29376	1.75742	1.75	1.75	1.75		Failed

NCX 2024-7 Fatigue Crack Growth Data Sheet

Width: 4.004 in. Thick: 0.25 in. Area: 1.001 in²

Precrack Information

Precrack Date: 3-Jan-12 Loading Condition: Constant Amplitude R=0.1
 Frequency: 20 Hz Hole Diameter: 0.4762 in. Peak Stress: 20 ksi
 Surface EDM Length: 0.0105 in.

Testing Information

Test Date: 11-Jan-12 Loading Condition: Spectrum
 Loading Rate: 500,000 lbs/s Hole Diameter: 0.50225 in.
 Peak Stress: 43.25 ksi Surface EDM Length: 0 in. Bore EDM Length: 0.0000 in.

Flight Hours	Actual Crack Length (inches)				Bore	Comments
	Surface of Hole					
	EDM		NEDM			
	A	B	A	B		
0	0.04264				0.028287	
47	0.04942				0.045563	
134	0.05976				0.053916	
299	0.0673				0.067639	
677	0.0838				0.097255	
857	0.09164				0.114179	
995	0.0972				0.120688	
1300	0.11114				0.141544	
1606	0.12938				0.174279	
1783	0.14138				0.190687	
1913	0.15834				0.202701	
2211	0.17368				0.231721	
2375	0.18616		0.05894			
2487	0.19466		0.07468			
2600	0.20572		0.10244			
2740	0.21974		0.12234			
2846	0.23216		0.14352			
3005	0.2486		0.16744			
3249	0.27424		0.19656			
3463	0.29248		0.22044			

NCX 2024-7 Test Data (Continued)

Flight Hours	Actual Crack Length (inches)				Bore	Comments
	Surface of Hole					
	EDM		NEDM			
	A	B	A	B		
3608	0.31072		0.24248			
3782	0.32926		0.26338			
4050	0.36002		0.29856			
4174	0.3703	0.01692	0.31708			
4300	0.39536	0.01712	0.34528	0.00786		
4379	0.4032	0.02368	0.35822	0.0101		
4440	0.41452	0.02618	0.36212	0.01426		
4502	0.43398	0.0312	0.38954	0.04768		
4563	0.4512	0.05226	0.41302	0.07068		
4658	1.75	1.75	1.75	1.75		Failed

PC-CX 2024-1 Fatigue Crack Growth Data Sheet

Width: 4.0005 in. Thick: 0.253 in. Area: 1.0121 in²

Precrack Information

Precrack Date: 29-Sep-11 Loading Condition: Constant Amplitude R=0.1
 Frequency: 20 Hz Hole Diameter: 0.475795 in. Peak Stress: 20 ksi
 Surface EDM Length: 0.01076 in.

Testing Information

Test Date: 25-Oct-11 Loading Condition: Spectrum
 Loading Rate: 500,000 lbs/s Hole Diameter: 0.500875 in.
 Peak Stress: 33 ksi Surface EDM Length: 0.00512 in. Bore EDM Length: 0.0051 in.

Flight Hours	Actual Crack Length (inches)				Bore	Comments
	Surface of Hole					
	EDM		NEDM			
	A	B	A	B		
0	0.04436				0.04912	Started test 25-Oct-2011
238	0.0561				0.061433	
3598	0.07304				0.090577	
6237	0.081				0.097225	
7918	0.08818				0.10158	Heat Exchanger Maintenance
11277	0.08844				0.117331	
13437	0.09238				0.12912	
16317	0.09824				0.12948	Stopped test at 5:15, 25-Oct-2011
18248	0.10072				0.133311	Resumed test 27-Oct-2011 @ 8:20
23516	0.10836				0.181089	
28076	0.11502				0.198608	
35708	0.12676				0.210659	
37367	0.13156				0.219959	
39676	0.14388				0.234957	
41556	0.1509		0.02538		0.258076	
42972	0.15574		0.04826			
44524	0.1615		0.06424			
46563	0.16778		0.0739			
48563	0.17606		0.07836			
50642	0.18574		0.0961			

PC-CX 2024-1 Test Data (Continued)

Flight Hours	Actual Crack Length (inches)				Bore	Comments
	Surface of Hole					
	EDM		NEDM			
	A	B	A	B		
53513	0.20576		0.11432			
56237	0.22768		0.14714	0.03508		
58511	0.2526	0.00336	0.1808	0.0685		
60653	0.28026	0.00448	0.21678	0.07844		
62236	0.30426	0.0157	0.23768	0.0907		
64340	0.33626	0.01684	0.27758	0.10254		
65502	0.36182	0.11354	0.30168	0.12272		
66448	0.38206	0.129	0.31732	0.13086		
67849	0.42416	0.1502	0.36504	0.14872		
69256	0.46918	0.18806	0.4301	0.18268		
70088	0.51144	0.21312	0.4581	0.20446		
71107	0.56884	0.2663	0.54744	0.24554		
71776	0.64968	0.33816	0.60084	0.3037		
72131	0.72554	0.40704	0.7132	0.36982		
72164	1.75512	1.75	1.75	1.75		Failure

PC-CX 2024-2 Fatigue Crack Growth Data Sheet

Width: 3.9995 in. Thick: 0.253 in. Area: 1.0118 in²

Precrack Information

Precrack Date: 29-Sep-11 Loading Condition: Constant Amplitude R=0.1
 Frequency: 20 Hz Hole Diameter: 0.47577 in. Peak Stress: 20 ksi
 Surface EDM Length: 0.01378 in.

Testing Information

Test Date: 22-Dec-11 Loading Condition: Spectrum
 Loading Rate: 500,000 lbs/s Hole Diameter: 0.500825 in.
 Peak Stress: 33 ksi Surface EDM Length: 0.00768 in. Bore EDM Length: 0.0067 in.

Flight Hours	Actual Crack Length (inches)				Bore	Comments
	Surface of Hole					
	EDM		NEDM			
	A	B	A	B		
0	0.04788				0.049065	Started 22-Dec-2011
40	0.0513				0.058872	
2200	0.07246				0.083876	
7572	0.08742				0.107785	
47809	0.1509				0.227325	
55308	0.16626		0.02544			
60505	0.18304		0.05214			
64524	0.1966		0.06772			
89612	1.7572675		1.749588			Failed

PC-CX 2024-3 Fatigue Crack Growth Data Sheet

Width: 3.9995 in. Thick: 0.253 in. Area: 1.0118 in²

Precrack Information

Precrack Date: 29-Sep-11 Loading Condition: Constant Amplitude R=0.1

Frequency: 20 Hz Hole Diameter: 0.47572 in. Peak Stress: 20 ksi

Surface EDM Length: 0.01034 in.

Testing Information

Test Date: 4-Jan-12 Loading Condition: Spectrum

Loading Rate: 500,000 lbs/s Hole Diameter: 0.50085 in.

Peak Stress: 33 ksi Surface EDM Length: 0.00598 in. Bore EDM Length: 0.0014 in.

Flight Hours	Actual Crack Length (inches)				Bore	Comments
	Surface of Hole					
	EDM		NEDM			
	A	B	A	B		
0	0.05932				0.055941	Started 4-Jan-2012
1079	0.07738				0.070265	
11242	0.09778				0.129206	
20233	0.11548				0.1765	5-Jan-12
53140	0.19362	0.0446	0.09592	0.00544		
56639	0.21302	0.0513	0.11874	0.00776		
60547	0.23706	0.06158	0.15286	0.01224		
62740	0.25674	0.0633	0.1785	0.01448		
65076	0.28022	0.0766	0.21086	0.01998		
66912	0.30408	0.08306	0.2331	0.02262		
68754	0.33024	0.09074	0.28898	0.02814		
70718	0.35962	0.09812	0.30218	0.03606		
72055	0.38374	0.1085	0.32392	0.04726		
73057	0.40644	0.11796	0.35002	0.0558		
74140	0.43094	0.12962	0.37548	0.07268		
74871	0.45186	0.13918	0.39416	0.08406		
78884	1.755555	1.749575	1.749575	1.749575		Failed

PC-CX 2024-4 Fatigue Crack Growth Data Sheet

Width: 4.0005 in. Thick: 0.2525 in. Area: 1.0101 in²

Precrack Information

Precrack Date: 29-Sep-11 Loading Condition: Constant Amplitude R=0.1

Frequency: 20 Hz Hole Diameter: 0.47592 in. Peak Stress: 20 ksi

Surface EDM Length: 0.01026 in.

Testing Information

Test Date: 22-Jan-12 Loading Condition: Spectrum

Loading Rate: 500,000 lbs/s Hole Diameter: 0.500875 in.

Peak Stress: 30 ksi Surface EDM Length: 0.0059 in. Bore EDM Length: 0.0031 in.

Flight Hours	Actual Crack Length (inches)				Bore	Comments
	Surface of Hole					
	EDM		NEDM			
	A	B	A	B		
0	0.04848				0.054539	
3092	0.073				0.074736	
9572	0.0783				0.089048	
50739	0.10566				0.15823	
69305	0.11492				0.188097	
108202	0.13902	0.02462			0.222827	
122658	0.14854	0.03888	0.03264			
162067	0.24218	0.08442	0.17512	0.03666		
164374	0.25666	0.08754	0.19646	0.04246		
167424	0.282	0.09348	0.23386	0.04922		
169651	0.30428	0.0964	0.26156	0.05576		
171653	0.32712	0.10102	0.28734	0.06018		
173895	0.35402	0.10742	0.3176	0.06412		
175639	0.38084	0.11306	0.34512	0.0746		
177071	0.40192	0.1189	0.3725	0.08128		
178909	0.43632	0.12914	0.40562	0.0921		
179865	0.45914	0.1351	0.42456	0.09984		
180790	0.48122	0.1438	0.45254	0.1064		
181729	0.50742	0.15282	0.47434	0.11392		
182145	0.5204	0.15926	0.4861	0.11938		
187482	1.7559	1.75	1.75	1.75		Failed at 25 kip, not max

PC-CX 2024-5 Fatigue Crack Growth Data Sheet

Width: 4 in. Thick: 0.252 in. Area: 1.008 in²

Precrack Information

Precrack Date: 27-Sep-11 Loading Condition: Constant Amplitude R=0.1
 Frequency: 20 Hz Hole Diameter: 0.475845 in. Peak Stress: 20 ksi
 Surface EDM Length: 0.01454 in.

Testing Information

Test Date: 6-Dec-11 Loading Condition: Spectrum
 Loading Rate: 500,000 lbs/s Hole Diameter: 0.500925 in.
 Peak Stress: 25 ksi Surface EDM Length: 0.01116 in. Bore EDM Length: 0.0041 in.

Flight Hours	Actual Crack Length (inches)				Bore	Comments
	Surface of Hole					
	EDM		NEDM			
	A	B	A	B		
0	0.04914				0.058817	Started at 7:30 on 6-Dec-2011
1207	0.05396				0.064779	Hydraulic pump overheated at 8:15
2689	0.06024				0.070516	Started at 1:00, overheated at 1:30
53865	0.08064				0.08712	Started at 12:27 PM on 7-Dec-2011
76825	0.08526				0.09571	
128038	0.09654				0.113596	Ran constantly over weekend
307360	0.11554				0.147668	7:30 on 12-Dec-2011
373167	0.12186	0.05874			0.16379	8:30 on 13-Dec-2011
435273	0.12674	0.06556	0.01846			8:00 on 14-Dec-2011
573678	0.14788	0.08332	0.01972			1:00 PM on 16-Dec 2011
704450	0.18	0.09562	0.03026			Failed in Grip; 2:42 PM, 18-Dec-2011
831642	1.75	1.75	1.75	1.75		Restarted 17-Feb-2012; Failure

PC-CX 2024-6 Fatigue Crack Growth Data Sheet

Width: 4.001 in. Thick: 0.2525 in. Area: 1.0102 in²

Precrack Information

Precrack Date: 27-Sep-11 Loading Condition: Constant Amplitude R=0.1
 Frequency: 20 Hz Hole Diameter: 0.47562 in. Peak Stress: 20 ksi
 Surface EDM Length: 0.00872 in.

Testing Information

Test Date: 9-Jan-12 Loading Condition: Spectrum
 Loading Rate: 500,000 lbs/s Hole Diameter: 0.500875 in.
 Peak Stress: 43.25ksi Surface EDM Length: 0.00536 in. Bore EDM Length: 0.0041 in.

Flight Hours	Actual Crack Length (inches)					Comments
	Surface of Hole				Bore	
	EDM		NEDM			
	A	B	A	B		
0	0.04888				0.061998	
60	0.05822				0.071743	
240	0.07168				0.090555	
483	0.08346				0.121337	
1060	0.08958				0.139252	
1461	0.11216				0.161131	
1941	0.12488				0.18396	
2385	0.13968				0.208254	
2601	0.14678				0.221202	
3122	0.16372		0.02236			
3591	0.1788		0.05638			
3962	0.19456		0.07634			
4251	0.20504		0.09088			
4476	0.21488		0.10202			
5028	0.23808		0.12606			
5463	0.26164		0.15458			
5809	0.28408	0.01262	0.17884			
6118	0.31246	0.03412	0.21328	0.01272		
6352	0.34508	0.09346	0.26438	0.02406		
6398	0.36268	0.11128	0.28766	0.06694		
6409	1.7549225	1.749563	1.749563	1.749563		Failed

PC-CX 2024-7 Fatigue Crack Growth Data Sheet

Width: 4.0015 in. Thick: 0.253 in. Area: 1.0124 in²

Precrack Information

Precrack Date: 29-Sep-11 Loading Condition: Constant Amplitude R=0.1
 Frequency: 20 Hz Hole Diameter: 0.475595 in. Peak Stress: 20 ksi
 Surface EDM Length: 0.00878 in.

Testing Information

Test Date: 6-Jan-12 Loading Condition: Spectrum
 Loading Rate: 500,000 lbs/s Hole Diameter: 0.50095 in.
 Peak Stress: 43.25 ksi Surface EDM Length: 0.00494 in. Bore EDM Length: 0.0027in.

Flight Hours	Actual Crack Length (inches)				Bore	Comments
	Surface of Hole					
	EDM		NEDM			
	A	B	A	B		
0	0.04812				0.060487	
167	0.06364				0.077348	
496	0.08088				0.102024	
1189	0.10064				0.141689	
1611	0.1139				0.158363	
2159	0.1314				0.196956	
2572	0.1477				0.220509	
2988	0.165		0.03686			
3322	0.18157		0.07242			
3701	0.19882		0.09972			
4214	0.2263		0.1264			
4654	0.25042		0.15712			
4866	0.26656		0.1719			
5085	0.28164	0.00918	0.18792			
5403	0.30628	0.0111	0.20856			
5691	0.33746	0.02226	0.25438	0.0118		
5745	0.35122	0.03242	0.26928	0.02902		
5826	0.36344	0.0467	0.28064	0.04344		
5858	1.754465	1.749525	1.749525	1.749525		Failure

PC-CX 2024-8 Fatigue Crack Growth Data Sheet

Width: 4.0005 in. Thick: 0.253 in. Area: 1.0121 in²

Precrack Information

Precrack Date: 29-Sep-11 Loading Condition: Constant Amplitude R=0.1
 Frequency: 20 Hz Hole Diameter: 0.475945 in. Peak Stress: 20 ksi
 Surface EDM Length: 0.0155 in.

Testing Information

Test Date: 3-Jan-12 Loading Condition: Spectrum
 Loading Rate: 500,000 lbs/s Hole Diameter: 0.500875 in.
 Peak Stress: 43.25 ksi Surface EDM Length: 0.00934 in. Bore EDM Length: 0.0057 in.

Flight Hours	Actual Crack Length (inches)				Bore	Comments
	Surface of Hole					
	EDM		NEDM			
	A	B	A	B		
0	0.04726				0.0456	
598	0.07632				0.089481	
1447	0.0984				0.125407	
2327	0.12086				0.170337	
3243	0.15178				0.223979	
3813	0.17872		0.06616			
4407	0.20824		0.11156			
4754	0.22426		0.13984			
5213	0.25376		0.16758			
5664	0.28596	0.0104	0.19942			
6210	0.3472	0.06424	0.26508	0.04124		
6338	1.7589025	1.749563	1.749563	1.749563		Failure

PC-CX 2024-9 Fatigue Crack Growth Data Sheet

Width: 4.0015 in. Thick: 0.254 in. Area: 1.0163 in²

Precrack Information

Precrack Date: 11-Oct-11 Loading Condition: Constant Amplitude R=0.1
 Frequency: 20 Hz Hole Diameter: 0.475675 in. Peak Stress: 20 ksi
 Surface EDM Length: 0.01452 in.

Testing Information

Test Date: 15-Nov-11 Loading Condition: Constant Amplitude R=0.1
 Frequency: 20 Hz Hole Diameter: 0.50095 in.
 Peak Stress: 25 ksi Surface EDM Length: 0.00932 in. Bore EDM Length: 0.0061 in.

Total Cycles	Actual Crack Length (inches)				Bore	Comments
	Surface of Hole					
	EDM		NEDM			
	A	B	A	B		
0	0.04376				0.055188	load at 8 kip for 20 min.
2569	0.0496				0.056441	
29536	0.08228				0.080818	
55418	0.10036				0.110951	
145706	0.1235				0.126526	
239786	0.14386				0.198406	
335214	0.16398		0.04244			
443084	0.21084	0.11488	0.06776	0.04784		
451015	0.2199	0.11762	0.0687	0.05138		
470943	0.25114	0.12346	0.073586	0.05328		
477442	0.26598	0.12432	0.07518	0.0539		many cracks on N-EDM-A
489345	0.3107	0.12924	0.0762	0.0541		
499617	0.41318	0.13288	0.0762	0.0541		
504898	0.5156	0.13518	0.08232	0.0541		
508291	1.75932	1.75	1.75	1.75		Failure

PC-CX 2024-10 Fatigue Crack Growth Data Sheet

Width: 4.002 in. Thick: 0.2535 in. Area: 1.0145 in²

Precrack Information

Precrack Date: 11-Oct-11 Loading Condition: Constant Amplitude R=0.1
 Frequency: 20 Hz Hole Diameter: 0.47565 in. Peak Stress: 20 ksi
 Surface EDM Length: 0.01544 in.

Testing Information

Test Date: 17-Nov-11 Loading Condition: Constant Amplitude R=0.1
 Frequency: 20 Hz Hole Diameter: 0.501 in.
 Peak Stress: 25 ksi Surface EDM Length: 0.00612 in. Bore EDM Length: 0.0095 in.

Total Cycles	Actual Crack Length (inches)				Bore	Comments
	Surface of Hole					
	EDM		NEDM			
	A	B	A	B		
0	0.04278				0.055053	
5060	0.06448				0.06964	
15227	0.0809				0.071885	
41947	0.10174				0.103916	
81259	0.12764				0.118844	
190033	0.14798				0.127549	
257826	0.16348	0.06246	0.02368			
329197	0.1816	0.07872	0.03418	0.05236		
375270	0.20288	0.09012	0.05018	0.06742		
408553	0.22272	0.09738	0.05778	0.06834		
430550	0.24712	0.1006	0.05934	0.06902		
443389	0.26992	0.10602	0.06098	0.06976		
451023	0.2988	0.10678	0.06108	0.0725		
454448	0.31816	0.10686	0.06128	0.07378		
457595	0.3417	0.10838	0.0621	0.07394		
459335	0.3611	0.109	0.06214	0.07412		
461583	0.3849	0.11036	0.06222	0.07825		
464143	0.41678	0.11198	0.0637	0.07846		
466083	0.43936	0.11268	0.06392	0.07656		
467831	0.4699	0.1145	0.06392	0.07696		

PC-CX 2024-10 Test Data (Continued)

Total Cycles	Actual Crack Length (inches)				Bore	Comments
	Surface of Hole					
	EDM		NEDM			
	A	B	A	B		
468947	0.49532	0.11686	0.06398	0.07696		
469805	0.5187	0.11732	0.06398	0.07694		
470830	0.55364	0.11806	0.08468	0.07786		
471360	0.5835	0.11834	0.4094	0.07916		
471863	0.6195	0.11846	0.46258	0.07934		
472381	0.66684	0.1202	0.6229	0.08156		
472922	0.74198	0.12212	0.75854	0.08596		
473455	1.04596	0.13568	1.0581	0.10268		
473555	1.75562	1.7495	1.7495	1.7495		Failure

PC-CX 2024-11 Fatigue Crack Growth Data Sheet

Width: 4.002 in. Thick: 0.2535 in. Area: 1.0145 in²

Precrack Information

Precrack Date: 11-Oct-11 Loading Condition: Constant Amplitude R=0.1
 Frequency: 20 Hz Hole Diameter: 0.475775 in. Peak Stress: 20 ksi
 Surface EDM Length: 0.01136 in.

Testing Information

Test Date: 10-Jan-12 Loading Condition: Constant Amplitude R=0.1
 Frequency: 20 Hz Hole Diameter: 0.50095 in.
 Peak Stress: 25 ksi Surface EDM Length: 0.00874 in. Bore EDM Length: 0.0060 in.

Total Cycles	Actual Crack Length (inches)				Bore	Comments
	Surface of Hole					
	EDM		NEDM			
	A	B	A	B		
0	0.04846				0.044954	
10740	0.07928				0.085295	
21861	0.09722				0.101782	
33402	0.11438				0.118295	
69835	0.12638				0.145224	
109782	0.13706	0.0559			0.166243	
153721	0.1501	0.07338			0.170802	
234897	0.17506	0.09088	0.04238	0.01204		
297514	0.1996	0.1022	0.0515	0.05048		
328966	0.2231	0.10826	0.057	0.05438		
345981	0.24622	0.1121	0.06046	0.05698		
356239	0.27926	0.1121	0.06046	0.0593		
359957	0.30732	0.11538	0.06046	0.0593		
361847	0.32564	0.11672	0.06046	0.0593		
363706	0.34706	0.11672	0.06046	0.0593		
365128	0.36488	0.11688	0.0644	0.06022		
367342	0.39158	0.11856	0.0644	0.06022		
368995	0.41902	0.1188	0.06476	0.06022		
370322	0.4435	0.11982	0.06476	0.06022		
370750	0.46542	0.1206	0.06962	0.06022		

PC-CX 2024-11 Test Data (Continued)

Total Cycles	Actual Crack Length (inches)				Bore	Comments
	Surface of Hole					
	EDM		NEDM			
	A	B	A	B		
372036	0.49404	0.12068	0.0767	0.06022		
372930	0.5284	0.12256	0.15456	0.06112		
373898	0.57332	0.12422	0.51422	0.06112		
374499	0.62028	0.12738	0.60878	0.06112		
375136	0.68562	0.12938	0.73194	0.07286		
375548	0.81412	0.13326	0.86582	0.07286		
375910	1.758265	1.749525	1.749525	1.749525		Failure

PC-CX 2024-12 Fatigue Crack Growth Data Sheet

Width: 4.002 in. Thick: 0.254 in. Area: 1.0165 in²

Precrack Information

Precrack Date: 11-Oct-11 Loading Condition: Constant Amplitude R=0.1
 Frequency: 20 Hz Hole Diameter: 0.47555 in. Peak Stress: 20 ksi
 Surface EDM Length: 0.00766 in.

Testing Information

Test Date: 30-Jan-12 Loading Condition: Spectrum
 Loading Rate: 500,000 lbs/s Hole Diameter: 0.501025 in.
 Peak Stress: 30 ksi Surface EDM Length: 0.00978 in. Bore EDM Length: 0.0059 in.

Flight Hours	Actual Crack Length (inches)				Bore	Comments
	Surface of Hole					
	EDM		NEDM			
	A	B	A	B		
0	0.05228				0.055842	
1128	0.06612				0.070301	
13652	0.08406				0.099134	
55709	0.11416				0.173333	
70693	0.1247				0.208967	
110799	0.15298				0.234179	
126831	0.16442	0.03664	0.0587			
165595	0.3432	0.06638	0.29034			
168672	0.38598	0.09612	0.34342	0.03558		
173307	0.4704	0.11224	0.43084	0.0453		
174222	0.49206	0.111812	0.45354	0.0453		
175288	0.51956	0.12456	0.48432	0.05124		
176349	0.55018	0.1327	0.51994	0.05416		
177100	0.57892	0.14506	0.54296	0.06536		
177855	0.60808	0.15256	0.5718	0.07976		
178434	0.63304	0.17028	0.6022	0.09222		

PC-CX 2024-12 Test Data (Continued)

Flight Hours	Actual Crack Length (inches)				Bore	Comments
	Surface of Hole					
	EDM		NEDM			
	A	B	A	B		
179008	0.6594	0.1804	0.63098	0.1083		
179527	0.68428	0.19588	0.65554	0.11796		
179924	0.70866	0.2109	0.68096	0.12828		
180490	0.74954	0.2408	0.71346	0.16796		
180884	0.78822	0.26708	0.74992	0.20422		
181080	0.81824	0.28484	0.78036	0.22558		
181232	0.84704	0.30482	0.80796	0.2459		
181360	0.89034	0.33438	0.86004	0.28318		
181526	1.75978	1.75	1.75	1.75		Failed

PC-CX 2024-13 Fatigue Crack Growth Data Sheet

Width: 4.0025 in. Thick: 0.2535 in. Area: 1.0146 in²

Precrack Information

Precrack Date: 11-Oct-11 Loading Condition: Constant Amplitude R=0.1
 Frequency: 20 Hz Hole Diameter: 0.47585 in. Peak Stress: 20 ksi
 Surface EDM Length: 0.01034 in.

Testing Information

Test Date: 6-Feb-12 Loading Condition: Spectrum
 Loading Rate: 500,000 lbs/s Hole Diameter: 0.50115 in.
 Peak Stress: 30 ksi Surface EDM Length: 0.00812 in. Bore EDM Length: 0.0057 in.

Flight Hours	Actual Crack Length (inches)				Bore	Comments
	Surface of Hole					
	EDM		NEDM			
	A	B	A	B		
0	0.0514				0.056745	
829	0.06182				0.067147	
8711	0.07538				0.087261	
12413	0.07846				0.089696	
52284	0.10744				0.147844	
70970	0.1138				0.170686	
126662	0.1427	0.02346			0.246777	
162054	0.17272	0.04306				
166681	0.17714	0.04442	0.08022	0.03958		
178915	0.20206	0.0542	0.10046	0.04168		
183470	0.22306	0.06446	0.12442	0.047		
215843	1.75812	1.75	1.75	1.75		Failed

PC-CX 2024-14 Fatigue Crack Growth Data Sheet

Width: 4.003 in. Thick: 0.252 in. Area: 1.0088 in²

Precrack Information

Precrack Date: 12-Oct-11 Loading Condition: Constant Amplitude R=0.1
 Frequency: 20 Hz Hole Diameter: 0.4755 in. Peak Stress: 20 ksi
 Surface EDM Length: 0.01418 in.

Testing Information

Test Date: 28-Nov-11 Loading Condition: Constant Amplitude R=0.1
 Frequency: 20 Hz Hole Diameter: 0.50085 in.
 Peak Stress: 20 ksi Surface EDM Length: 0.00816 in. Bore EDM Length: 0.0040 in.

Total Cycles	Actual Crack Length (inches)				Bore	Comments
	Surface of Hole					
	EDM		NEDM			
	A	B	A	B		
0	0.04486				0.065952	
1084272	0.11248				0.188415	
1118317	0.11248	0.07716			0.220711	
1262687	0.11344	0.08942	0.0283			
1547762	0.1135	0.09132	0.0312	0.01094		
1768982	0.1141	0.09712	0.03124	0.0149		
3176132	0.11646	0.09984	0.03188	0.01528		
5688576	0.11646	0.09984	0.03188	0.01528		Failed at grip

PC-CX 2024-15 Fatigue Crack Growth Data Sheet

Width: 4.0025 in. Thick: 0.2535 in. Area: 1.0146 in²

Precrack Information

Precrack Date: 12-Oct-11 Loading Condition: Constant Amplitude R=0.1
 Frequency: 20 Hz Hole Diameter: 0.47565 in. Peak Stress: 20 ksi
 Surface EDM Length: 0.01392 in.

Testing Information

Test Date: 2-Dec-11 Loading Condition: Constant Amplitude R=0.1
 Frequency: 20 Hz Hole Diameter: 0.500775 in.
 Peak Stress: 20 ksi Surface EDM Length: 0.00904 in. Bore EDM Length: 0.0060 in.

Total Cycles	Actual Crack Length (inches)				Bore	Comments
	Surface of Hole					
	EDM		NEDM			
	A	B	A	B		
0	0.04988				0.050295	
10983	0.05912				0.069009	
29157	0.07466				0.074332	
55158	0.08442				0.083183	
91509	0.0893				0.090106	
183180	0.09748				0.109865	
218734	0.10126				0.117116	
1403233	1.7586525					Failed

PC-CX 2024-16 Fatigue Crack Growth Data Sheet

Width: 4.002 in. Thick: 0.2535 in. Area: 1.0145 in²

Precrack Information

Precrack Date: 12-Oct-11 Loading Condition: Constant Amplitude R=0.1
 Frequency: 20 Hz Hole Diameter: 0.4756 in. Peak Stress: 20 ksi
 Surface EDM Length: 0.01526 in.

Testing Information

Test Date: 19-Dec-11 Loading Condition: Constant Amplitude R=0.1
 Frequency: 20 Hz Hole Diameter: 0.500875 in.
 Peak Stress: 20 ksi Surface EDM Length: 0.00438 in. Bore EDM Length: 0.0021 in.

Total Cycles	Actual Crack Length (inches)				Bore	Comments
	Surface of Hole					
	EDM		NEDM			
	A	B	A	B		
0	0.0407				0.045205	
22383	0.06144				0.060544	
53390	0.06872				0.071643	
1076376	0.10694	0.0657	0.032			
1165948	0.1072	0.07662	0.03474	0.03036		
1329599	0.11844	0.09508	0.03566	0.03154		
1521614	0.12214	0.1019	0.0373	0.03154		
2904440	0.19208	0.12152	0.03976	0.02486		
2954676	0.21182	0.1216	0.04008	0.02594		
3001800	0.23878	0.12052	0.04008	0.02996		
3023755	0.31094	0.12052	0.04008	0.02996		
3034633	0.39284	0.1208	0.04008	0.02996		
3037500	0.42634	0.12186	0.04008	0.02996		
3038466	0.43878	0.12186	0.04008	0.02996		
3039836	0.4597	0.12186	0.04008	0.02996		
3040991	0.47966	0.12186	0.04008	0.02996		
3041926	0.50046	0.12186	0.04008	0.02996		
3042542	0.52122	0.12186	0.04008	0.02996		

PC-CX 2024-16 Test Data (Continued)

Total Cycles	Actual Crack Length (inches)				Bore	Comments
	Surface of Hole					
	EDM		NEDM			
	A	B	A	B		
3044049	0.56512	0.12246	0.04008	0.02996		
3045633	0.60752	0.12246	0.54364	0.02996		
3046843	0.663	0.12246	0.61564	0.02996		
3047941	0.72608	0.12246	0.696	0.02996		
3048543	0.7646	0.12246	0.75852	0.02996		
3049109	0.80952	0.12246	0.84906	0.02996		
3049578	0.86914	0.12246	0.9043	0.02996		
3049985	0.9309	0.12246	0.96014	0.02996		
3050350	1.01438	0.12246	1.01844	0.02996		
3050740	1.13212	0.1357	1.13122	0.03512		
3050999	1.7539425	1.749563	1.749563	1.749563		Failure

PC-CX 2024-17 Fatigue Crack Growth Data Sheet

Width: 4.0015 in. Thick: 0.2535 in. Area: 1.0144 in²

Precrack Information

Precrack Date: 12-Oct-11 Loading Condition: Constant Amplitude R=0.1
 Frequency: 20 Hz Hole Diameter: 0.47555 in. Peak Stress: 20 ksi
 Surface EDM Length: 0.01386 in.

Testing Information

Test Date: 18-Jan-12 Loading Condition: Constant Amplitude R=0.1
 Frequency: 20 Hz Hole Diameter: 0.50105 in.
 Peak Stress: 20 ksi Surface EDM Length: 0.00612 in. Bore EDM Length: 0.0057 in.

Total Cycles	Actual Crack Length (inches)				Bore	Comments
	Surface of Hole					
	EDM		NEDM			
	A	B	A	B		
0	0.04372				0.044866	
21013	0.06538				0.065482	
30557	0.06842				0.074431	
135184	0.08374				0.088373	
219448	0.09168				0.104811	
548428	0.09462				0.13754	
1761149	0.11502		0.03196			
2365870	0.11738	0.0966	0.03318	0.0271		
3435185	0.12386	0.10802	0.03418	0.02954		
3630344	0.13076	0.10804	0.03418	0.03062		
3986797	0.13492	0.10804	0.03442	0.03062		
7041458	0.15054	0.10866	0.03442	0.03062		Failed in the grip

APPENDIX C

SPECIMEN CRACK GROWTH CURVES

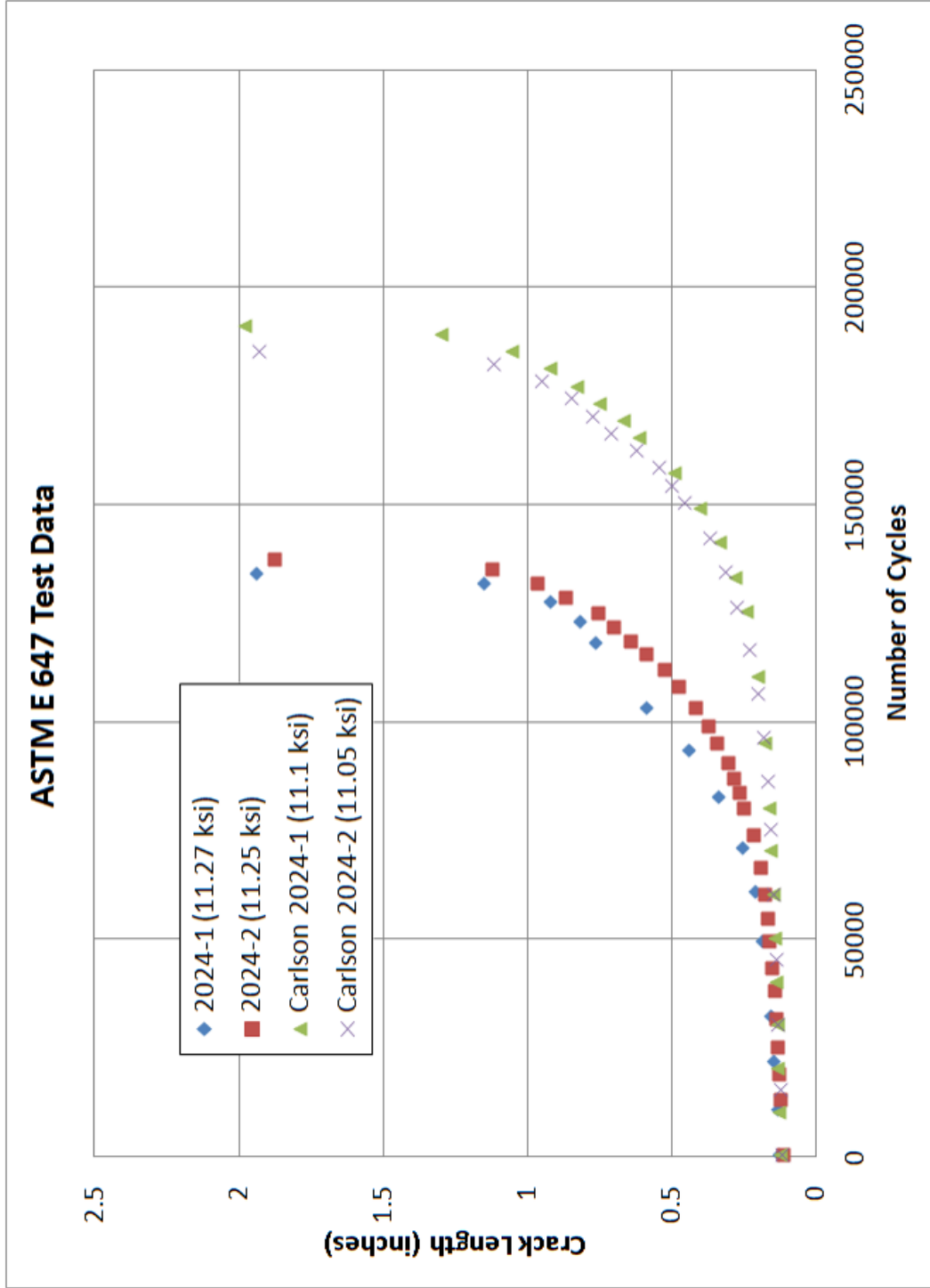


Fig. 51 Crack Growth Curves for ASTM E 647 Tests

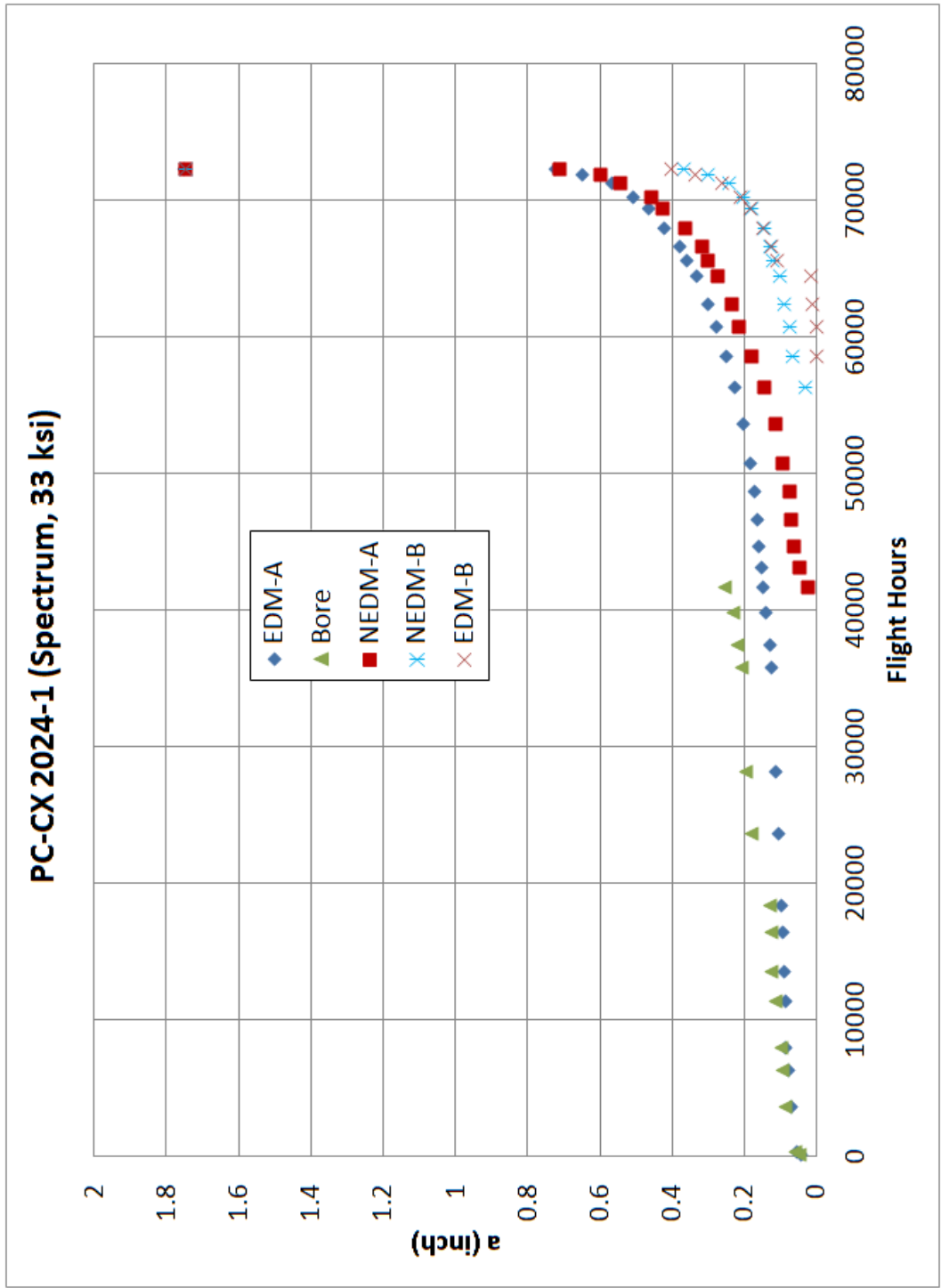


Fig. 52 Crack Growth Curve for NCX 2024-1

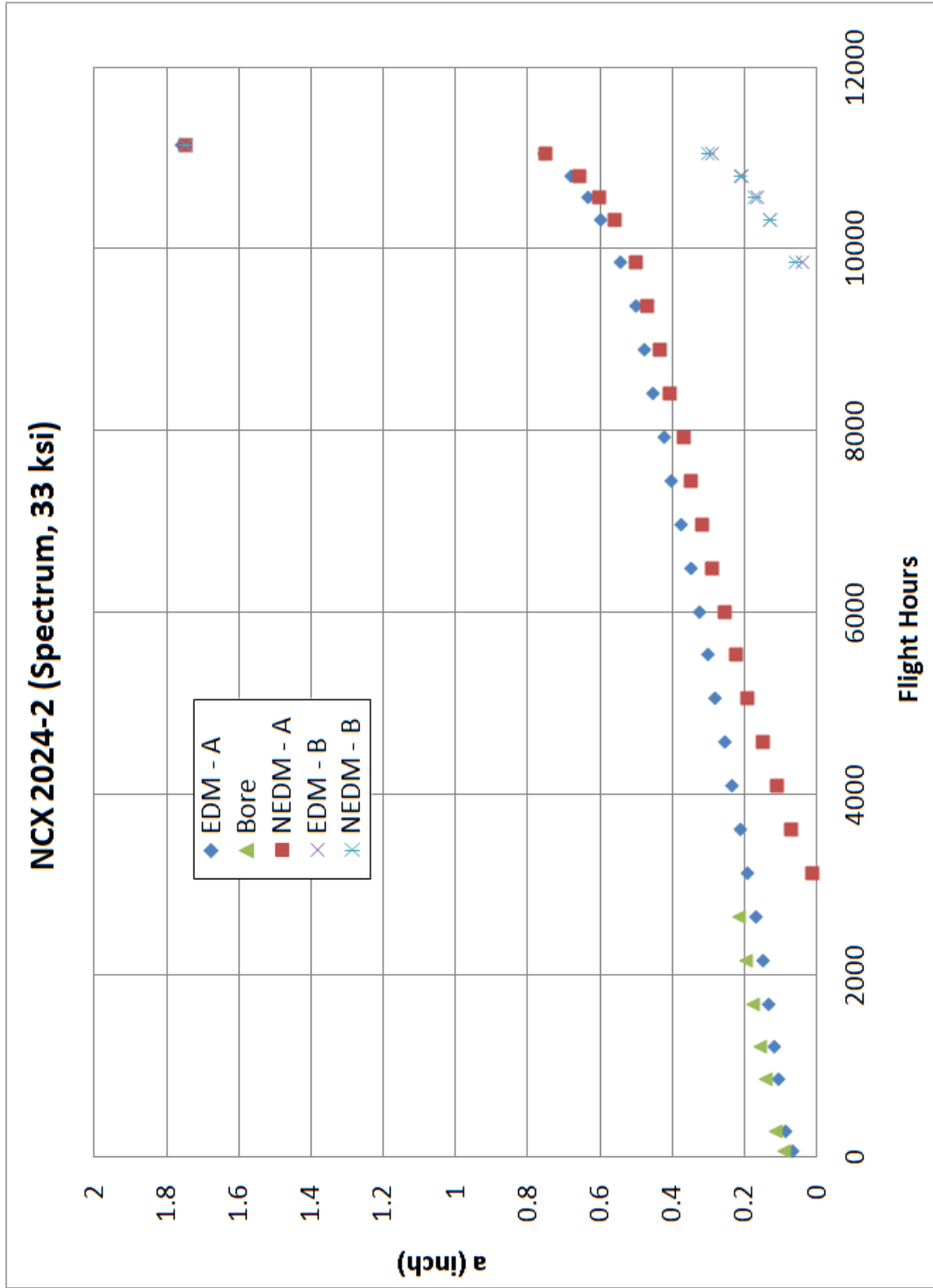


Fig. 53 NCX 2024-2 Crack Growth Curve

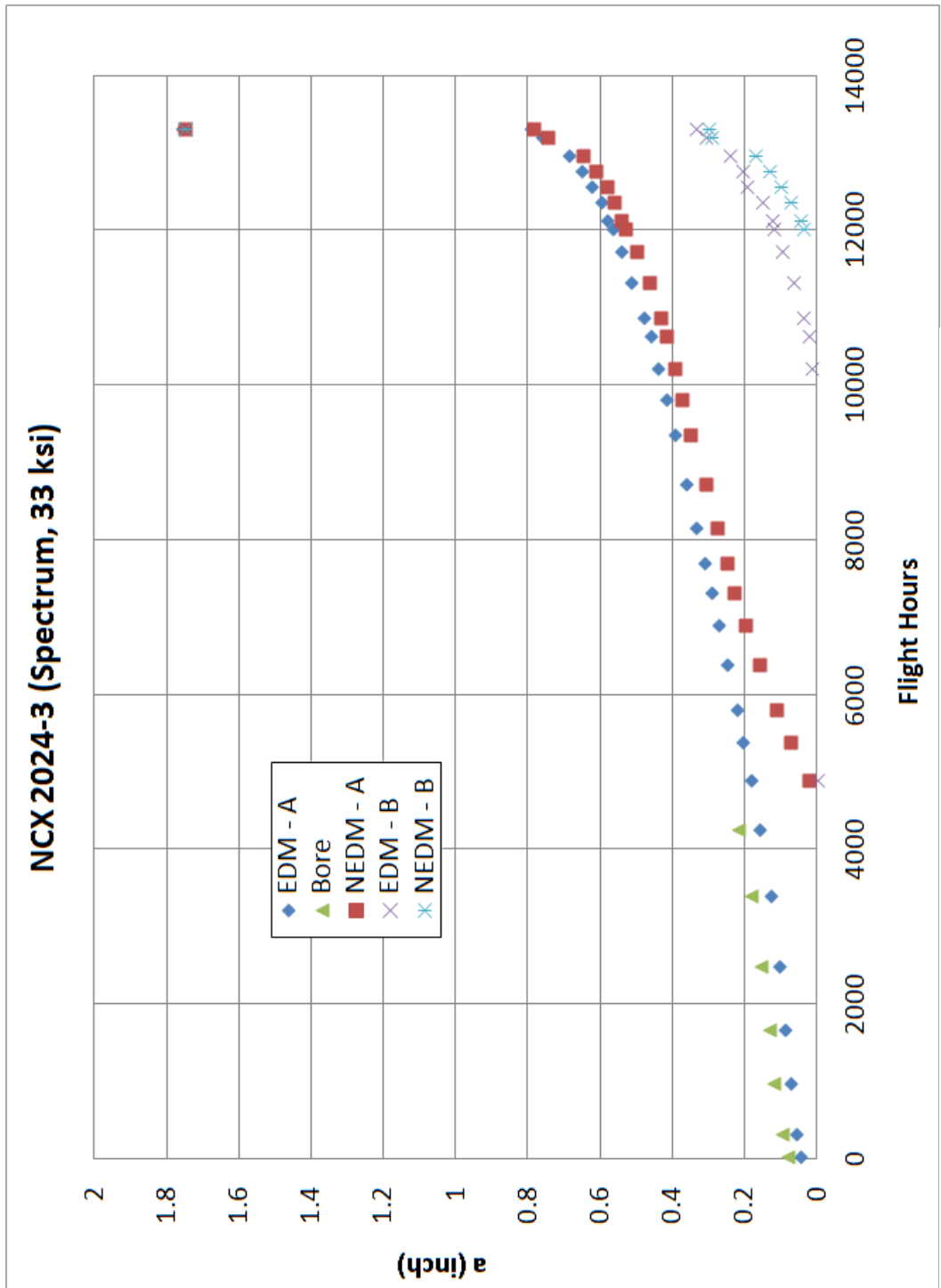


Fig. 54 NCX 2024-3 Crack Growth Curve

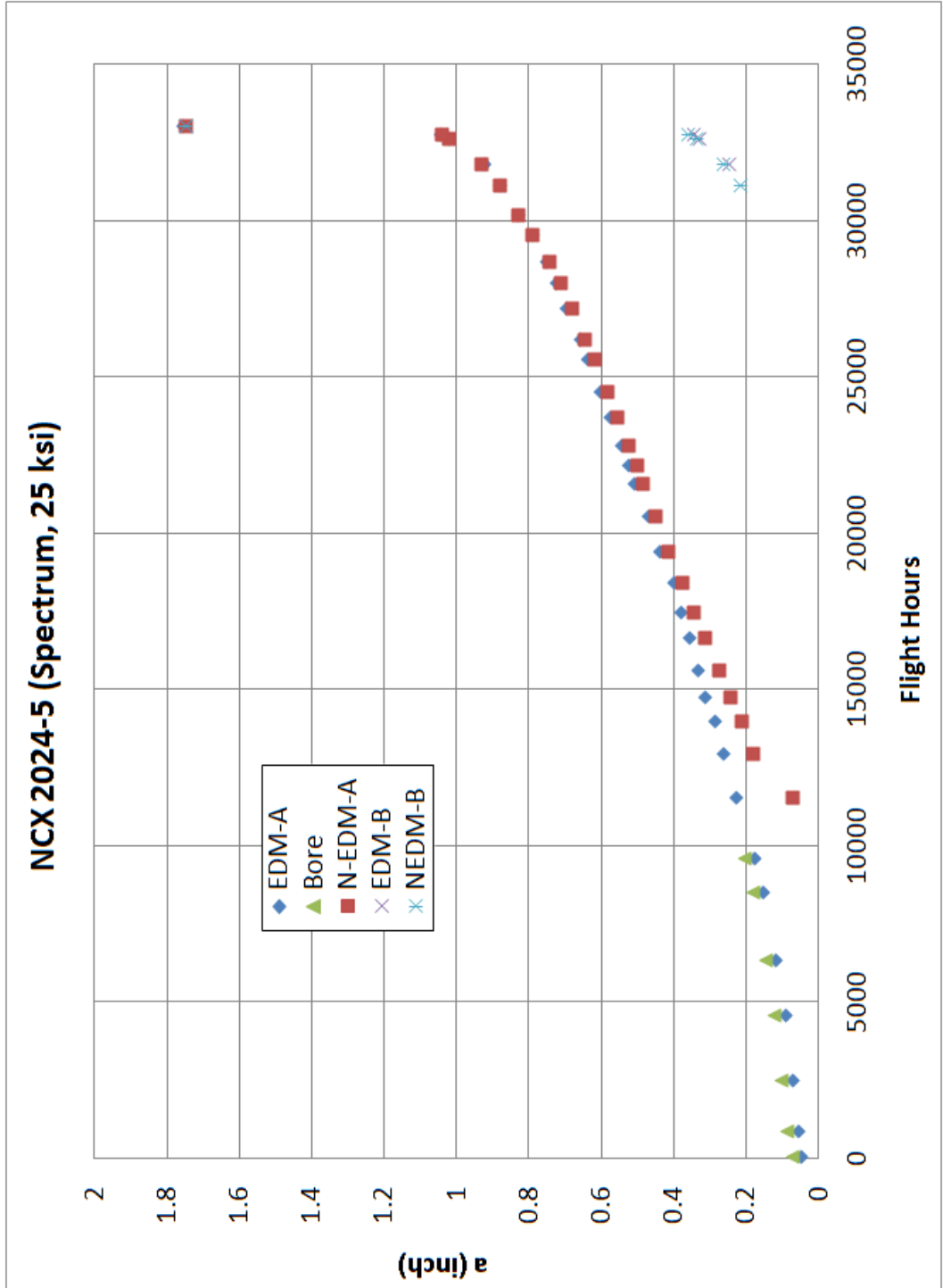


Fig. 55 NCX 2024-5 Crack Growth Curve

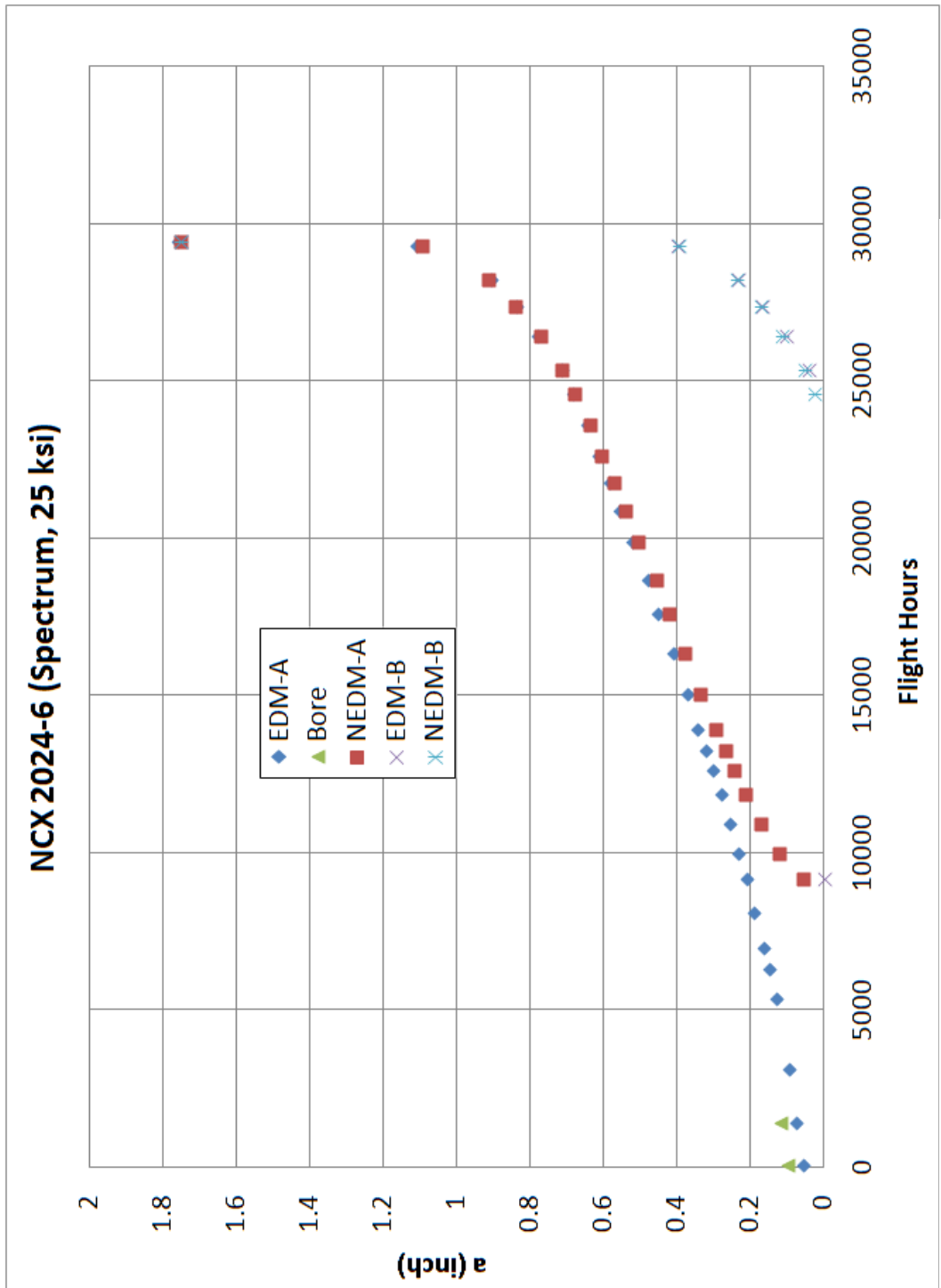


Fig. 56 NCX 2024-6 Crack Growth Curve

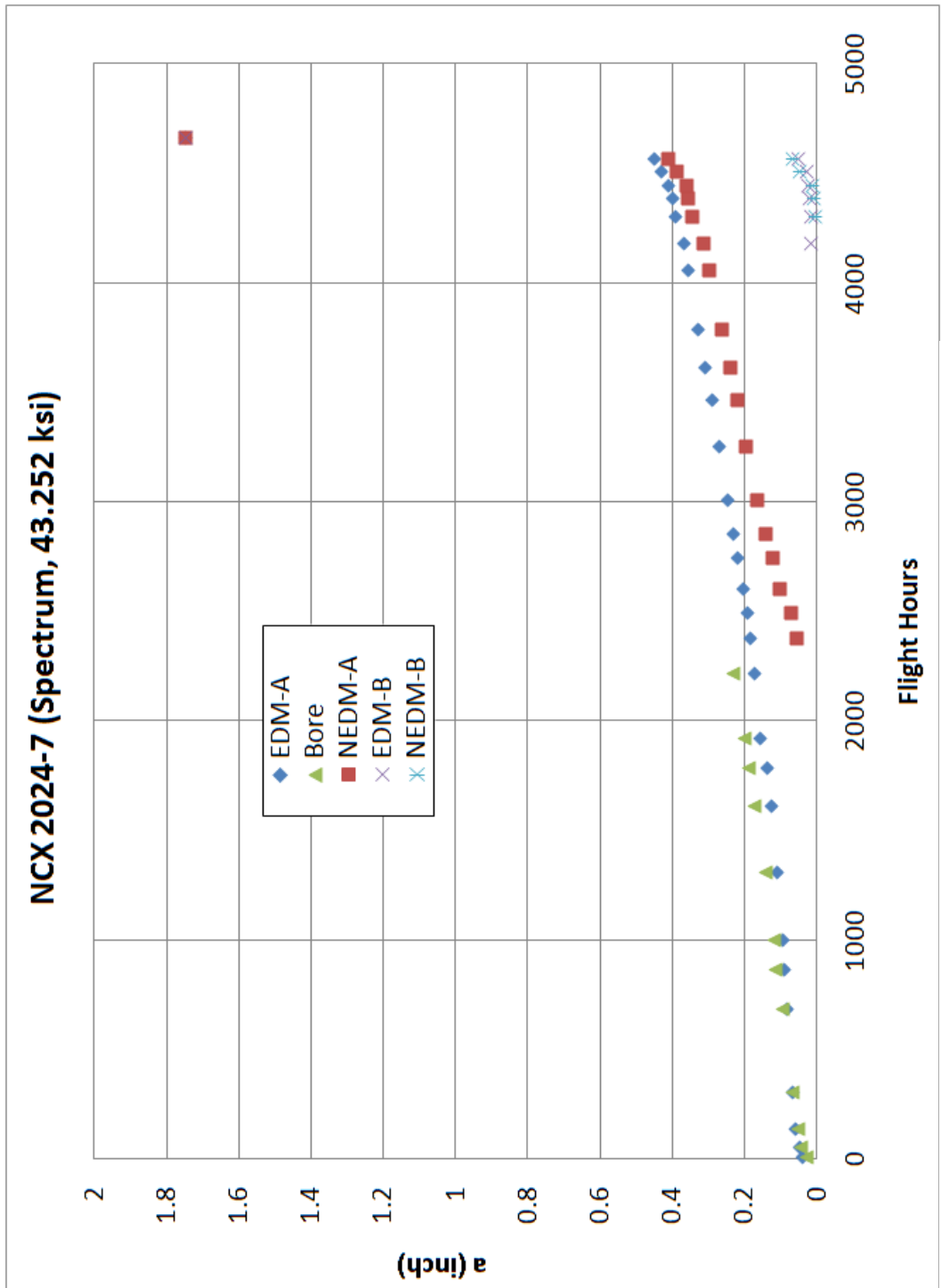


Fig. 57 NCX 2024-7 Crack Growth Curve

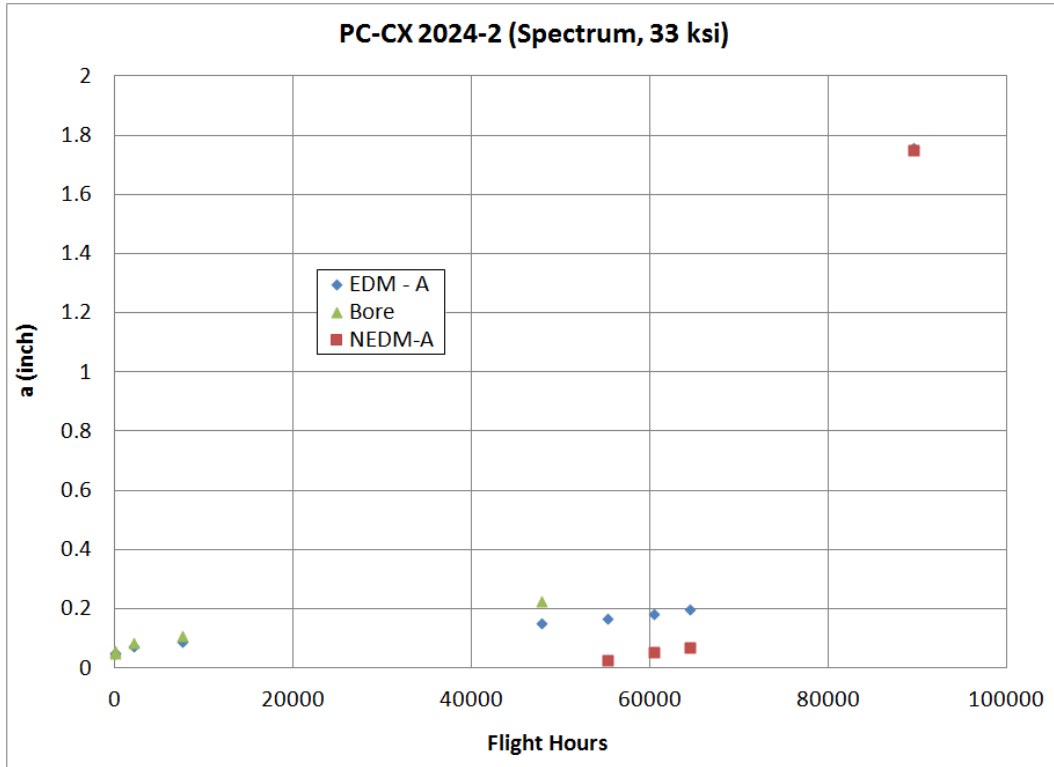


Fig. 58 PC-CX 2024-2 Crack Growth Curve

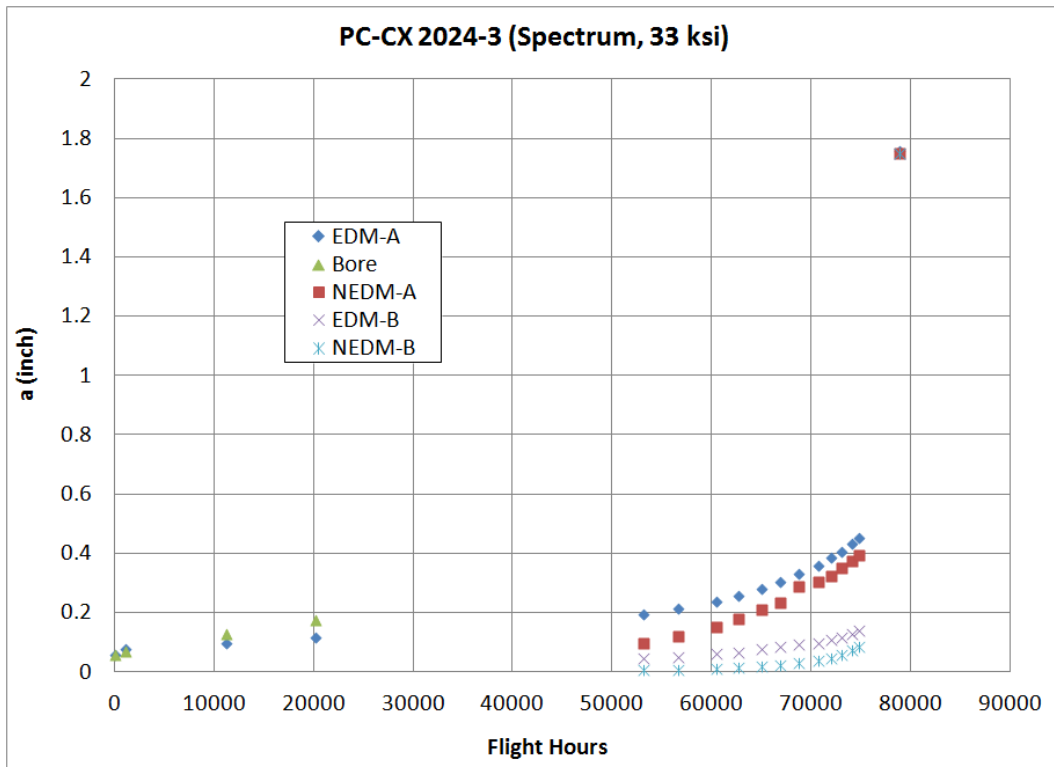


Fig. 59 PC-CX 2024-3 Crack Growth Curve

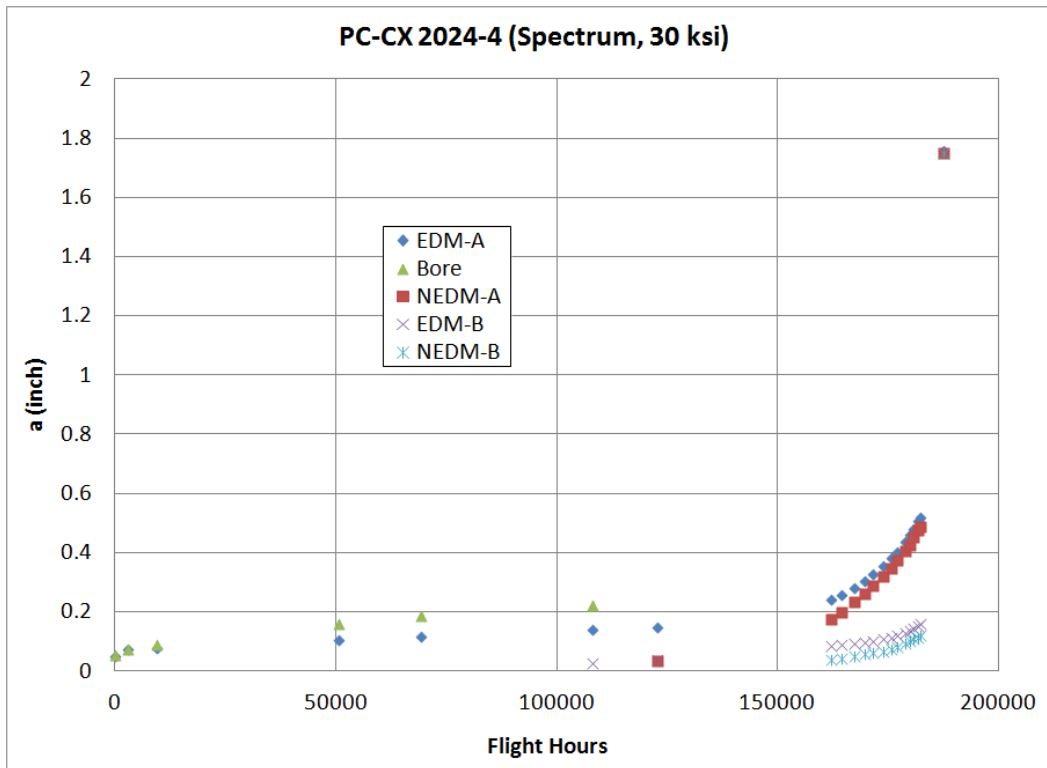


Fig. 60 PC-CX 2024-4 Crack Growth Curve

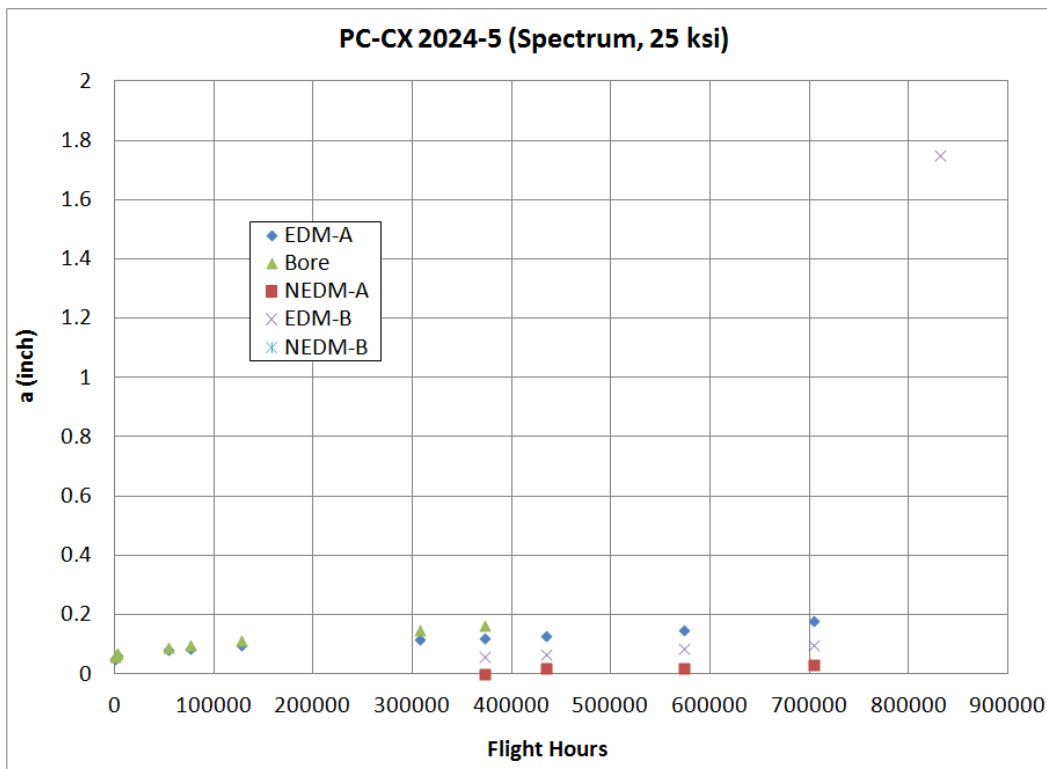


Fig. 61 PC-CX 2024-5 Crack Growth Curve

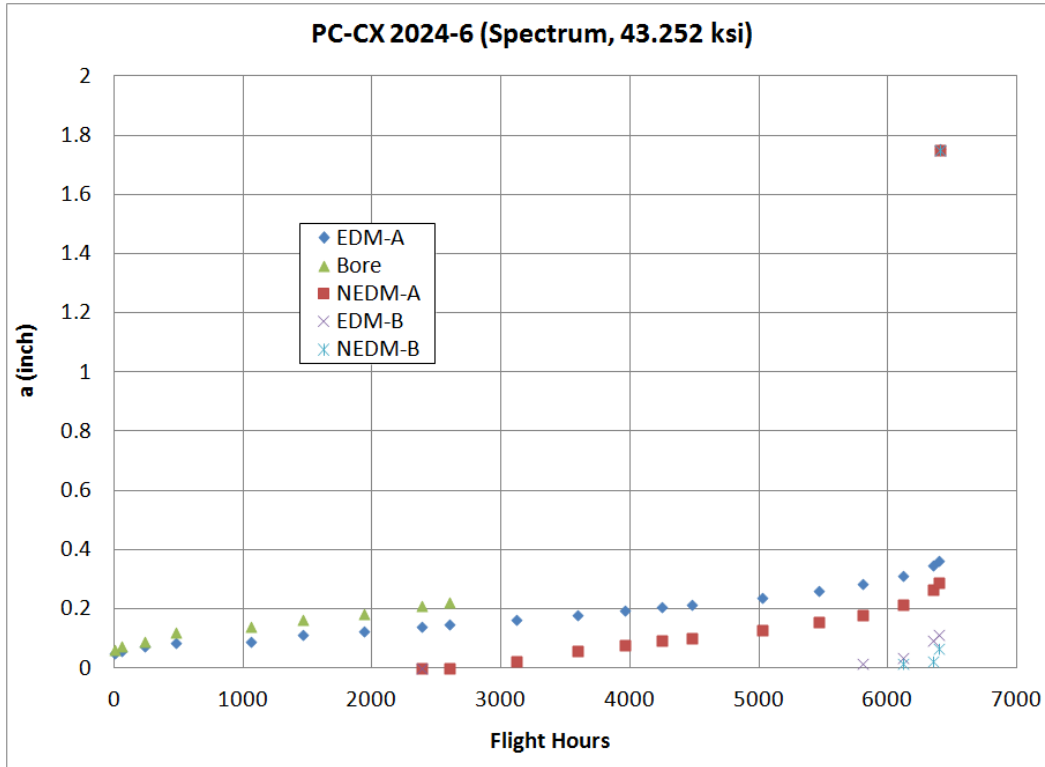


Fig. 62 PC-CX 2024-6 Crack Growth Curve

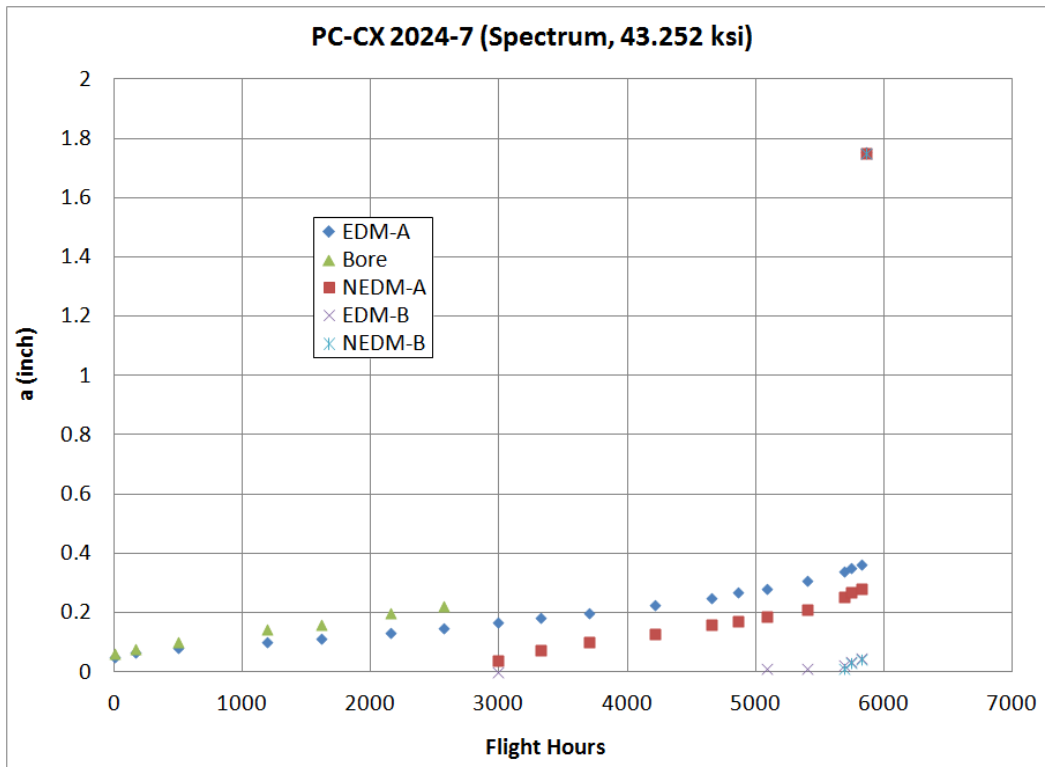


Fig. 63 PC-CX 2024-7 Crack Growth Curve

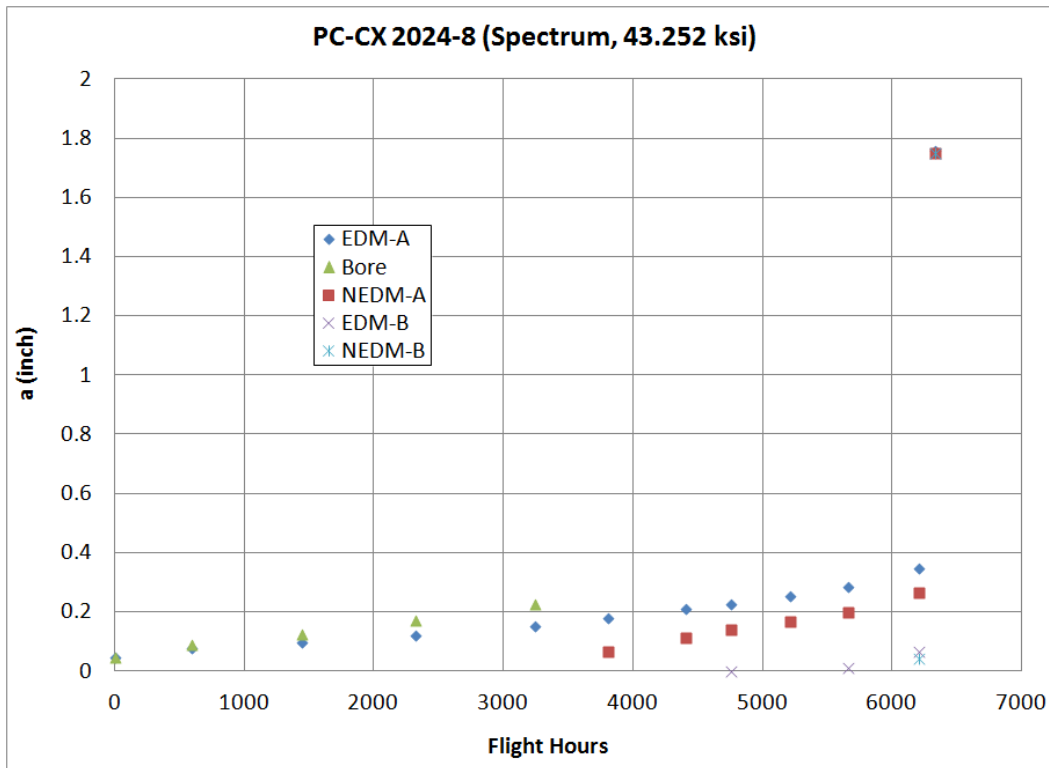


Fig. 64 PC-CX 2024-8 Crack Growth Curve

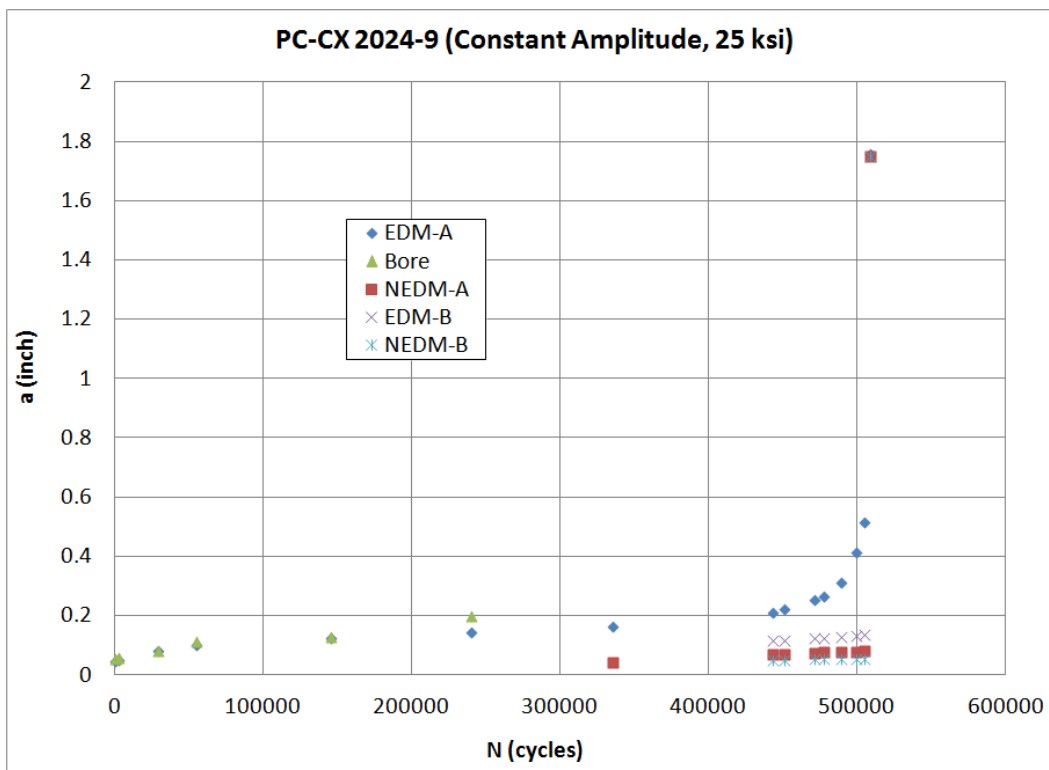


Fig. 65 PC-CX 2024-9 Crack Growth Curve

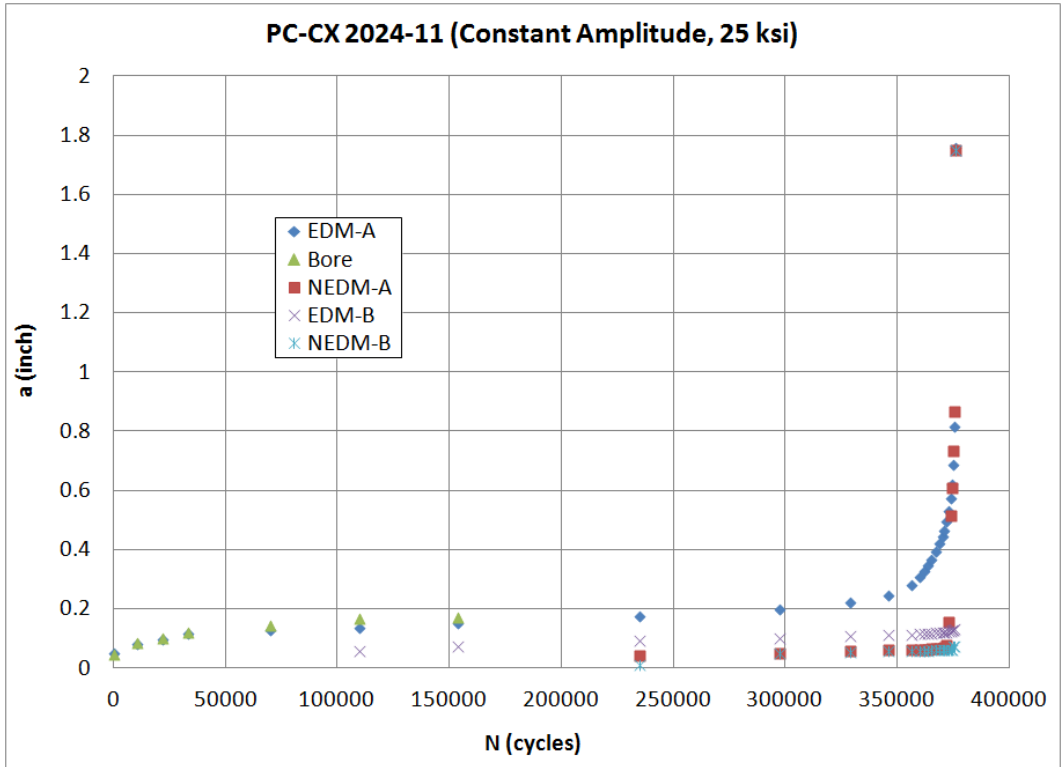


Fig. 66 PC-CX 2024-11 Crack Growth Curve

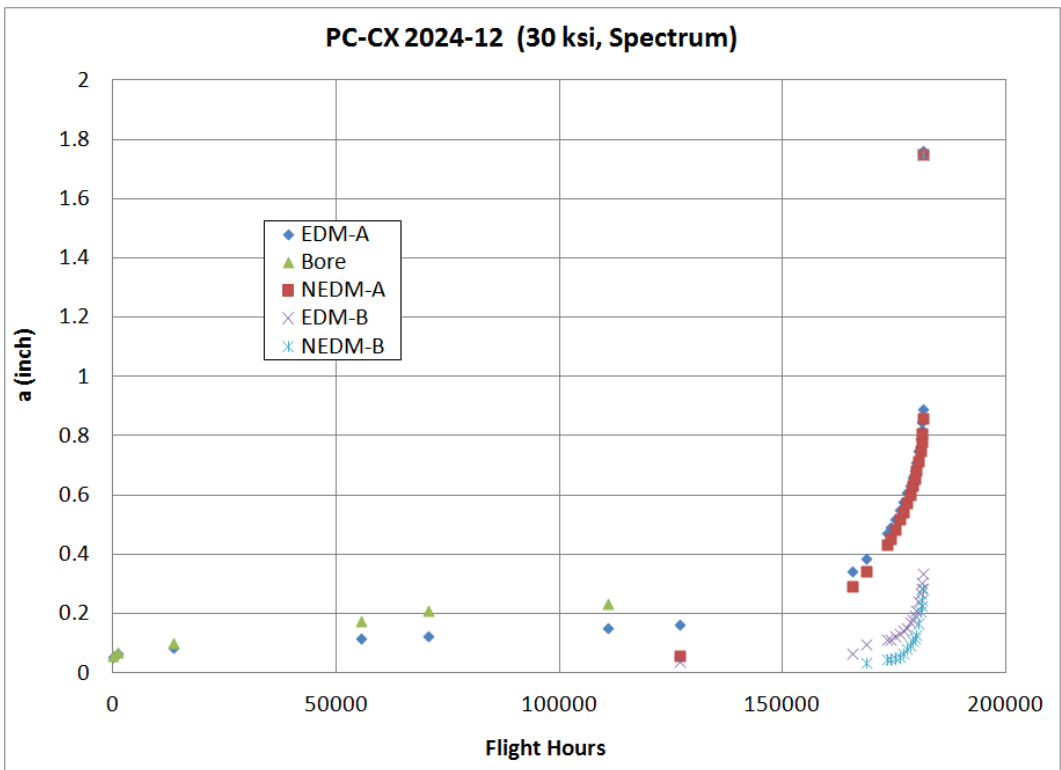


Fig. 67 PC-CX 2024-12 Crack Growth Curve

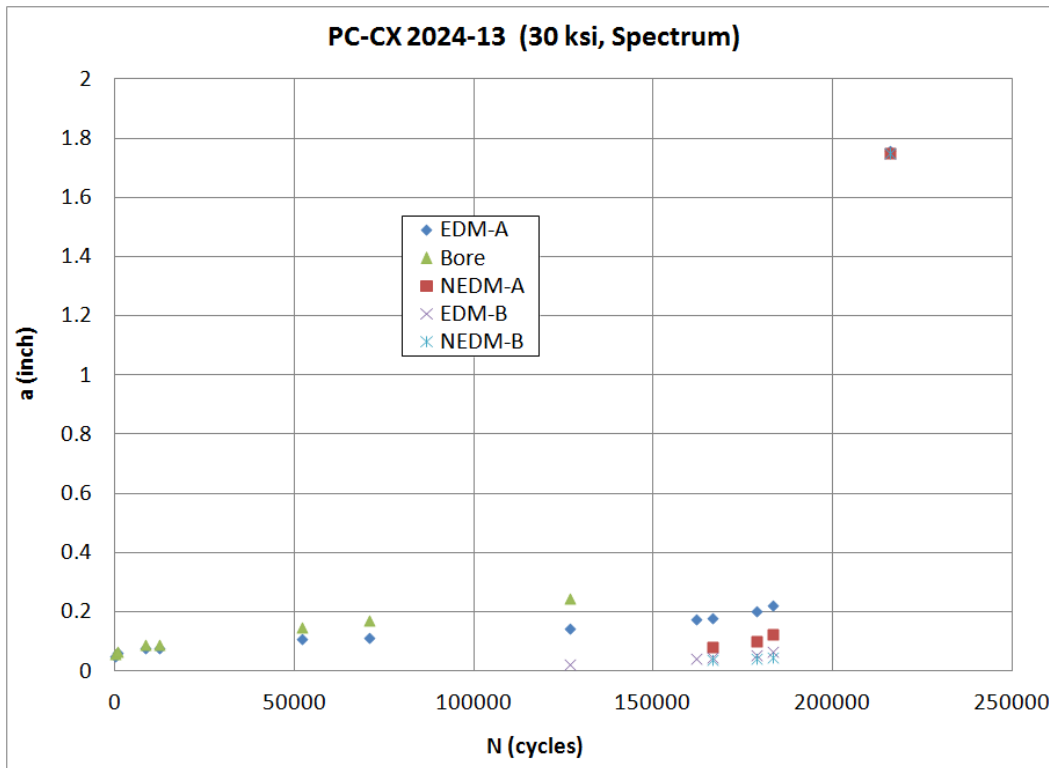


Fig. 68 PC-CX 2024-13 Crack Growth Curve

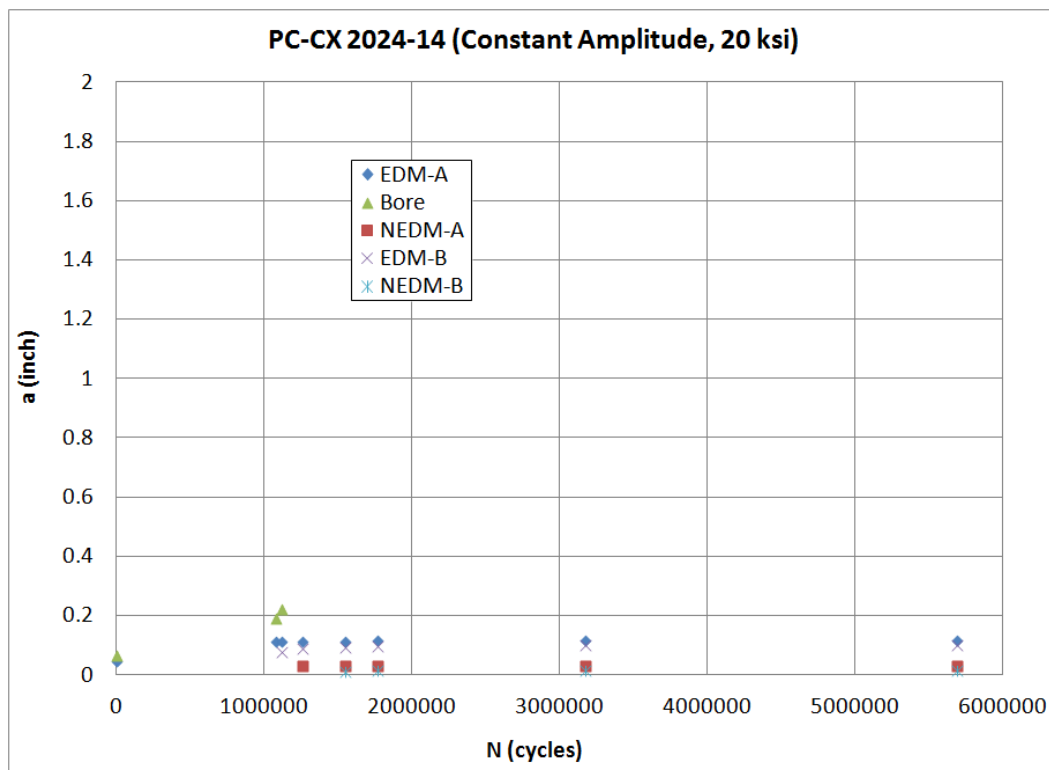


Fig. 69 PC-CX 2024-14 Crack Growth Curve

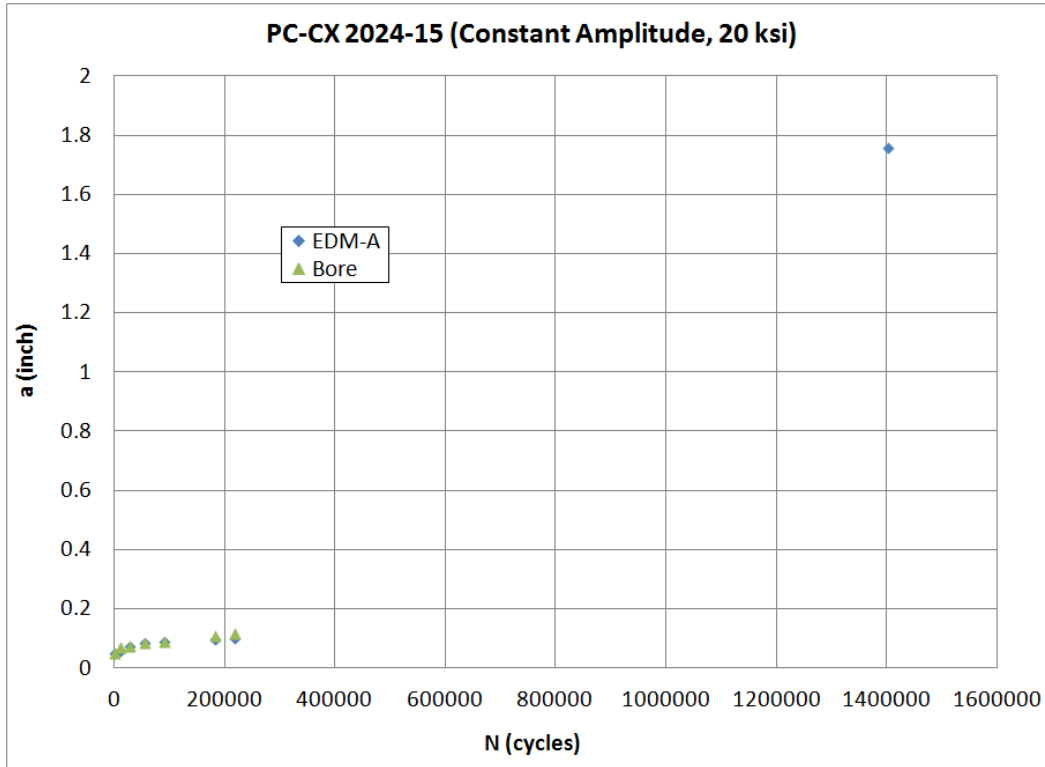


Fig. 70 PC-CX 2024-15 Crack Growth Curve

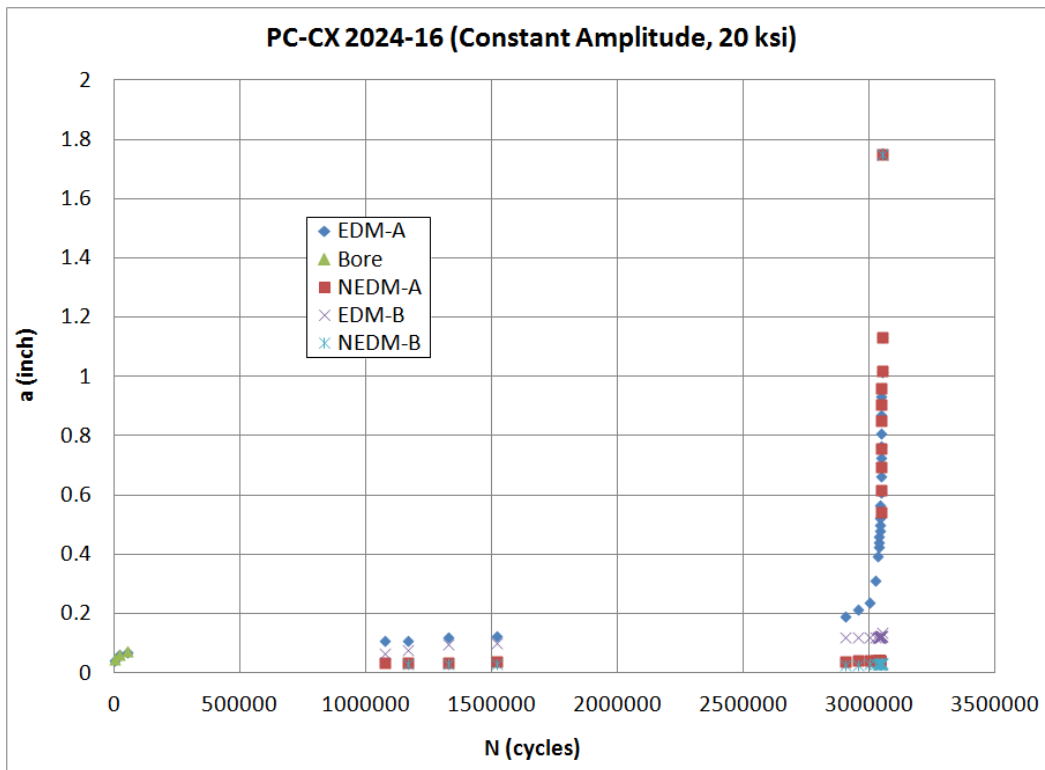


Fig. 71 PC-CX 2024-16 Crack Growth Curve

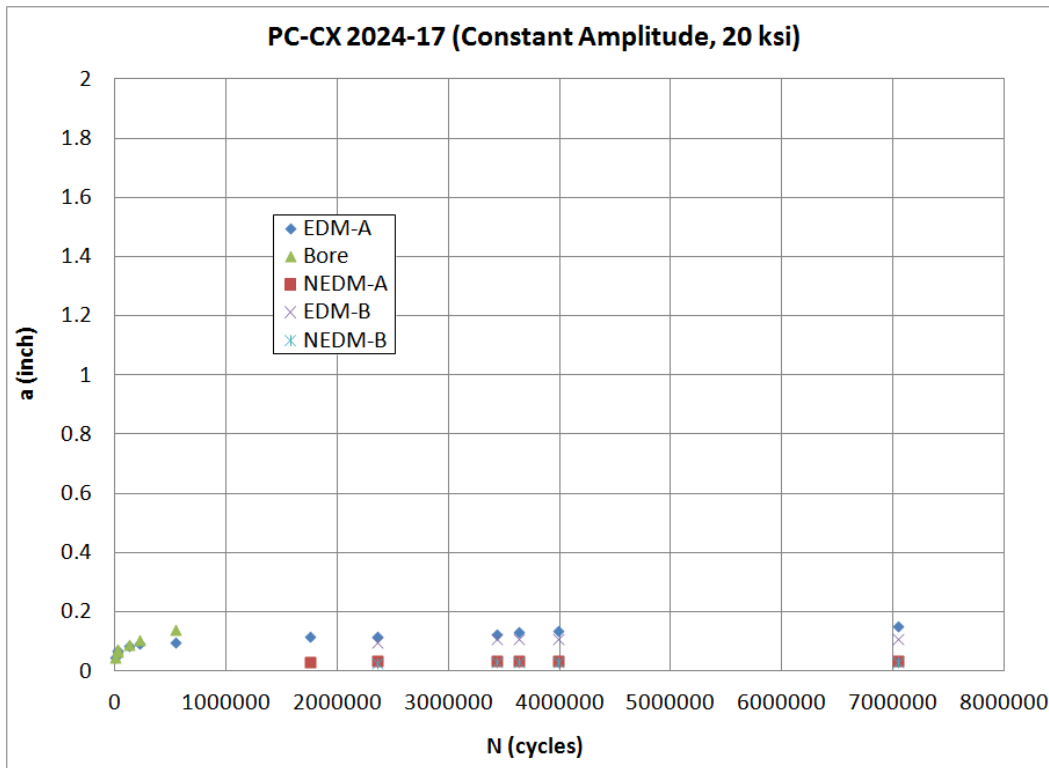


Fig. 72 PC-CX 2024-17 Crack Growth Curve

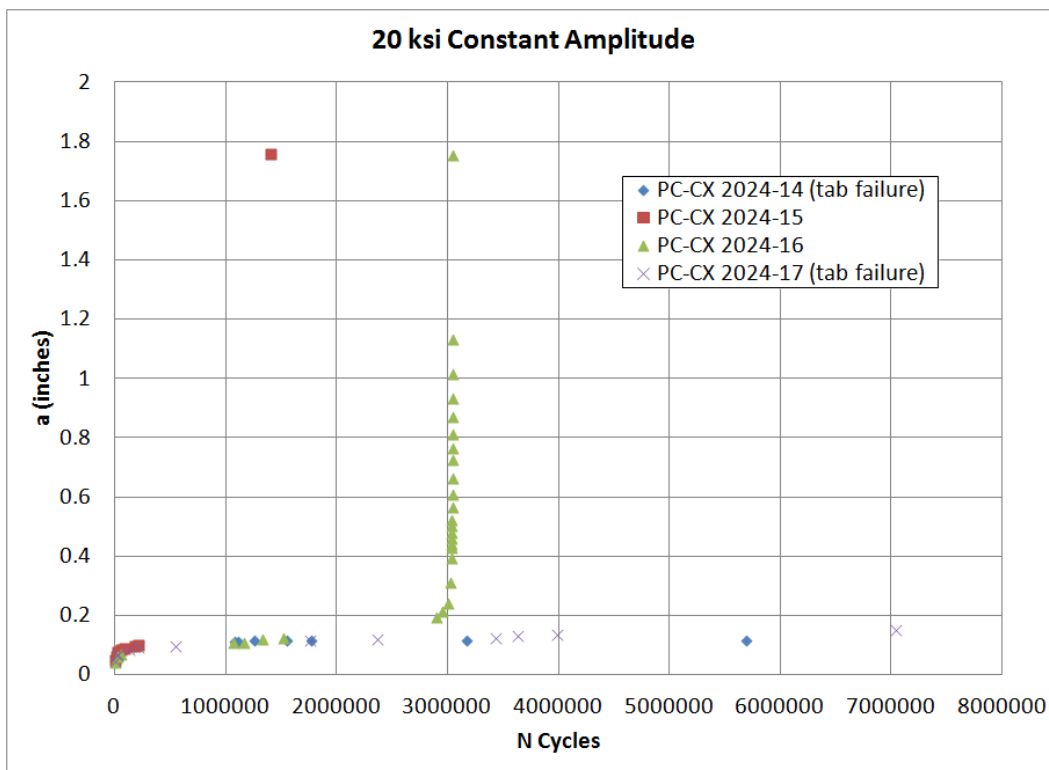


Fig. 73 All 20 ksi Constant Amplitude Tests

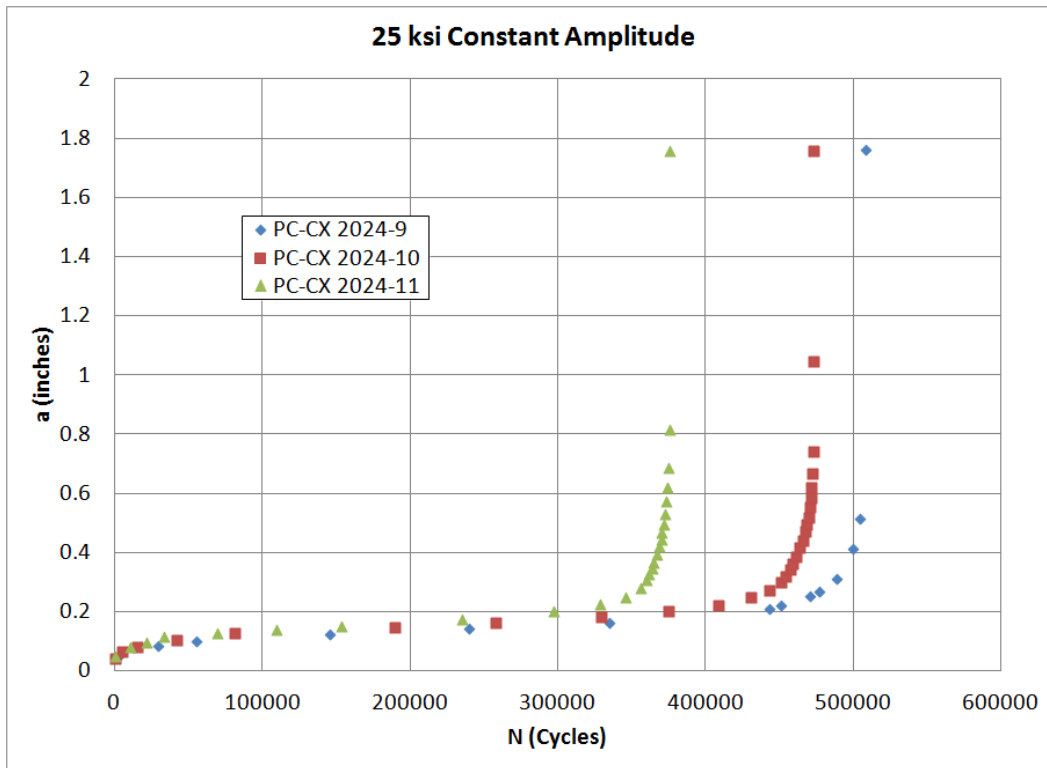


Fig. 74 All 25.00 ksi Constant Amplitude Tests

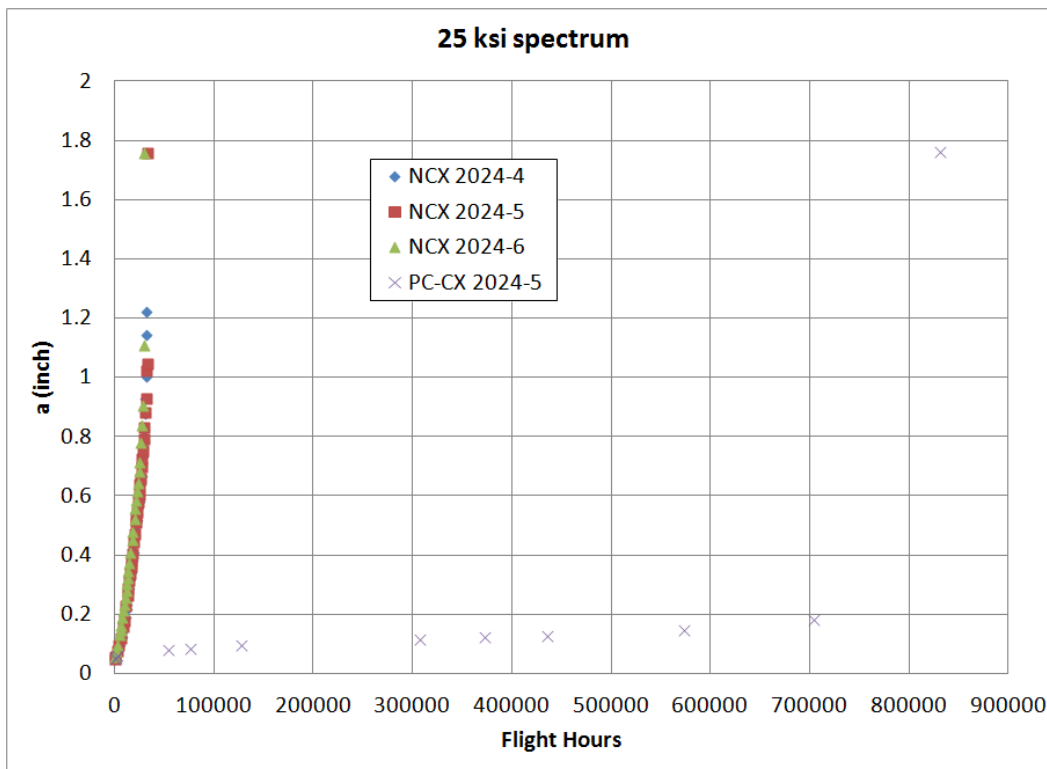


Fig. 75 All 25.00 ksi Spectrum Tests

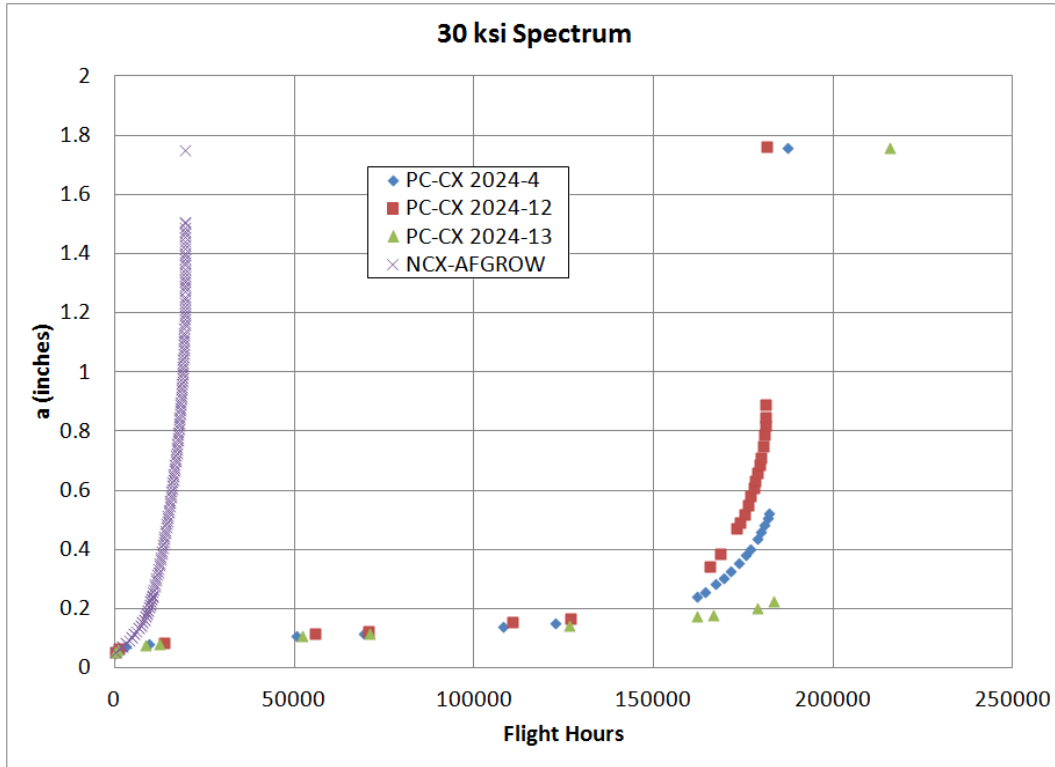


Fig. 76 All 30.00 ksi Spectrum Tests

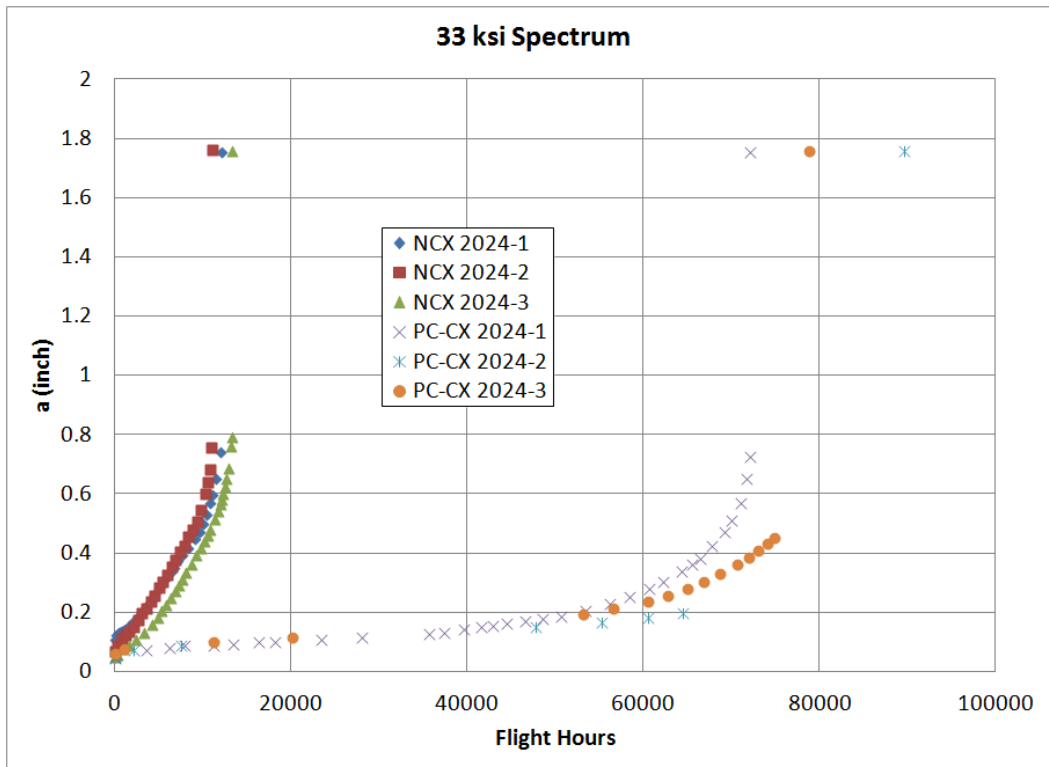


Fig. 77 All 33.00 ksi Spectrum Tests

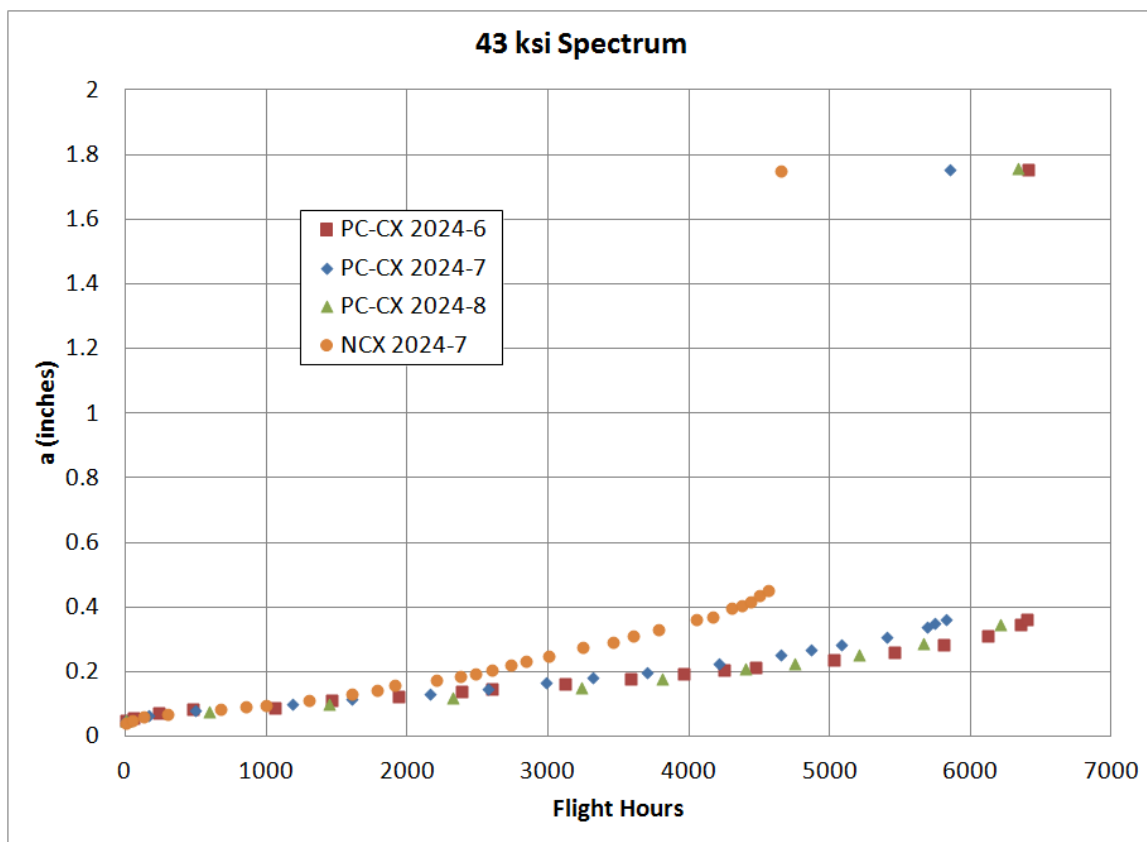


Fig. 78 All 43.25 ksi Spectrum Tests

APPENDIX D

AFGROW PREDICTIONS

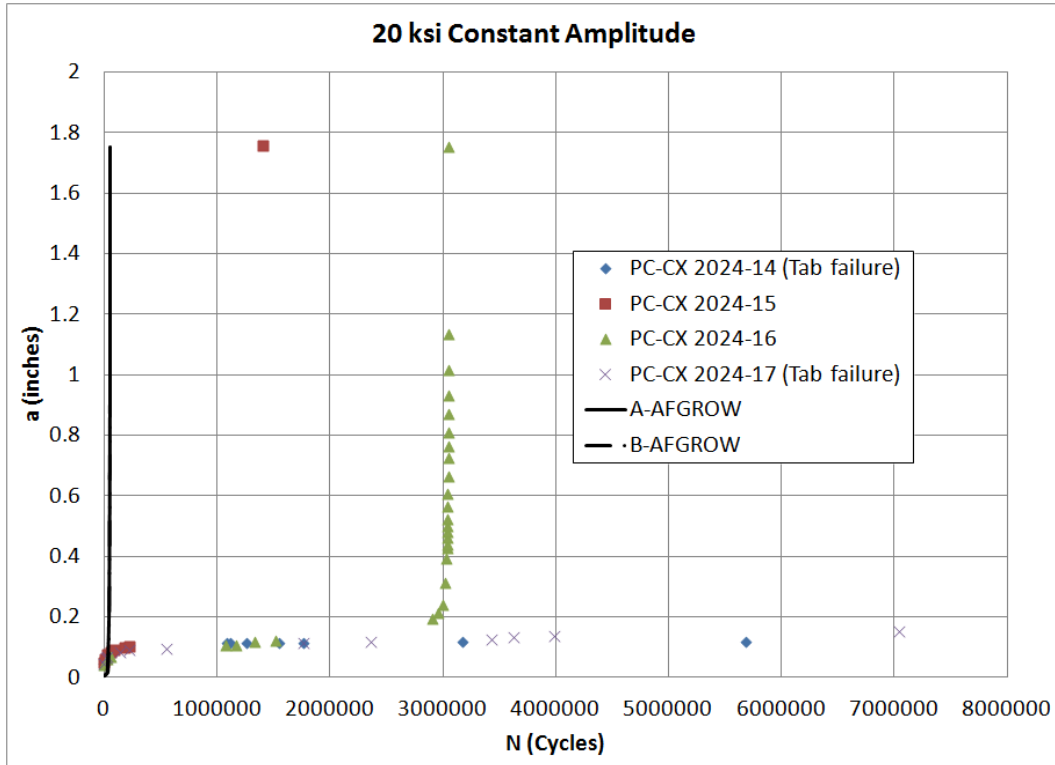


Fig. 79 All 20 ksi Constant Amplitude Tests and AFGROW 0.005 inches IFS Predictions

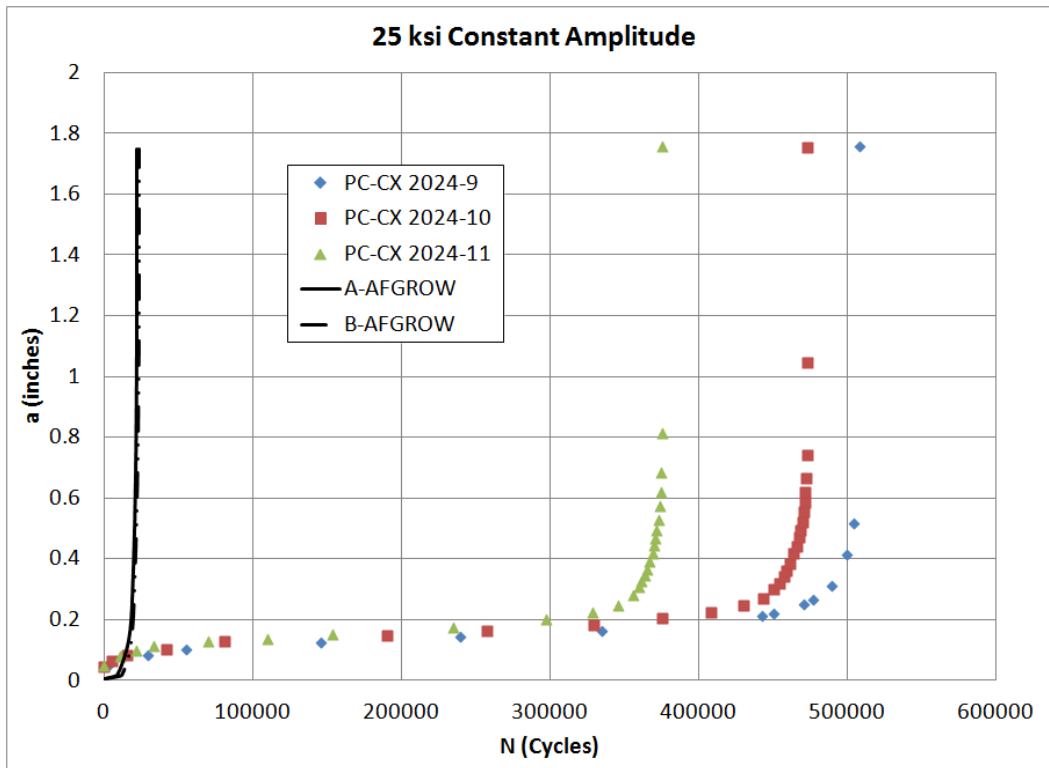


Fig. 80 All 25.00 ksi Constant Amplitude Tests and AFGROW 0.005 inches IFS Prediction

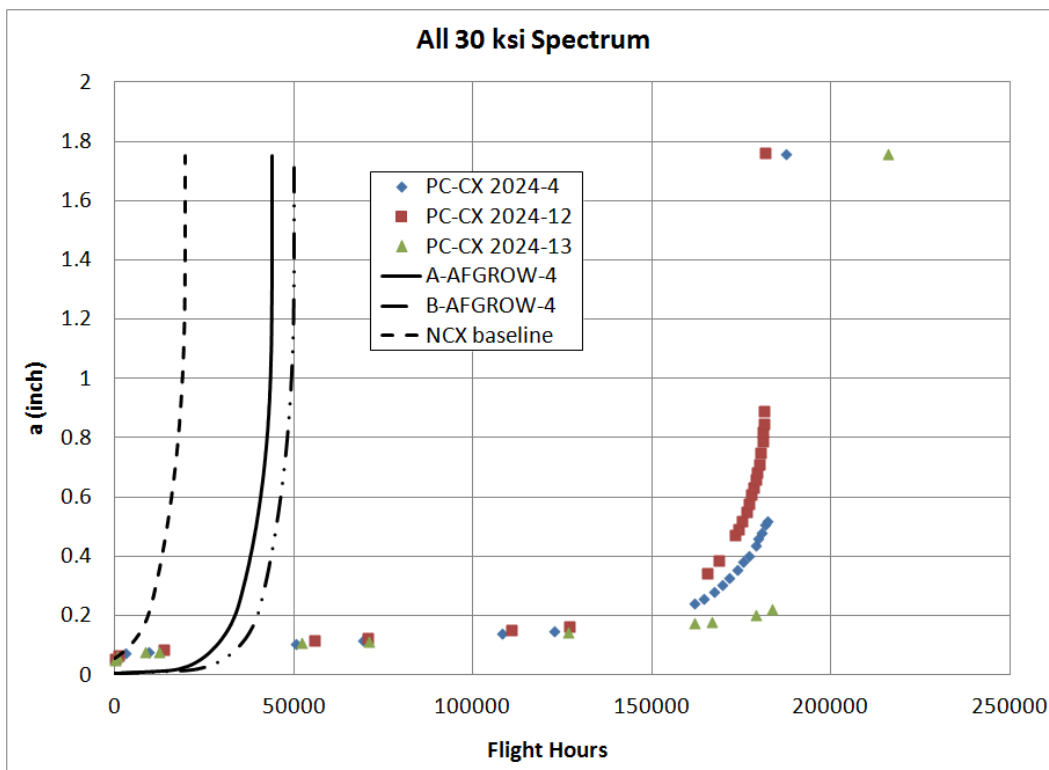


Fig. 81 All 30.00 ksi Spectrum Tests and AFGROW 0.005 inches IFS Predictions

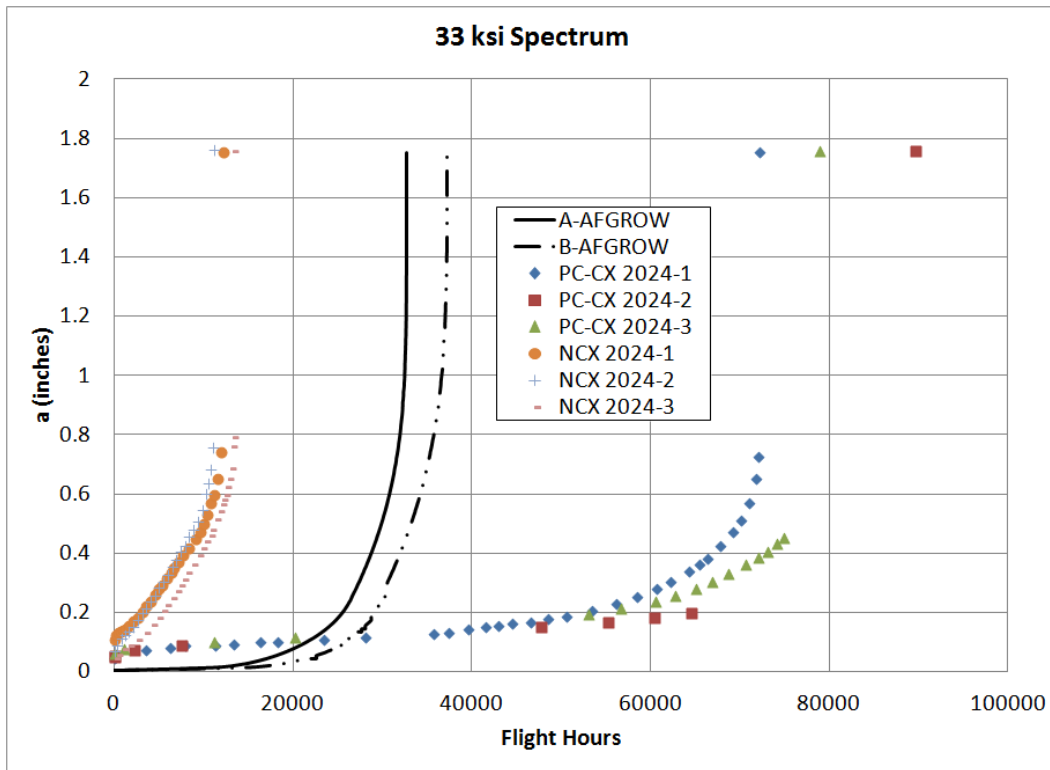


Fig. 82 All 33.00 ksi Spectrum Tests and AFGROW 0.005 inches IFS Predictions

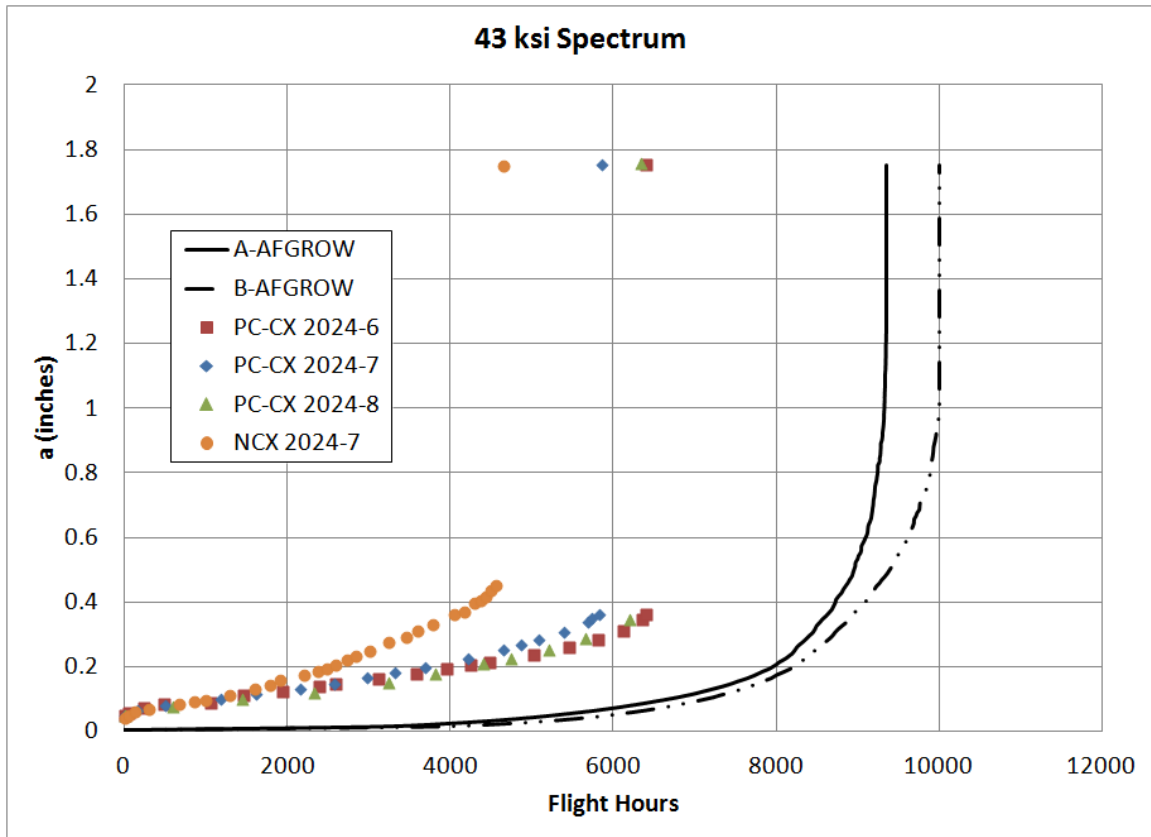


Fig. 83 All 43.25 ksi Spectrum Tests and AFGROW 0.005 inches IFS Predictions

APPENDIX E

FRACTOGRAPHIC IMAGES

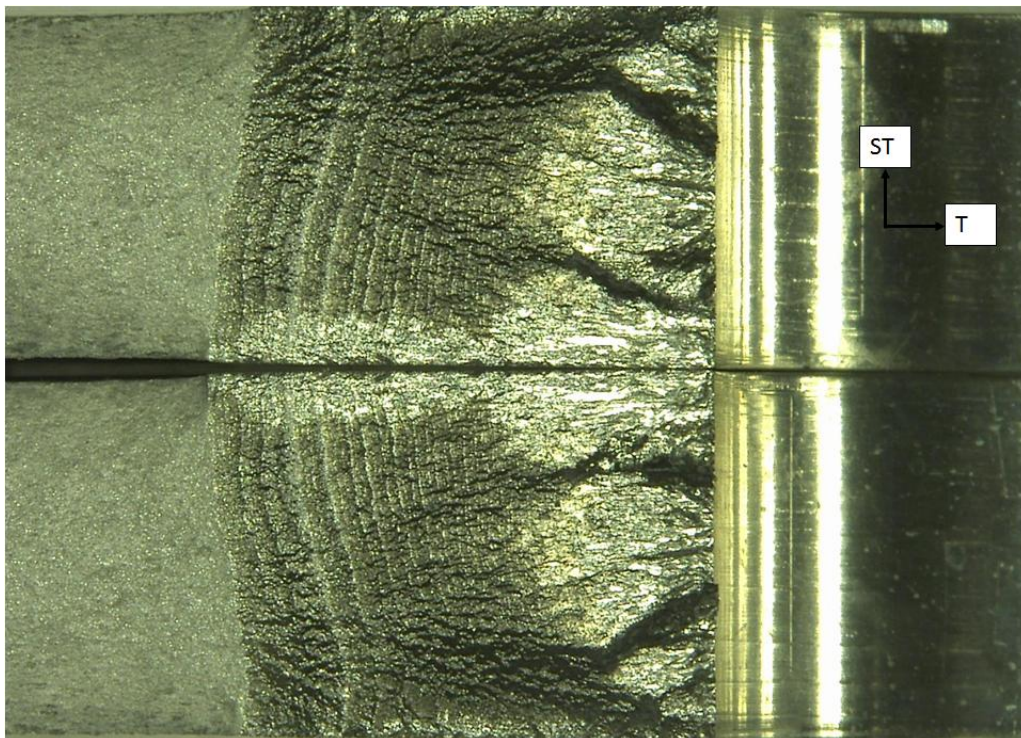


Fig. 84 Beachmarks and Multiple Bore Nucleation Sites on Side B of Precracked Cold-Expanded Spectrum Test with Peak Stress 33.00 ksi. (PC-CX 2024-2)

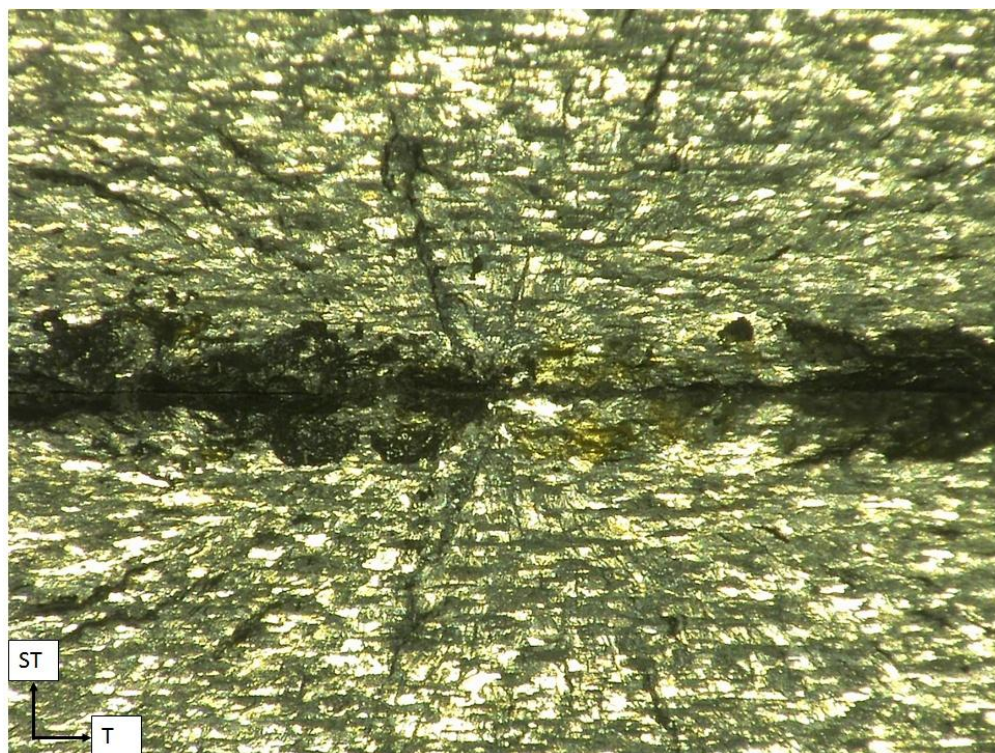


Fig. 85 Nucleation Site of Grip Failure in PC-CX 2024-5 Test

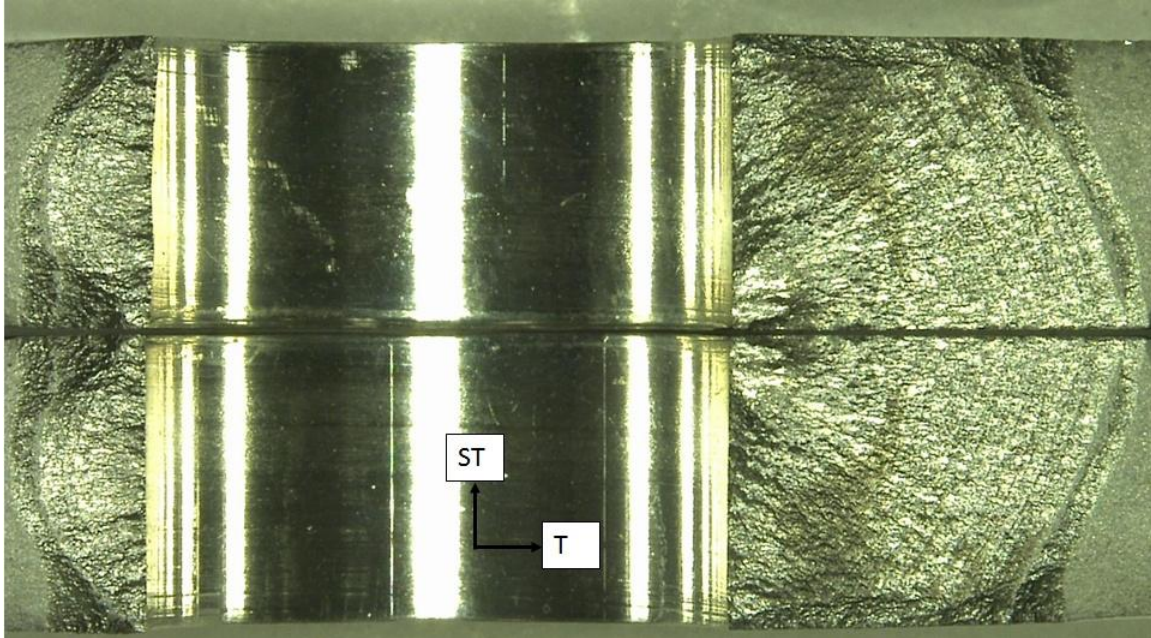


Fig. 86 Beachmarks on Precracked Cold-Expanded Spectrum Test at 43.25 ksi Peak Stress

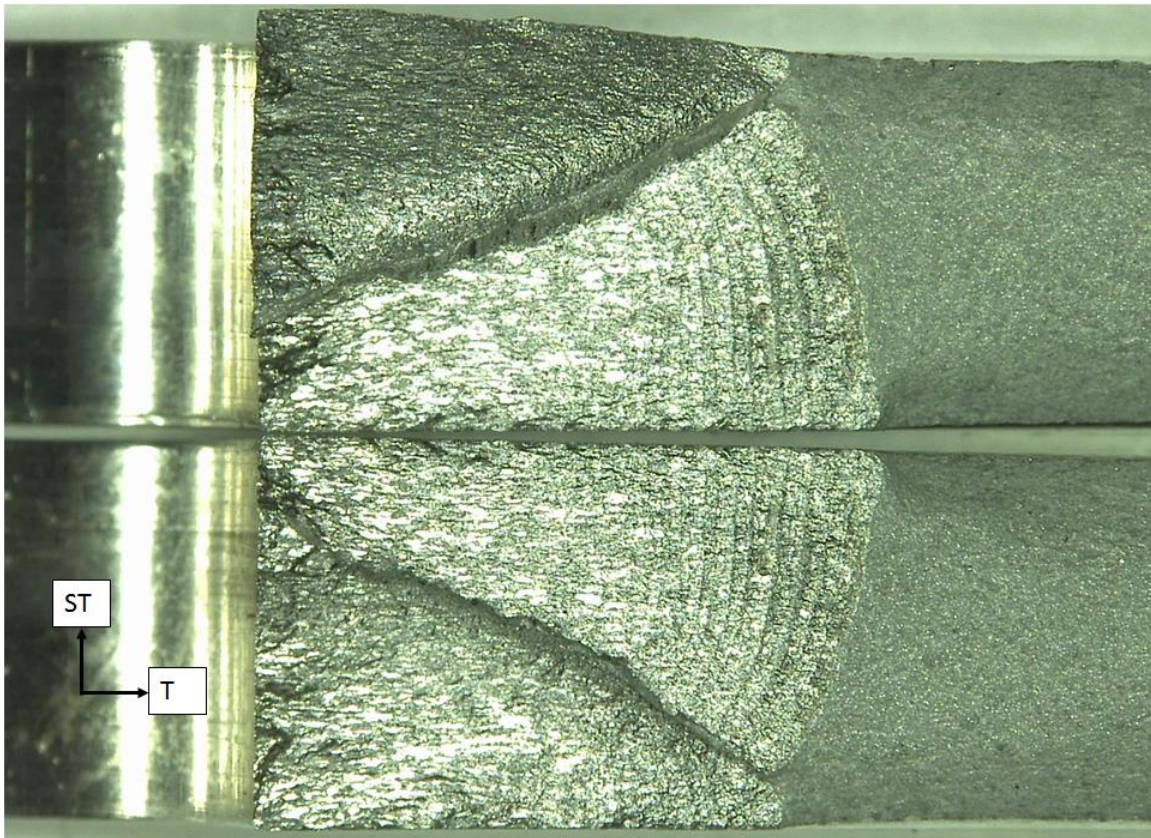


Fig. 87 Two Cracks Nucleated on Different Planes in the Bore of Precracked Cold-Expanded, Constant Amplitude Test with Max Stress of 25.00 ksi.

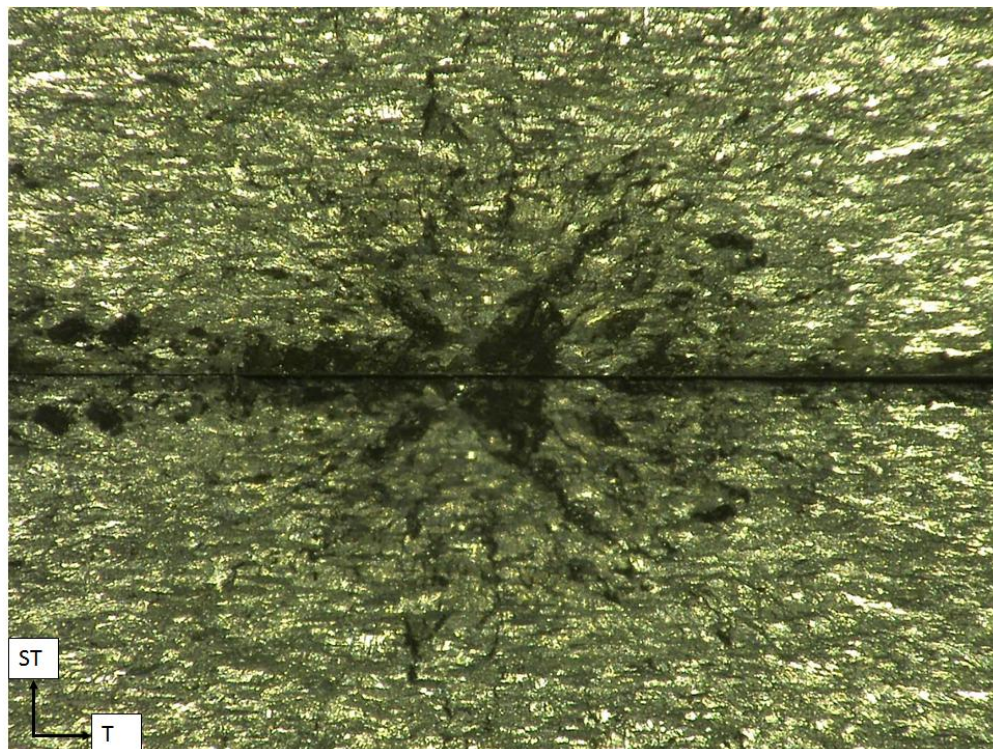


Fig. 88 Nucleation Site of Grip Failure in Constant Amplitude 20 ksi Peak Stress Test (PC-CX 2024-14)

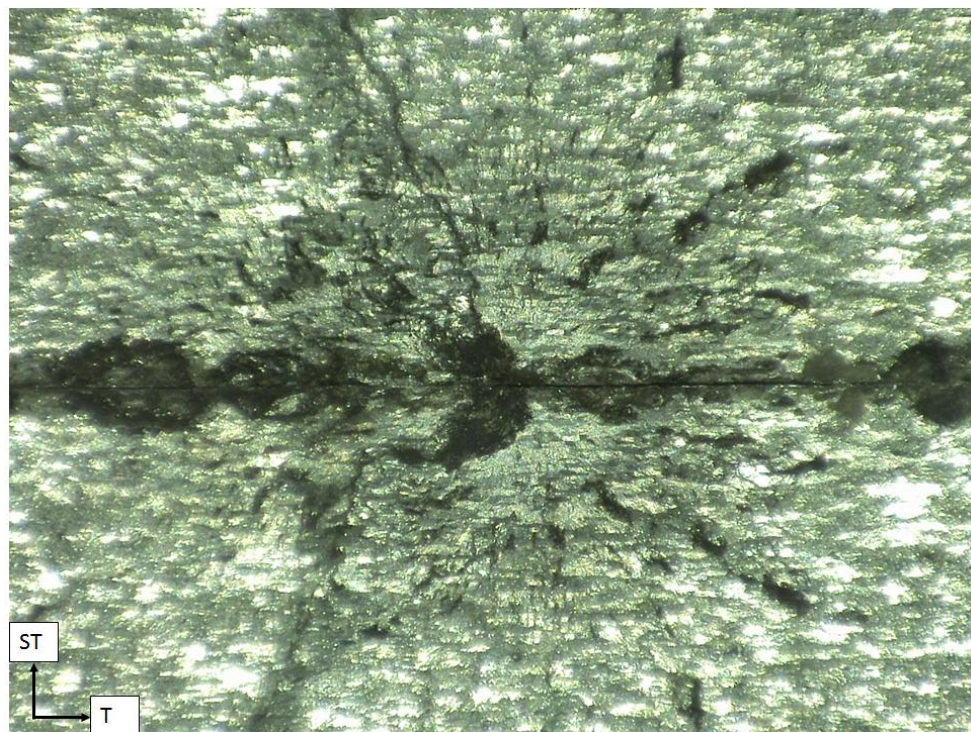


Fig. 89 Nucleation Site of Grip Failure in Constant Amplitude 20 ksi Peak Stress Test (PC-CX 2024-17)

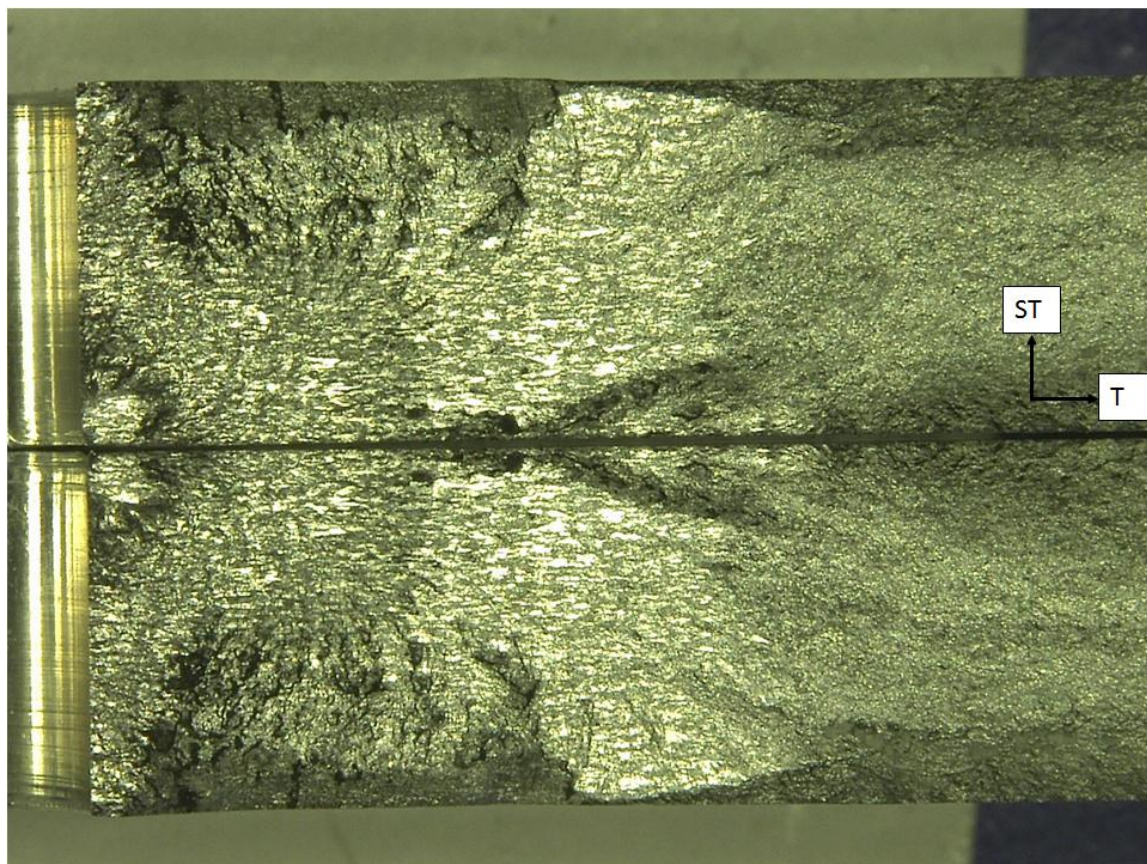


Fig. 90 P Shape Crack Front in Precracked Cold-Expanded Constant Amplitude 20 ksi Peak Stress Test (PC-CX 2024-15)

APPENDIX F

da/dN VS. ΔK DATA

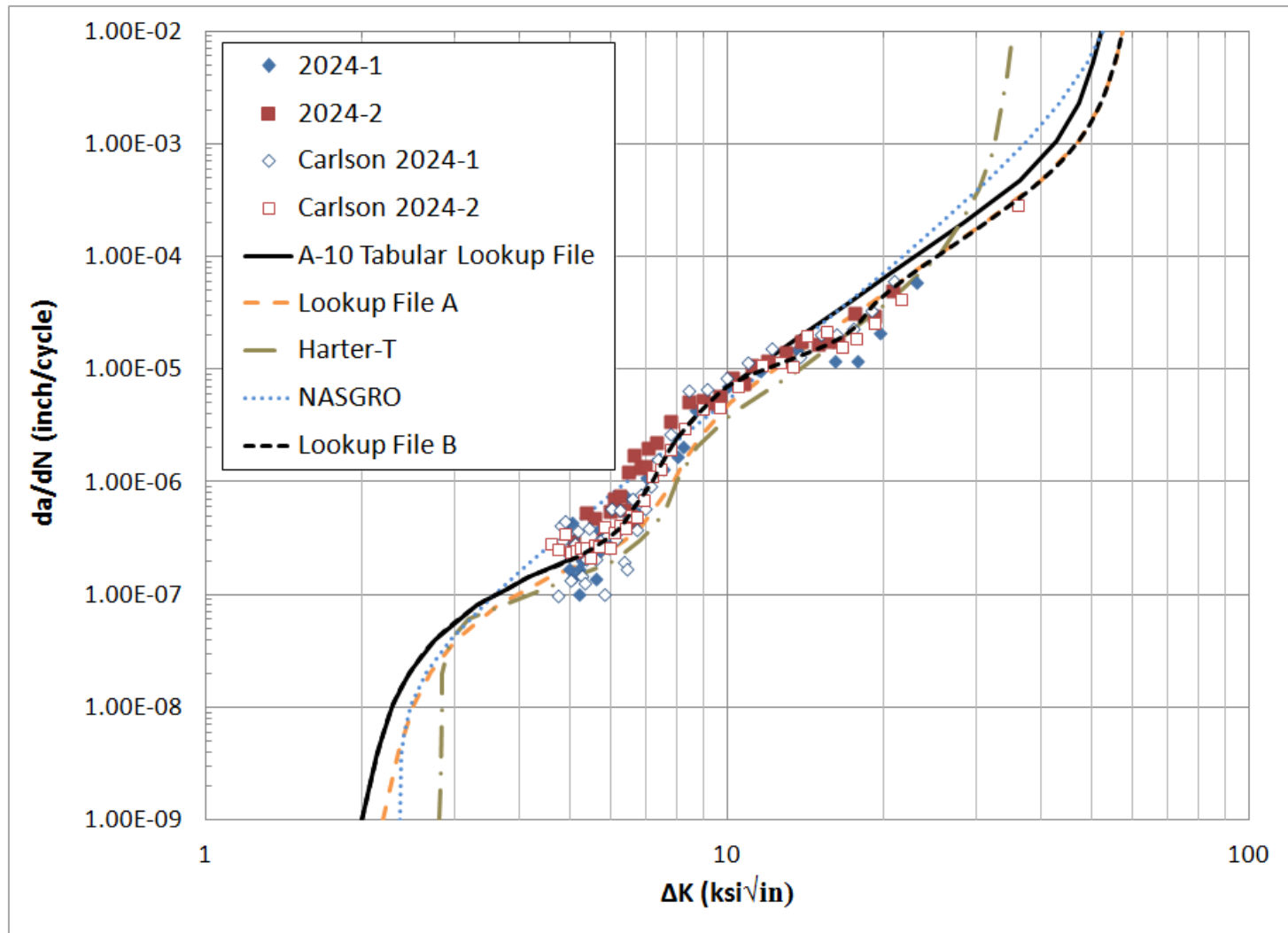


Fig. 91 da/dN vs. delta K Data and Common Curve Fits

APPENDIX G

DAMAGE TOLERANCE ANALYSIS GROUND RULES FOR A-10A
RECONFIGURED POST-DESERT STORM SPECTRUM

This document outlines the approach for conducting damage tolerance analyses for the A-10 Damage Tolerance Analysis (DTA) and Force Structural Maintenance Plan (FSMP) update. This update is a joint effort between USAF, Southwest Research Institute and Northrop Grumman. These ground rules apply to analyses using the USAF crack growth software AFGROW.

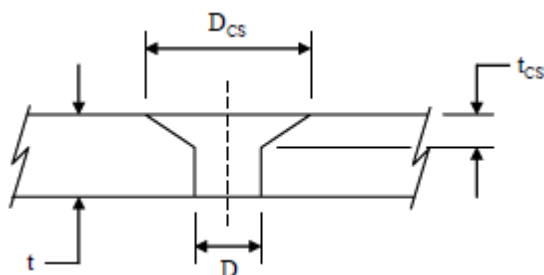
1. Version 4.10.13.0 of AFGROW released 02/03/2006
 - a. Prepare AFGROW Electronic Input file (.dax) as part of deliverable.
 2. Title: Brief description of model.
 3. Material: reference RPDS DTR Master Document for guidance related to material model (Forman Lookup or Tabular Lookup) as well as material properties for cp locations. Reference “A-10 Material Reference” document for new analysis not covered by the RPDS Master Document. This document is a general guide and some material properties may need to be adjusted based on manufacturing thicknesses or other factors. Reference the RPDS DTR Master Document and the “Metallic Materials Properties Development and Standardization” (formerly MIL HNDBK 5) document to verify correct material properties.
 - a. Tabular Lookup File
 - i. Select appropriate tabular lookup file from A-10 Materials Folder.
 1. **Verify** correct material properties *for each control point* as prescribed in RPDS DTR Master Document.

NOTE: Ultimate strength and RLO default to 66ksi and -1.0; these values will need to be modified in accordance with the RPDS DTR Master Document. Altering the ultimate strength does not seem to affect the result from AFGROW.
 - b. Forman Lookup File
 - i. Select appropriate Forman lookup file from A-10 Materials Folder.
 1. **Verify** correct material properties *for each control point* as prescribed in RPDS DTR Master Document
 2. Special note: Fracture Toughness
 - a. Kc: “FR Kcut” from the RPDS DTR Master Document under Grumman CP1-72 Forman Constants must be entered as the Plain Stress Fracture Toughness, KC, value in AFGROW material properties. Do **not** use USAF “Kc” in AFGROW material properties.
 - b. USAF “Kc” from RPDS DTR Master Document must be entered into AFGROW » Predict Function Preferences » Propagation Limits » User Defined ‘Kmax’

NOTE: RLO defaults to -1.0; this value will need to be modified in accordance with the RPDS DTR Master Document, typically - 0.3
 - c. Material Properties. Select from RPDS DTR Master Document.
4. Model:

- a. Classic models
- i. Select appropriate geometric model
 - ii. Enter problem geometric factors including: thickness, width, hole diameter, initial flaw size (IFS), offset, etc
 1. 1. Keep A/C constant=YES (checked)
 - a. Note: Keep A/C constant=NO [For specific cases as noted in SA220R0207 (2nd 6000 Hour DTR)]
 2. Oblique through crack=NO (unchecked)
 3. Initial Flaw Size: Unless otherwise specified, the initial flaw size should be the same in both the “A” & “C” directions. See Section 10 for appropriate initial flaw sizes.
 4. Countersunk Holes:
 - a. A weighted average hole diameter should be used in the geometric model if the hole is countersunk
 - b. The weighted average hole diameter is calculated as the cross-sectional area of the hole divided by the thickness, i.e.,

$$D_{ave} = \frac{D(t - t_{cs}) + [(D + D_{cs})/2]t_{cs}}{t}$$

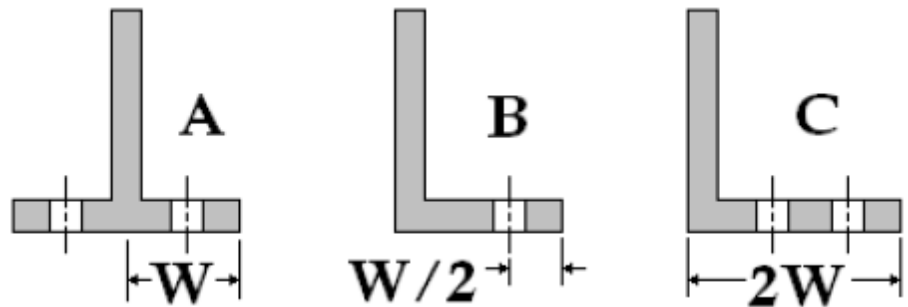


- c. Knife edge fasteners ($t_{cs} \geq t$) are not allowed in airframe design because of fatigue requirements. The maximum countersink depth is

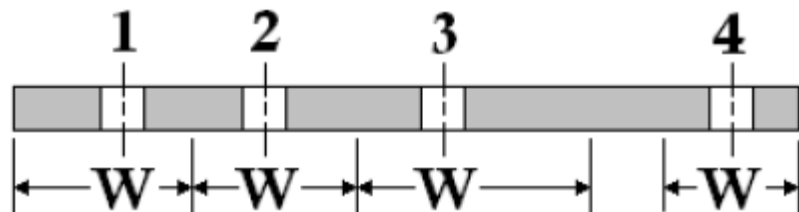
$$t_{cs} = \frac{2}{3}(t)$$

- iii. Load: Ratio of tension or bearing stress to reference stress must be input for each load case (tension stress fraction = 1.0, if bearing stress is zero).
- iv. For pin loaded fastener holes, the tension stress fraction should reflect the reduced bypass stress fraction (i.e.: 20% load transfer equates to 80% tension stress fraction).
 1. Effective Widths: Refer to RPDS DTR Master Document for appropriate Effective Width for each CP.
 - a. New analysis: For the purpose of determining the Bearing Stress Fraction (BrSF) in AFGROW the following approach should be used.
 - b. For all capstrips, angles etc., the effective width as shown in the figure below: A) the length of the leg,

B) the offset doubled, or C) one-half the leg length as in the case of a leg with a double row of fasteners. In cases where multiple cases could be applicable, use the smallest effective width.



- c. In situations where there is a line of fasteners the effective width can be taken as 1) offset plus half the distance to the neighboring hole, 2 & 3) the sum of half the distance to the neighboring holes, or 4) offset doubled, whichever is less.



- d. The final method of finding the BrSF is to determine it directly from the load reports. The far field stress is easily determined using the load and the cross-sectional area, the bearing stress is the load taken out by the fastener divided by (width * thickness). Typically, doing this method in lieu of the above technique should result in the same BrSF.
2. Further modeling may be necessary via, FEM, Stress-Check, etc.
 - v. The “Filled Unloaded Hole” option is not typically used unless engineering judgment overrides this approach. If used, justification must be provided in the analysis report.
- b. Lug Model
- i. Use AFGROW default preferences (see Predict Function Preferences in this document).
5. Spectrum:
- a. Stress Multiplication Factor (SMF)
 - i. Enter maximum stress (normalized spectrum will be used for all analyses).

1. Maximum stresses come from Northrop Grumman stress equations (reference SA220R0474), these values are also listed in the RPDS DTR Master Document.
 - b. Residual Strength Requirement (Pxx)
 - i. Enter the higher of either the maximum spectrum stress or the limit stress if known.
 - c. Open existing spectrum file
 - i. Use only RPDS severe spectrum from approved spectrum folder.
 1. A common spectrum electronic folder will be utilized.
 2. Spectrum files are:
 - a. Flight-by-flight
 - b. Base-peak-base converted
 - c. Normalized
 - ii. In the event an AFGROW ready spectrum file (filename.sp3) is not in existence, use the spectrum converter file to be certain the spectrum file is in the proper format to be read by AFGROW.
6. Retardation:
- a. Generalized Willenborg Retardation
 - i. Turn OFF the “Adjust Yield Zone Size for Compressive Cycles” toggle.
 - ii. For all SOLR values, see the RPDS DTR Master Document and/or Appendix F.
7. Predict Function Preferences:
- a. Growth Increment
 - i. Cycle by Cycle Beta and Spectrum calculation
 1. For advanced models use “Cycle by Cycle Spectrum calculation”.
 - a. Use default % Max. Growth Increment of 1%.
 - b. Output Intervals
 - i. Specify Crack Growth Increments.
Increment = 0.01”.
 - ii. Number of Hours per Pass.
 1. Spectra based on 240 hours for all except landing gear
 2. Landing gear spectra based on 250 landings (assumes 1.5 hours per landing).
 - c. Output Options (AFGROW output files are part of deliverables).
 - i. Output
 1. Data File
 2. Plot File
 - d. Propagation Limits
 - i. Kmax failure criteria (If using Forman: see 3.b.i.2.a of these ground rules)

- ii. Net section yield: to be evaluated on a case-by-case basis
 - e. Transition to Through Crack
 - i. Default = 95% (Stick with default unless documented otherwise.)
 - f. Lug Boundary Conditions
 - i. Use default of combined bearing and spring solution and default values:
 - 1. Bearing: 70%
 - 2. Spring 80%
- 8. Stress State
 - a. Use Stress State to be determined automatically.
- 9. Betas
 - a. Use AFGROW standard solution betas for standard geometries.
 - b. Non-standard geometries shall be dealt with on a case-by-case basis (User Defined Betas: Legacy, NASGRO, StressCheck, etc.)
- 10. Inspection intervals
 - a. Initial inspection intervals based upon the safety limit (Initial Flaw Size** to fracture) divided by 2. **Ref: JSSG-2006 Table XXX, page 449.
 - i. New Structure Initial Flaw Sizes (IFS)
 - 1. Non-Cold Worked Holes:
 - a. Aluminum: IFS = 0.05"
 - b. Steel: IFS = 0.05"
 - 2. Cold Worked Holes:
 - a. Aluminum: IFS = 0.005"
 - b. Steel: IFS = 0.005"
 - 3. Surface Flaws
 - a. IFS = 0.05" = c (This is the half crack length)
 - b. Recurring inspection intervals based upon the field safety limit (Detectable Flaw Size** to fracture) divided by 3. **Ref: JSSG-2006 Table XXXII, page 450.
 - i. Field safety limit detectable flaw sizes (DFS)
 - 1. For Bolt Hole Eddy current inspections
 - a. Non Coldworked Holes
 - i. Aluminum: DFS = 0.05"
 - ii. Steel: DFS = 0.05"
 - b. Coldworked Fastener Holes
 - i. Aluminum: DFS = 0.03"
 - ii. Steel: DFS = 0.05"
 - 2. Eddy Current Surface Scan

- a. Around hole—Aluminum and Steel: $DFS = 0.10''$ + fastener head overlap, if applicable
 - b. Surface Flaw—Aluminum and Steel: $DFS = 0.10'' = 2c$ (this is the total crack length)
 - 3. Magnetic Particle
 - a. Steel: $DFS = 0.10''$
 - 4. Visual
 - a. $0.50''$
- 11. Continuing Damage Option
 - a. Use standard Air Force practice when justified.
 - i. JSSG 2006 Table XXXI, page 450.
- 12. Document analysis using A-10 USAF-SwRI-NGC DTA template

REFERENCES

- ¹Shutz, W. (1996) A history of fatigue. *Eng. Fract. Mech.* **54**, 263-300.
- ²Molnar, M. (2011) Southwest airlines scare. Popular Mechanics. [Cited Jan. 4, 2012] <<http://www.popularmechanics.com/technology/aviation/safety/how-southwest-airlines-flight-812-737s-fuselage-weakness-went-undetected-5519864>>.
- ³American Society for Testing and Materials (ASTM). (2010). Standard terminology relating to fatigue and fracture testing. (E 1823), *Am. Soc. For Testing and Materials*, West Conshohocken, PA, USA.
- ⁴Becker, W. T. and Shipley, R. J. (2002) *ASM Handbook*. Vol. 11: Failure analysis and prevention, Materials Park, OH.
- ⁵Griffith, A. A. (1920) "The phenomena of rupture and flow in solids." *Philosophical Transaction of the Royal Society*, London, Series A, **221**, Delft, Netherlands.
- ⁶Janssen, M., Zuidema, J. and Wanhill, R.J.H. (2002) *Fracture mechanics*. Delft University Press, 2nd ed., Delft, Netherlands.
- ⁷ASM International Handbook Committee (1996) *ASM handbook*. Vol. 19: Fatigue and fracture, ASM International.
- ⁸Department of Defense (2005). *Aircraft Structural Integrity Program (MIL STD 1530C)*, Department of Defense Standard Practice, United States Air Force.
- ⁹Fatigue Technologies Inc. (2002). *FTI process specification 8101D cold expansion of holes using the standard split sleeve system and countersink cold expansion (CsCx™)*, Seattle, WA, USA.
- ¹⁰Wagner, R. V., Reid, L., Easterbrook, E. T. and Rufin, A. C. (1992) Beneficial effects of Split Sleeve Cold Expansion(TM) on the fatigue lives of pre-cycled cold expanded structure. *Aircraft Structural Integrity Conference (ASIP)*, San Antonio, TX, USA.
- ¹¹Steensma, D. K. (1993) *Procurement of cold expansion tool kits by the Oklahoma City Air Logistics Center*. Technical Assessment Report, **94-018**, Arlington, VA, USA.
- ¹²Lam, Y.C. (1993) A comparative study on the effects of interference fit and cold expansion on the fatigue life of cracked holes. *Scr. Metall. Mater.* **27**, 191-195.

- ¹³ Reid, L and Restis, J. H. Life (1997) *Enhancement of repairs subject to the repair assessment program*. NASA/DoD/FAA First Conference on Aging Aircraft, Ogden, UT, USA.
- ¹⁴ Toor, P. M. (1976) Cracks emanating from precracked coldworked holes. *Eng. Fract. Mech.* **8**, 391-395.
- ¹⁵ Air Force Structures (2011). *Structures Bulletin EN-SB-08-012, Revision B – Nondestructive inspection capability guidelines for United States Air Force aircraft structures*, Wright-Patterson AFB, OH, USA.
- ¹⁶ Ball, D.L., Lowry, D.R., (1998) Experimental investigation on the effects of cold expansion of fastener holes. *Fatigue Fract. Engng. Mater. Struct.* **21**, 17-34.
- ¹⁷ Pell, R.A., Beaver, P.W., Mann, J.Y. and Sparrow, J.G. (1989) Fatigue of thick-section cold-expanded holes with and without cracks. *Fatigue Fract. Engng. Mater. Struct.* **12**, 553-567.
- ¹⁸ Zhang, X. and Wang, Z. (2003) Fatigue life improvement in fatigue-aged fastener holes using the cold expansion technique. *Int. J. Fatigue.* **25**, 1249-1257.
- ¹⁹ Phillips, J. L. (1974) Sleeve cold working fastener holes. *Air Force Materials Laboratory AFML-TR-74-10.* **1**, D6-26271-6. Wright Patterson Air Force Base.
- ²⁰ Chandawanich, N. and Sharpe, W. N., Jr. (1979) An experimental study of fatigue crack initiation and growth from coldworked holes. *Eng. Fract. Mech.* **2**, 609-620.
- ²¹ Lacarac, V., Smith, D. J., Pavier, M. J. and Priest, M. (1999) Fatigue crack growth from plain and cold expanded holes in aluminum alloys. *Int. J. Fatigue.* **22**, 189-203.
- ²² Buch, A. and Berkovits, A. (1985) Effect of cold-working by hole expansion on fatigue life of 7075-T351 and 7475-T761 aluminum lugs with and without initial flaws under maneuver loading spectrum. *Department of Aeronautical Engineering Technion - Israel Institute of Technology.* **561**, Haifa, Israel.
- ²³ Buxbaum, O., Huth, H. (1987) Expansion of cracked fastener holes as a measure for extension of lifetime to repair. *Eng. Fract. Mech.* **28**, 689-698.
- ²⁴ Petrak, G.J., Stewart, R.P. (1974) Retardation of cracks emanating from fastener holes. *Eng. Fract. Mech.* **6**, 275-282.
- ²⁵ Andrew, D. L. (2011) Investigation of cold expansion of short edge margin holes with preexisting cracks in 2024-T351 aluminum alloy. *Mechanical Engineering*. University of Utah, Salt Lake City , UT, USA.

- ²⁶ Carlson, S. (2008). Experimentally derived beta (β) corrections to accurately model the fatigue crack growth behavior at cold-expanded holes in 2024-T351 aluminum alloys. *Mechanical Engineering*. University of Utah, Salt Lake City, UT, USA.
- ²⁷ Pilarczyk, R. (2008). Experimentally derived beta corrections to predict fatigue crack growth at cold-expanded holes in 7075-T651 aluminum alloy. *Mechanical Engineering*. University of Utah, Salt Lake City, UT, USA.
- ²⁸ Cathey, W.H., Grandt, A.F. Jr. (1980) Fracture mechanics consideration of residual stresses introduced by coldworking fastener holes. *J. Eng. Mater. Technol.* **102**, 85-91.
- ²⁹ Pasta, S. (2006) Fatigue crack propagation from a cold-worked hole. *Eng. Fract. Mech.* **74**, 1525-1538.
- ³⁰ American Society for Testing and Materials (ASTM). (1997) Standard test method for plane-strain fracture toughness of metallic materials (E 399), *Am. Soc. For Testing and Materials*, West Conshohocken, PA, USA .
- ³¹ American Society for Testing and Materials (ASTM). (2000). Standard test method for measurement of fatigue crack growth rates (E 647), *Am. Soc. For Testing and Materials*, West Conshohocken, PA. USA.
- ³² Gaertner Scientific Corporation (2010) Packing List. Chicago, IL, USA.
- ³³ Gaertner Scientific Corporation (2010) Measuring Microscopes. Micrometer Slide with Readout M303LE. [Cited: January 25, 2012.]
<<http://www.gaertnerscientific.com/microscope/m303le.htm>>.
- ³⁴ Grube, K. P., Burnside, H., and Clark, P. (2011) A-10 Aircraft Structural Integrity Program Damage Tolerance Re-Assessment: Reconfigure Post Desert Storm Sever Spectrum (SA220R0207). *Ogden Air Logistics Center Engineering Services*, Ogden, UT, USA.
- ³⁵ Pilarczyk, R. and Allred, T. (2010) Damage Tolerance Analysis Ground Rules for A-10A Reconfigured Post Desert Storm - Rev W. *Aircraft Structural Integrity Program (ASIP)*. Hill Air Force Base, UT, USA.
- ³⁶ Wood, H.A., Engle, R.M. (1979). *USAF damage tolerance design handbook: Guidelines for the analysis and design of damage tolerant aircraft*. USAF Systems Command, Wright-Patterson Air Force Base, OH, USA.
- ³⁷ LexTech Inc. (2010) *AFGROW (fracture mechanics and fatigue crack growth analysis software)*, version 5.1.5.16.
- ³⁸ Department of Defense (2006). *DoD Joint Service Specification Guide, Aircraft Structures*, USA.

- ³⁹ Department of Defense (2002) *Composite materials handbook (MIL-HDBK-17-3F)*. Vol. 3: Polymer matrix composites materials usage, design, and analysis, USA.
- ⁴⁰ Hoepfner, D.W. (1981) Estimation of component life by application of fatigue crack growth threshold knowledge. In: *Fatigue, creep, and pressure vessels for elevated temperature service*. Presented at: *The winter annual meeting of the American Society of Mechanical Engineers*, 15-21 Nov. 1981, Washington D.C.
- ⁴¹ Hoepfner, D. W. (2011) Overview of HOLSIP. *FASIDE International Inc.* Salt Lake City, UT, USA.
- ⁴² Thomsen, M. L. (2011) Fracture mechanics course notes. *Mechanical Engineering*. University of Utah, Salt Lake City, UT, USA.
- ⁴³ McKeighan, P. C., Fess II, F. E., Petit, M. and Campbell, F. S. (2002) Quantifying the magnitude and effect of loading errors during fatigue crack growth testing under constant and variable amplitude loading. In: *Applications of Automation Technology in Fatigue and Fracture Testing and Analysis (ASTM STP 1411)*. Vol. 4, pp. 146-164.